RSC Advances

REVIEW

View Article Online
View Journal | View Issue

Cite this: *RSC Adv.*, 2025, **15**, 15951

Progress and obstacles in electrode materials for lithium-ion batteries: a journey towards enhanced energy storage efficiency

Rimsha Khalid, Afzal Shah, * Mohsin Javed and Hazrat Hussain

This review critically examines various electrode materials employed in lithium-ion batteries (LIBs) and their impact on battery performance. It highlights the transition from traditional lead-acid and nickel–cadmium batteries to modern LIBs, emphasizing their energy density, efficiency, and longevity. It primarily focuses on cathode materials, including $LiMn_2O_4$, $LiCoO_2$, and $LiFePO_4$, while also exploring emerging materials such as organosulfides, nanomaterials, and transition metal oxides & sulfides. It also presents an overview of the anode materials based on their mechanism, *e.g.*, intercalation–deintercalation, alloying, and conversion-type anode materials. The strengths, limitations, and synthesis techniques associated with each material are discussed. This review also delves into cathode materials, such as soft and hard carbon and high-nickel systems, assessing their influence on storage performance. Additionally, the article addresses safety concerns, recycling strategies, environmental impact evaluations, and disposal practices. It highlights emerging trends in the development of electrode materials, focusing on potential solutions and innovations. This comprehensive review provides an overview of current lithium-ion battery technology, identifying technical challenges and opportunities for advancement to promote efficient, sustainable, and environmentally responsible energy storage solutions. This review also examines the issues confronting lithium-ion batteries, including high production costs, scarcity of materials, and safety risks, with suggestions to address them through doping, coatings, and incorporation of nanomaterials.

Received 23rd March 2025
Accepted 5th May 2025

DOI: 10.1039/d5ra02042e

rsc.li/rsc-advances

1. Introduction

Energy serves as a fundamental necessity in today's world, and the United Nations has identified the provision of affordable and clean energy as the seventh Sustainable Development Goal (SDG). Since the beginning of civilization, humanity has been dependent on energy sources. Initially, the focus was primarily on non-renewable resources. However, the continuous growth in global energy demand and the awareness about the depletion of fossil fuel reserves highlighted the critical necessity for renewable energy alternatives. Additionally, the growing environmental concerns associated with carbon dioxide emissions and rising fuel prices have intensified the drive for the advancement of hybrid and electric vehicles.[1] In this regard, guaranteeing a secure and sustainable energy supply is arguably our most urgent societal challenge. Therefore, collaborative initiatives are being pursued to find solutions that mitigate air pollution from internal combustion engines, while simultaneously advancing effective technologies for the generation and storage of electrical energy derived from solar and wind sources. Rechargeable batteries are viewed as the most promising alternatives in this scenario.[2] They store chemical energy, which can be converted into electrical energy on demand.[3,4]

The first rechargeable battery was developed in the mid-19th century, with Gaston Plante's lead-acid batteries debuting in 1859.[5] The quest for higher energy density, enhanced efficiency, and more environmentally friendly options spurred the evolution of rechargeable batteries, transitioning from lead-acid to nickel–cadmium (NiCd) and ultimately to lithium-ion technology. While lead-acid batteries remain in use, their limited lifespan, low energy density, and considerable weight have prompted the search for superior alternatives. Nickel–cadmium batteries offered improved energy density, durability, and performance across various temperatures, yet their environmental impact and health risks due to cadmium toxicity posed significant challenges. A pivotal breakthrough occurred in the 1990s with the advent of lithium-ion batteries, which have since become the predominant battery technology, largely due to their reduced environmental footprint.[5]

The shift from lead-acid batteries to nickel–cadmium and subsequently to lithium-ion batteries was driven by pressing practical requirements rather than solely by technological progress. As society increasingly prioritized mobility, electrification, and sustainability, there arose a demand for energy storage solutions that were lighter, more efficient, and environmentally friendly. Innovations in materials science,

Department of Chemistry Quaid-i-Azam University, Islamabad 45320, Pakistan. E-mail: afzals_qau@yahoo.com

particularly in the development of electrodes and electrolytes, largely addressed the limitations of earlier battery technologies. Additionally, the worldwide pursuit of cleaner technologies and the expansion of electric and portable electronics significantly accelerated the adoption of lithium-ion systems.[6]

LIB is rechargeable utilizing the reversible intercalation of Li^+ into electrically conducting electrodes to store energy. Typically, one electrode functions as the cathode, often composed of lithium cobalt oxide, while the anode is usually made of graphite. These materials are capable of absorbing and releasing lithium ions. The electrolyte, a specialized liquid that enables the transfer of Li^+ ions between the electrodes, commonly consists of a mixture of dimethyl carbonate and ethylene carbonate. A separator is also present to allow the flow of Li^+ ions while preventing direct contact between the electrodes. During charging, lithium is oxidized, prompting the power supply to drive Li^+ ions from the cathode to the anode through the electrolyte and separator. To maintain charge balance, electrons travel from the cathode to the anode *via* an external circuit instead of through the electrolyte. This entire process is reversed during discharging, where Li^+ ions migrate from the anode to the cathode through the electrolyte, and electrons follow the same path through the external circuit, generating power from the battery.[7]

LIBs have been a game changer in the battery market because of their distinct advantages over other commercially available rechargeable batteries in the context of their high specific energy, energy density and efficiency, longer cyclability, and extended shelf life.[8] LIBs are particularly advantageous for electric vehicles primarily because of their elevated energy density, allowing for better energy storage in a lighter and more compact form. They also deliver superior power output relative to their mass compared to traditional rechargeable batteries.[9] Presently, the majority of all hybrid vehicles in the market utilize Ni-MH batteries. However, research shows that this trend may change within a decade, with projections indicating that 70% of hybrids, 100% of plug-in hybrids, and almost all electric vehicles (EVs) will depend on LIBs.[10] A comparison of the energy density of LIBs with other materials and batteries can be seen in Fig. 1.

The idea behind the first LIB was based on the reversible transmission of Li^+ ions between anode and cathode materials of varying potentials. This mechanism has led to the common designation of "rocking chair battery", reflecting the oscillatory movement of lithium ions between the two electrodes.[11] The ability of the series of lithium incorporated transition metal oxides (TMOs) with the $LiFeO_2$ structure to intercalate and de-intercalate Li-ions reversibly at comparatively high potentials marked a ground-breaking discovery. Nickel and cobalt oxides and their mixtures with Al, Mn, and Fe were also found to demonstrate this capability. Among these materials, $LiCoO_2$ emerged as the active material for LIBs. Later on, a new form of MnO_2 was prepared from $LiMn_2O_4$ (LMO) that exhibited reversible oxidation and reduction reactions in a nonaqueous electrolyte at elevated potentials, making it an effective option for various commercial battery applications.[12,13] The recognition of materials suited for use as anode materials proved to be more intricate; initially, graphite and carbon-based materials were utilized, but they faced challenges due to the co-intercalation of solvent molecules, leading to solvent degradation and damage to the carbon structure. Eventually, petroleum coke (PC) was recognized superior to graphite due to its resistance to reduction and solvent co-intercalation, and the addition of ethylene carbonate further enhanced the stability of both petroleum coke and graphite.[14,15]

Currently, a variety of cathode materials are employed in batteries alongside the traditional options LCO and LMO. A newer alternative, lithium nickel manganese cobalt oxide (NMCO), is available in several formulations based on the ratios of nickel, manganese, and cobalt, including 111, 532, and 811, with the 111 and 532 variants being the most commonly utilized. Recently, lithium iron phosphate (LFP), characterized by its tunnel-like structure, has garnered significant interest from researchers. Each of these materials presents distinct advantages and disadvantages, influencing their specific applications.[16]

Despite significant advancements of LIBs over recent decades, they continue to exhibit certain shortcomings. The overall production costs of these batteries have fallen to approximately $190 per kW h, yet this figure remains considerably above the target of $125. The increasing demand for LIBs has heightened the strain on the availability of critical materials, including lithium carbonate. As the use of these batteries broadens, maintaining an adequate supply of necessary materials will become a considerable challenge. Furthermore, safety concerns related to lithium-ion batteries continue to exist, particularly regarding effective heat dissipation management, which poses challenges in high-temperature environments or within extensive battery setups.[17] An increase in battery temperature can trigger undesirable side reactions that may result in thermal runaway, characterized by the generation of excessive heat that is difficult to control. This situation poses risks of mechanical failure, electrical malfunctions, thermal damage, and even potential explosions. Consequently, it is crucial to comprehend the behaviour of LIBs under these hazardous conditions to enhance their safety.[18,19] This review article seeks to address the aforementioned safety issues by exploring various materials for electrodes and electrolytes and assessing their performance. Additionally, it offers a comprehensive overview of the impact of various electrode materials on the overall battery efficiency of LIBs.

2. Cathode materials used in LIBs

2.1 TMOs as cathode materials

Transition metal oxides are being extensively studied as promising materials for cathodes in LIBs due to their ability to provide high energy densities, a wide range of electrochemical characteristics, and a lower cost in comparison to other options. These materials typically comprise transition metals such as Co, Ni, Mn, or Fe bonded with oxygen.[20] The key advantages of using TMOs stem from their ability to undergo reversible lithium insertion and extraction during charge/discharge cycles, which makes them suitable for energy storage applications. The

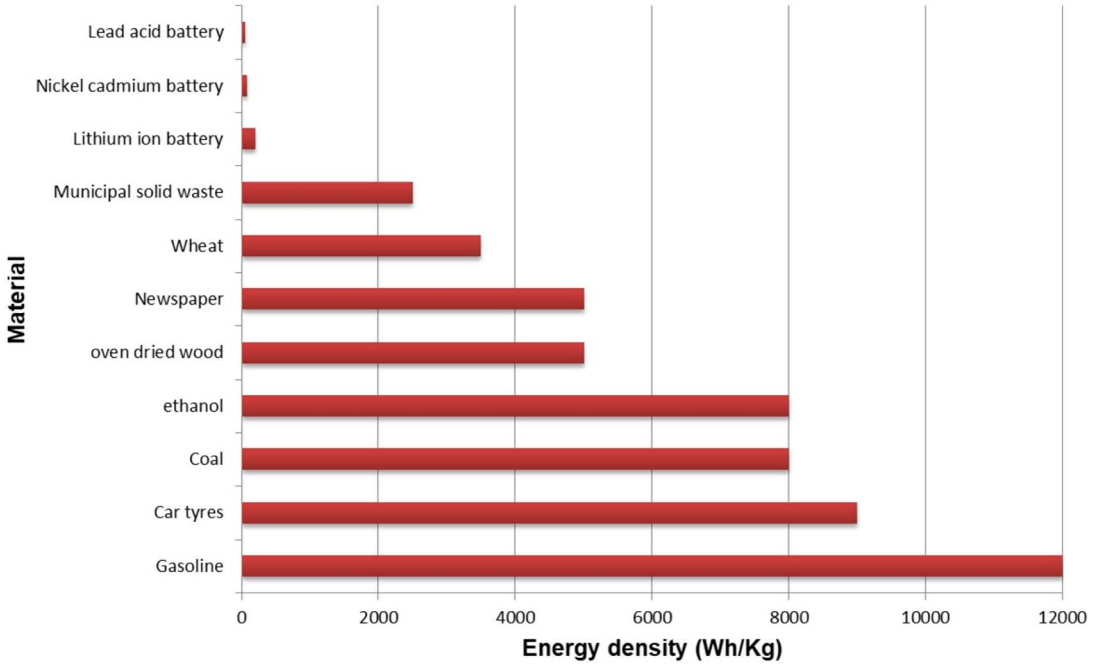

Fig. 1 Comparison of the energy density of different materials.

fundamental working principle of TMOs-based cathodes in LIBs is based on the processes of intercalation and de-intercalation of Li^+ ions within the layers of oxide structures. The TMOs' oxidation states, such as Ni^{2+}/Ni^{3+} in nickel-based oxides, Mn^{3+}/Mn^{4+} in manganese oxides, and Co^{3+}/Co^{4+} in cobalt oxides, play a critical role in facilitating these reversible processes.[21] This enables the cathode materials to store energy during charging and release it during discharge, thus powering devices such as EVs and portable electronics. These cathodes also exhibit relatively high voltage outputs, typically between 3.5 V and 4.5 V, which is favourable for achieving high energy densities. Several TMO materials have been investigated for LIBs as listed in Table 1.

Layered and spinel oxides have received special attention due to their high efficiency as cathode materials used in commercial LIBs. These oxides exhibit high capacitance and decent rate capability. Some of the layered and spinel oxides are discussed in the subsequent sections. Fig. 2 shows the schematic illustration of different cathode materials used for LIBs.

2.1.1 $LiCoO_2$ (LCO) as cathode material. LCO was initially proposed as a cathode material by Goodenough and Mizushima in 1980.[52] It continued to be a prevalent material in commercial Li-ion batteries because of its attributes such as higher discharge potential, energy density, cycling stability, and facile bulk preparation. One of the key advantages of LCO is its ideal layered structure when it is in a fully charged state. The difference in ionic radii between Li^+ and Co^{3+} facilitates this layered structure that allows for rapid 2D diffusion of lithium ions.[53] The layered architecture of $LiCoO_2$ contributes to its structural integrity during the processes of lithium ion intercalation and deintercalation, remaining stable even with the cycling of up to 0.5 Li^+ ions per formula unit. This compound boasts an impressive energy density of up to 840 W h kg^{-1} at 4.55 V, making it particularly well-suited for compact electronic devices that demand significant energy storage. Its ability to sustain consistent performance over numerous charge–discharge cycles ensures a prolonged battery life. Furthermore, $LiCoO_2$ maintains a stable and reliable voltage profile throughout the discharge cycle, which is crucial for sensitive electronic devices requiring a steady voltage supply.

Theoretically, LCO can achieve a capacitance of approx. 274 mA h g^{-1} when all the Li^+ ions are de-intercalated from its structure. However, in practice, it achieves only around 140 mA h g^{-1} within the potential range of 3.0–4.2 V.[54] $LiCoO_2$ exhibits greater volumetric density of 4.2 g cm^{-3} compared to numerous other cathode materials. This characteristic allows for greater energy storage within a compact volume, rendering it ideal for portable and miniaturized devices. Its widespread application in 3C devices—namely computers, communication tools, and consumer electronics—highlights its significance. Furthermore, the high energy density of $LiCoO_2$ suggests promising possibilities for use in electric vehicle applications.[55]

LCO can be prepared using various methods such as sol–gel method, solid-state reaction, co-precipitation, combustion synthesis, freeze-drying, mechano-chemical processes, hydrothermal methods, and microwave synthesis.[53,56] Among these methods, the solid-state reaction methodology is most commonly used. It involves grinding lithium and cobalt salts and heating the mixture at high temperatures. The synthesis method significantly influences the structure of the material and, consequently, affects the electrochemical performance. For instance, low-temperature synthesis often results in a high initial capacity, followed by rapid capacity degradation because

Table 1 TMOs as cathode materials in LIBs

Cathode materials	Method of preparation	Structure	Reversible capacity (mA h g^{-1})	Cycle number	Coulombic efficiency (%)	Ref.
α-$LiFeO_2$	Solid state method	Cubic with space group $Fm\bar{3}m$	500	30	>95	22
NCM@$LiFeO_2$ and Fe_2O_3	Sol–gel method followed by calcination	Layered structure	180	600	≈99	23
α-$LiFeO_2$/graphene nanocomposites	Hierarchical assembly	Cubic structure	238.9	50	>95	24
$0.7Li_2MnO_3.0.3LiFeO_2$	Dry synthesis	Layered structure	160	50	>95	25
α-$LiFeO_2$ nanorods	Solid state method	Nanorods	139.8	50	>85	26
$LiNi_{0.6}Mn_{0.37}Fe_{0.03}O_2$	Coprecipitation method	Layered $R3m$	185.3	500	>90	27
α-$LiFeO_2$/C composites	Solvothermal method	Cubic with $Fm\bar{3}m$	135.5	100	>90	28
Nanosized lithium cobalt oxide N-LCO	High-temperature solid-state reaction	Nanosized porous structure	168.7	300	>90	29
$LiCoO_2$ sintered disk cathode	High-temperature sintering method	Sintered thick and dense structure	135.8	>50	Good coulombic efficiency	30
$LiCoO_2$ nano polyhedron on Au-coated Cu foam	Microwave-assisted route followed by annealing	Hexagonal layered structure	136.4	600	>95	31
$Li_{1.2}Mn_{0.54}Co_{0.13}Ni_{0.13}O_2$ microspheres	Co-precipitation method	Layered structure with super-lattice reflections	202	100	>95	32
$LiNiO_2$ doped with 0.5% Mg and 0.3% Cu	Co-precipitation method	Rhombohedral	213	200	>80	33
$LiNiO_2$	By varying the partial pressure of oxygen during the calcination process	A structure having t_{2g}/e_g symmetry	204	100	92.5	34
$LiNiO_2$	Precipitation followed by calcination	The rhombohedral unit cell ($R3m$ space group)	231.7	400	91.3	35
Mg/Mn–$LiNiO_2$	The co-precipitation method followed by high-temperature calcination	Layered with rhombohedral unit cell	216	350	86	36
$LiNiO_2$ with $LiYO_2$–YO_3 coating	The co-precipitation method followed by calcination	Layered with rhombohedral unit cell	225	100	93.4	37
$LiNi_{0.95}Mn_{0.05}O_2$	The co-precipitation method followed by calcination	Layered structure	189.6	100	≈99	38
Niobium treated $LiNiO_2$	Facile incorporation of Nb into $LiNiO_2$	Layered structure	160	500	≈99	39
$LiNi_{0.95}Al_{0.04}Mg_{0.01}O_2$	Solid state interface elemental inter-diffusion strategy	Layered structure	200.8	200	79.46	40
Selenium coated $LiNiO_2$	Solid-phase mixing combined with low-temperature sintering	Layered structure	200.1	300	>95	41
Pre-oxidized $LiNiO_2$	Precursor peroxidation method	Layered structure	190.9	100	>90	42
$LiNiO_2$ with Al_2O_3 artificial coating layer	Atomic layer deposition	Layered hexagonal structure	170	50	>95	43
Al^{3+} and Ti^{4+} doped $LiNiO_2$	Sol–gel method	Layered structure with $R\bar{3}m$ space group	223	300	81.59	44
$LiMnO_2$ and rGO nanocomposite cathode	One pot hydrothermal route	Layered structure	185.6	100	>95	45
$LiMnO_2$–$LiMn_2O_3$ composites	Hydrothermal method	Orthorhombic structure	265	80	>95	46

Table 1 (*Contd.*)

Cathode materials	Method of preparation	Structure	Reversible capacity (mA h g^{-1})	Cycle number	Coulombic efficiency (%)	Ref.
$LiMnO_3$ nanowires	Low-temperature reduction process	Nanowires	120.1	100	>90	47
$Li_{0.98}MnO_{1.992}$	Tuneable electrochemical conversion using protonated Mn_3O_4	Spinel layered heterostructures	250.5	1000	98.8	48
Li_2Se–$LiTiO_2$	Two-step solid-phase synthesis method	Cubic $LiTiO_2$ in which Li_2Se are uniformly distributed	398	100	>95	49
$LiNi_{0.6}Co_{0.2}Mn_{0.2}O_2$	Ball-milling and tempering method	Rock salt type	≈ 180	200	80.01	50
$LiCu_2O_2$	Solid phase sintering technique	Crystalline structure	423	>50	Good coulombic efficiency	51

of disordered Co^{3+} and Li^+ ions placement, resulting in a spinel-like LCO phase.[57]

Along with its merits LCO also faces some challenges as a cathode material. Its main issue is the phase transition during the deintercalation of Li^+, causing lattice distortions. In particular, a reduction in the lattice dimensions at around 50% Li^+ extraction (beyond 4.2 V) results in capacity fading due to non-uniform strain, leading to particle fractures. Cobalt dissolution at high voltages (above 4.2 V) is another issue, leading to further capacity loss. This is partly triggered by oxygen loss from the lattice during deep Li^+ extraction.[58–60] The instability of LCO at high voltages and the loss of active elements such as Li^+ and Co also cause compatibility problems with the electrolyte, binders, and conductive additives, affecting the whole battery system. These issues lead to reduced electrochemical performance and can even pose safety concerns. The interface between LCO and other components, like the electrolyte, is also a significant challenge. Moreover, disruption of the solid electrolyte interface due to oxidation of the electrolyte leads to interface instability and capacity fading. The commonly used electrolyte salt, $LiPF_6$, has low thermal stability and is sensitive to hydrolysis. At high voltages, it decomposes and triggers side reactions with the cathode, which worsens battery performance and raises safety risks, including thermal runaway.[13,61] These high-voltage challenges can be addressed by doping and coating. Doping can improve the structure of LCO, enhancing its stability. In contrast, coating materials like Al_2O_3, $CePO_4$, $FePO_4$, $Li_4Ti_5O_{12}$, SnO_2, TiO_2, ZnO, and ZrO_2 can improve conductivity, stabilize the material, and choke unwanted reactions between the electrolyte and electrode and accounts for improved C_s and longer cycle life.[62] Another practical approach to enhance LCO's cycle life and discharge capacity is metal doping, using elements such as Al, Cr, Ni, Ti, or Mg.[63]

Future advancements in $LiCoO_2$ cathode materials will leverage innovative engineering strategies to enhance performance, stability, and safety. One promising approach is advanced defect engineering, which employs techniques such as high-temperature shock to deliberately introduce controlled imperfections in the material. These defects can potentially boost electrochemical performance and enhance lithium-ion mobility. Additionally, morphology engineering plays a vital role by designing specific particle shapes and structures, such as core–shell configurations, which can significantly improve structural stability and prolong cycle life. Furthermore, there is a growing demand for precise control over doping and surface coating processes to ensure uniform distribution and optimal amounts of modifying agents. This precision will further enhance the electrochemical properties and long-term durability of $LiCoO_2$, thereby increasing its efficiency and reliability for next-generation lithium-ion batteries.[64]

2.1.2 $LiMn_2O_4$ (LMO) as cathode material. Spinel $LiMn_2O_4$ is an appealing choice due to its cost-effectiveness, low toxicity, and admirable voltage profile. The abundance and cost-effectiveness of manganese render $LiMn_2O_4$ a more economical and accessible alternative to cobalt-based cathode materials. Additionally, manganese's environmental advantages and lower toxicity align with the increasing emphasis on sustainable

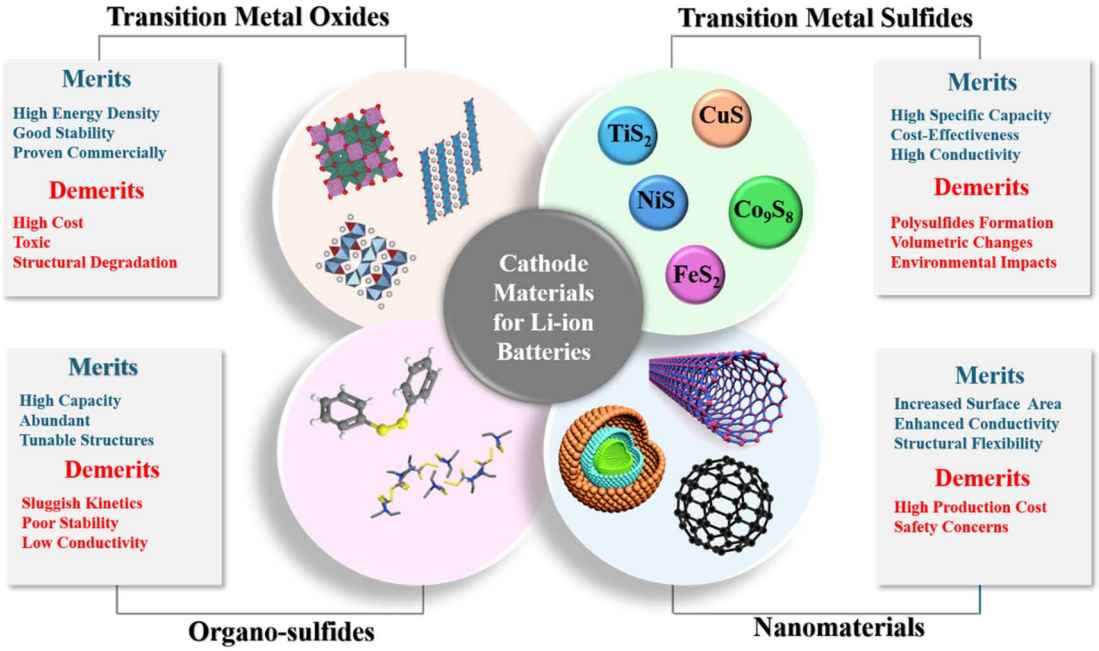

Fig. 2 Cathode materials for LIBs.

energy solutions. The spinel structure of $LiMn_2O_4$ promotes rapid lithium ion diffusion, enhancing both charging and discharging rates. These attributes position $LiMn_2O_4$ as a promising candidate for widespread use in electric vehicle batteries. However, they are not recommended for use under high temperature because their efficiency drops at around 60 °C, as their manganese dissolves into the acidic liquid electrolyte solution. This efficiency loss needs to be addressed for large scale utilization of LMOs in high-temperature applications.[65,66]

Traditionally, LMOs are synthesized through solid-state reactions involving oxides or carbonates having lithium and manganese ions. These reactions are followed by calcination at high temperatures. Though this process is widely used, it suffers from several drawbacks, including inhomogeneity, irregular particle morphology, large particle sizes, broad size distribution, long heating times, and the need for multiple grinding and annealing steps.[67,68] To address these limitations several alternate methods such as Pechini process, sol–gel, emulsion, and citric acid methods, have been developed by producing spinel materials with smaller, more uniform particle sizes. Preparing LMO by spray drying technique offers several benefits including simplicity, low cost, and scalability for large production quantities. Spray drying allows for the fabrication of microscale particles and enables the synthesis of high-purity materials at lower temperatures. It also allows the formation of homogeneous multi-component systems by blending precursor solutions.[69–71]

Despite these advances in synthesis, the issue of efficiency loss at elevated temperatures remains a challenge. Researchers have attempted to address this challenge by coating the surface of LMO with inorganic materials such as Al_2O_3, $AlPO_4$, AlF_3, ZrO_2, and SiO_2 to shield the LMO from direct exposure to the electrolyte, thereby enhancing its stability. Overly thick coatings affect the material's electrochemical performance.[72,73] Therefore, to avoid resistance researchers use electrically active materials as coatings. For instance, electrically conductive carbon coatings enhance LMO's electrochemical performance and room temperature stability. Nevertheless, when LMO coated with carbon is tested at 60 °C, its performance rapidly deteriorates under the same experimental conditions.[74] Surface coatings with electrochemically active materials like $LiCoO_2$, $LiNi_{0.5}Mn_{1.5}O_4$, $LiNi_{0.05}Mn_{1.95}O_4$ and $Li_4Ti_5O_{12}$, have been found to demonstrate some improvements in room-temperature performance. But still these approaches are less successful at higher temperatures. For instance, $LiMn_2O_4$ coated with $Li_4Ti_5O_{12}$ show a discharge capacity of approximately 90 mA h g^{-1}, showing less than 80 percent of its original capacity after 40 cycles at 55 °C.[75]

2.1.3 $LiFePO_4$ (LEF) as cathode material. LFP is both economically viable and environmentally sustainable, boasting a theoretical capacity of 170 mA h g^{-1} and a stable discharge voltage of 3.4 V in relation to the Li/Li^+ system. It also demonstrates commendable cycling performance and thermal stability.[76–78] Nevertheless, LFP encounters certain obstacles, such as slow electronic conduction and a reduced diffusion rate of Li^+ ions, which hinder its overall performance. To address these issues, researchers have explored various modifications. A common approach to improve its conductivity involves coating LFP particles with highly conducting materials such as carbon, metals, or metal oxides. This coating helps enhance electron flow, allowing for better battery performance.[79,80] Reducing the particle size of $LiFePO_4$ has also been explored to increase surface area, thereby improving lithium-ion diffusion.[81] In one particular research, $LiFePO_4$/C cathode was developed with minute particle size by mixing lithium acetate, iron oxalate, ammonium phosphate, and glucose followed by thorough

Table 2 Comparison of $LiCoO_2$, $LiMn_2O_4$ and $LiFePO_4$ as cathodes

Property	$LiCoO_2$	$LiMn_2O_4$	$LiFePO_4$
Theoretical capacity	~140 mA h g^{-1}	~120 mA h g^{-1}	~170 mA h g^{-1}
Energy density	High	Moderate	Moderate
Cycle life	Moderate (~500–1000 cycles)	Moderate (~500–1000 cycles)	Long (>2000 cycles with good retention)
Thermal stability	Low – prone to thermal runaway	Better than $LiCoO_2$, but still moderate	Excellent – stable at high temperatures
Environmental impact	High (toxic cobalt, difficult recycling)	Lower than $LiCoO_2$, but Mn dissolution can be an issue	Low (non-toxic, environmentally benign)
Safety	Moderate to low – can overheat	Better safety profile than $LiCoO_2$	Very safe – minimal risk of fire or explosion
Cost	High (due to cobalt content)	Lower cost than $LiCoO_2$	Low (iron and phosphate are abundant)
Electronic conductivity	High	Moderate	Low (requires carbon coating or doping)
Rate capability	Moderate	Good	Moderate (can be improved with nanostructuring)
Low-temperature performance	Poor to moderate	Poor to moderate	Poor
Structural stability	Moderate – suffers from capacity fading	Good – spinel structure provides better stability	Excellent – stable olivine structure
Applications	Mobile phones, laptops, consumer electronics	Power tools, electric vehicles (low-cost variants)	EVs, solar storage, grid storage

grinding with water and a PVA binder for 8 hours. The resulting mixture was dried using a spray drier with hot air and then heated in two steps: 300 °C for 5 h, then 600 °C for 10 h in an inert N_2 atmosphere to form the final product. After cooling, the material was ground again for 8 hours, producing $LiFePO_4$/C powder. Electrodes were fabricated by blending $LiFePO_4$ with carbon and a binder, applied onto aluminium, and tested in a battery utilizing the counter electrode of Li metal and adding an electrolyte solution. The battery's electrochemical properties were evaluated through charging and discharging between 2.0 and 4.2 volts, along with electrochemical impedance spectroscopy. The battery's performance was tested at various charge/discharge rates (C-rates), with promising results. At C/5, the battery delivered 134.6 mA h g^{-1}; at 1C, it provided 129.5 mA h g^{-1}; and at 5C, it yielded 120.1 mA h g^{-1}. Further, at 5C, it maintained 95.6% of its original capacity even after 50 cycles, demonstrating a minimum of 0.08% capacity loss per cycle and indicating strong cycling stability.[82–84]

A composite cathode of $LiFePO_4$ and polypyrrole (PPy–$LiFePO_4$) was explored for examining the influence of conductive coatings on the battery performance of $LiFePO_4$. Three variations of the PPy–$LiFePO_4$ composites were created, incorporating 5%, 10%, and 20% PPy content. The pure $LiFePO_4$ exhibited crystal sizes ranging from 2 to 5 μm, whereas the 10% PPy–$LiFePO_4$ sample featured $LiFePO_4$ crystals enveloped in a cotton-like PPy layer, which effectively reduced resistance and enhanced conductivity. In terms of discharge capacity, pure $LiFePO_4$ demonstrated a limited capacity of 112 mA h g^{-1} due to its inadequate electrical conductivity. In contrast, while PPy alone showed an even lower capacity of 69 mA h g^{-1}, the 10% PPy–$LiFePO_4$ sample outperformed both, as the PPy coating significantly improved conductivity, facilitating a more efficient utilization of $LiFePO_4$. Regarding cycling performance, the 10% PPy–$LiFePO_4$ electrode outperformed the others after multiple charge and discharge cycles. Pure $LiFePO_4$ lost capacity quickly due to its poor conductivity, while the PPy coating improved lithium-ion transfer, enhancing both capacity and cycling stability.[84] The comparison of the $LiCoO_2$, $LiMn_2O_4$, and $LiFePO_4$ is given in Table 2.

2.2 Nanomaterials as cathodes

Commercially available lithium-ion batteries utilize transition metal oxides as cathode materials, facilitating the intercalation of lithium ions. Significant research efforts have focused on enhancing these lithium-ion cells' electrochemical performance through various cathode materials. In this context, nanomaterials have surfaced as a promising alternative.[85] Recent progress in nanoscience and nanotechnology has led many researchers to concentrate on nano-architectonic cathode materials, aiming to create lithium-ion cells that demonstrate superior charge and discharge capacity, better rate performance, lower costs, and longevity. Research indicates that nanostructured materials can enhance the thermodynamics and kinetics of electrochemical reactions to a certain degree. Nanomaterials reduce the diffusion distance for electrons or ions and provide an increased surface area for electrode reactions.[86,87] To overcome the deficiencies of conventional cathode materials, nano-sized cathode materials with distinct morphologies have been prepared. They range from 0D nanoparticles to 1D structures including nanorods, nanowires, nanotubes, 2D constituting nano-sheets or nano-plates, and 3D hierarchical nanostructures. These have been prepared using grinding, solution synthesis, and sol–gel methods. The materials demonstrate distinctive lithium-ion storage capacity and superior electrochemical performance; characterized by enhanced rate capability, charge/discharge capacity, cyclic stability, and safety features. Nevertheless, there are also disadvantages associated with them. The oxidation of nanoparticles is enhanced, resulting in greater electrolyte decomposition and the formation of a thicker solid electrolyte interphase (SEI) layer on the nanoparticle surface.[88,89] Nanostructured cathode materials enhance the kinetic properties of

lithium-ion cells by facilitating shorter pathways for Li^+ ion diffusion. Nevertheless, this characteristic is not the sole determinant of the kinetic efficiency of these cells. Consequently, investigating the impact of nanoscale structures on the electrochemical performance of Li^+ ion cells represents a complex and intriguing field of research.[90–93]

Nanosheets are a game-changer in energy storage due to their distinctive characteristics. Olivine-type transition metal phosphates, specifically $LiMPO_4$ where M represents metals like Fe, Co, Mn, or Ni, have demonstrated considerable potential as effective cathode materials for LIBs. Their advantages include impressive thermal stability, elevated energy density, eco-friendliness, and low raw material costs. However, these materials are not without their drawbacks, particularly in terms of low electronic conductivity and slow kinetics for lithium ion diffusion. Despite these challenges, their overall promise in energy storage applications remains noteworthy. To test the impact of nanosize on these properties, $LiMPO_4$ nanosheets with thicknesses 2.7–4.6 nm were synthesized using a liquid phase exfoliation approach. Exfoliation was succeeded by solvothermal lithiation conducted in supercritical fluids under conditions of high pressure and elevated temperature. It produced ultrathin monodispersed nanosheets, and their electrochemical performance was tested by measuring the time required for Li^+ ions diffusion and rate capabilities. The diffusion time of Li^+ ion over a length of <5 nm was found to be 2.5, 25, and 250 microseconds for $LiFePO_4$, $LiMnPO_4$, and $LiCoPO_4$ nanosheets, respectively, and this was 5 times higher in magnitude than that of their corresponding bulk materials, showcasing the potential of nanotechnology in energy storage. The energy density and rate capabilities for $LiFePO_4$ nano sheets were 18 kW kg^{-1} and 90 W h kg^{-1}, which were also higher than the corresponding bulk materials, further highlighting the impressive performance of nanosheets.[94]

The 3D crystal structures of spinel $LiMn_2O_4$ are promising contenders as cathode materials for LIBs as they are economical, environmentally friendly, and exhibit excellent voltage profiles.[95,96] At the same time, they are hindered by a lower power density, which arises from significant polarization effects at elevated charge–discharge rates.[97,98] To address this issue, researchers are developing lithium intercalated compounds in nanoscale dimensions and various morphologies, such as nanoparticles,[99] nanowires,[100] nanotubes,[101] hollow spheres,[102] mesoporous materials, and so on.[103] In one such attempt, highly crystalline spinel $LiMn_2O_4$ with representative morphologies of 1D nanorods, 3D nano thorn microspheres, and 3D hollow nanospheres were prepared using topochemical methods, and their electrochemical properties were investigated and compared. It was found that $LiMn_2O_4$ nanorods and nano-thorns showed two distinct discharge plateaus (4.1 V and 3.95 V), while hollow nano spheres showed less distinct plateaus and lower capacity. The diffusion rate of Li^+ in hollow nanospheres was higher than in nanorods and nano-thorn microspheres because of the high surface area. Their cycling performance was also better than that of other $LiMn_2O_4$ structures. Hollow nanospheres retained 99% of their capacity after 100 cycles, while nanorods and nano-thorn microspheres retained 90% and 98%. Regarding rate performance, hollow nanospheres retained 89% of their capacity at a higher C-rate (5C), while it was 85% for nanorods and 83% for nano-thorn microspheres. This better electrochemical performance of these nanostructures compared to other structures of $LiMn_2O_4$ was perhaps due to high crystallinity and larger surface area. It enhanced Li^+ ion diffusion because of the smaller particle size.[104]

2.3 Organosulfides as cathode materials

The functional groups of organic compounds can be modified to adjust their properties and electrochemical behaviour, making them highly customizable. Among organic compounds, organosulfides have emerged as promising alternatives to traditional cathode materials. Organodisulfides contain a single sulfur–sulfur (S–S) bond, which can break and reform as the battery charges and discharges, making them rechargeable. However, compared to traditional TMO cathode materials, organodisulfides have struggled to compete due to their limited capacities and energy densities. Despite this slow progress, recent advancements have revealed the potential of organosulfides as cathode materials. In particular, organosulfides with longer sulfur chains are more appealing owing to their high capacity and the beneficial characteristics of organic electrode materials. These contain both polymers (–S–R–S_n–, where $n \geq 1$) and linear molecules (R–S_n–R, where $n \geq 3$). These materials help improve lithium–sulfur battery performance by reducing electrolytes, enhancing discharge voltage, and improving discharge product adsorption through functional groups. These features make them promising candidates for addressing some of the inherent problems associated with sulfur cathodes in Li–S batteries.[105,106]

Numerous organodisulfides were developed for use in batteries with TETD initially proposed by Visco and colleagues for applications in rechargeable batteries.[107] However, TETD exhibited low electrochemical efficiency and slow reaction kinetics, resulting in significant polarization during the charging and discharging processes. Consequently, the achieved potential was only 36% of its theoretical potential. Since then, researchers have studied other organodisulfides due to their promising theoretical capacities. For example, 2,5-dimercapto-1,3,4-thiadiazole (DMcT) is a well-known organosulfide with a theoretical capacity of 362 mA h g^{-1}. However, DMcT exhibits subpar performance at ambient temperature owing to its lower charge conductivity, which restricts the effective use of the active material in the battery.[108] In another study, researchers prepared a new organodisulfide called TPQD (2,3,4,6,8,9,10,12-octathia biscyclopenta[*b*,*c*]-5,11-anthraquinone-1,7-dithione) to utilize as a high-performing cathode material for LIBs. Due to its strong backbone structure, TPQD did not dissolve in ether-based electrolytes like DME/DOL and stayed stable throughout the battery's charge and discharge cycles. The compound had a theoretical capacity of about 324 mA h g^{-1}, based on the expectation of a six-electron transfer process from the disulfide and quinone (BQ) groups. The inclusion of BQ group into TPQD resulted in enhancing energy density and accelerating the reaction kinetics; attributed to its π-conjugation structure.

When TPQD was evaluated as a cathode in lithium-ion batteries, it underwent charging and discharging within a voltage range of 1.4 to 3.5 V. In the initial cycle, the discharge capacity achieved 251.7 mA h g^{-1}, whereas the charge capacity was recorded at 227.6 mA h g^{-1}, resulting in an efficiency of 91.7%. The researchers ascribed the initial loss in capacity to the formation of a SEI or the depletion of Li products. Over the first ten cycles, the capacity slightly increased as the material activated. After 50 cycles, the TPQD electrode stabilized at around 200 mA h g^{-1}. The TPQD electrode demonstrated strong cycle stability and retained 130 mA h g^{-1} following 200 cycles at a rate of 5C with a minimal capacity loss per cycle. The resistance to charge transfer also decreased after the first few cycles, improving the performance. Cyclic voltammetry tests showed that the carbonyl bonds performed well at higher current rates, while the disulfide bonds reacted more slowly, limiting the overall capacity at those rates. Overall, the TPQD-Li system demonstrated improved rate capability, good specific capacity, steady cyclability, and high coulombic efficiency compared to previously known disulfide-based electrodes. The results offered a novel strategy for enhancing the slow kinetics of organodisulfide materials and guided future designs for development of high-performance organic electrodes in LIBs.[109]

2.4 TMSs as cathodes for LIBs

The $2e^-$ electrochemical reaction ($CuS + 2Li^+ + 2e^- \rightarrow Li_2S + Cu$) allow CuS to attain a theoretical capacity of 560 mA h g^{-1}. Two key strategies, namely complexing and nano-structuring, are commonly utilized to improve electrochemical performance while tackling issues such as volume expansion and the electronic insulating characteristics of the discharge product (Li_2S). To combat challenges such as expansion of volume, synthesis of nanostructures has frequently been employed to facilitate the conversion of reaction-based materials. Cheng *et al.*, employed a simple *in situ* melt diffusion method to synthesize a mesoporous network of CuS sheets and particles on top of 3D monolithic Cu foam without using a binder for LIB. For the first and 100th cycles at 0.2C (1C = 560 mA h g^{-1}), the synthesized cathode has an exceptional capacity of 185.1 and 468.3 mA h g^{-1}. This CuS cathode outperformed many others already available in the market thanks to its outstanding rate capability, which allowed the capacity recovery to reach 83.9% after cycling at various current rates.[110] Another possibility is 1D nano-structures, which can provide the desired axial electronic conduction and a shorter ion diffusion channel. Furthermore, it facilitates improved accommodation of volumetric changes during reversible charging and discharging. A solvothermal approach that does not require a template was used by Feng *et al.* to synthesize CuS nanowire bundles.[111] At room temperature and a rate of 0.2C, the initial releasing capacity was 831 mA h g^{-1}, and the corresponding coulombic efficiency was 62.3%. At 0.2C and 0.4C, the reversible capacities following 100 cycles were approximately 570 and 200 mA h g^{-1}.

Wang and co-workers synthesized nanosized cobalt sulfide powders at ambient temperature. The exploration of cobalt sulfide powder as a prospective cathode material for LIBs was conducted *via* electrochemical testing. The findings from CV measurements indicated that the Li/Co_9S_8 cell undergoes a discharge process characterized by two distinct steps.[112] Hollow spheres of mesocrystal Co_9S_8 exhibited a capacity of 254.9 mA h g^{-1} at a rate of 100 mA g^{-1} following 100 cycles and were prepared by Jin *et al. via* solvothermal method.[113] NiS was subjected to charging/discharging at 80 °C, utilizing a PEO solid polymer electrolyte. The *ex situ* XRD measurements indicated that NiS transformed various phases during the discharging process, including the formation of nickel, Ni_3S_2, and sulphur. The start discharge capacity was reported as 580 mA h g^{-1} for the NiS cathode material at a 1.5 V voltage of *vs.* Li/Li^+. The cycling performance was impressive, maintaining 93% of starting discharge capacity following 200 cycles.[114]

Porous FeS_2 nanoparticles wrapped by rGO were synthesized using a solvothermal method and employed as a cathode for LIBs. It demonstrated good cyclic stability and rate capability. Furthermore, FeS_2 composite was found to maintain a discharge capacity of more than 170 mA h g^{-1} under high current density conditions, following 2000 cycles.[115] Zhang and co-workers synthesized a 1D porous FeS_2@C nanowires which proved to be a highly effective cathode material. These nanowires not only promoted efficient electron transport but also improved diffusion kinetics and acted as a reliable buffer against volume expansion. The unique combination of porous nanostructures and the surrounding amorphous carbon resulted in FeS_2@C nanowires exhibiting remarkable lithium storage capabilities, achieving a capacitance of 889 mA h g^{-1} at a current rate of 0.1 A g^{-1} and 521 mA h g^{-1} at 10 A g^{-1}. The discharge energy density is 1225 W h kg^{-1} at 2 A g^{-1} and remains at 637 W h kg^{-1} even after 1000 cycles, surpassing the performance LCO cathode.[116] Pan *et al.* presented a hydrolysis-sulfurization approach for fabricating FeS_2/C nanotube arrays utilizing glucose carbonization and a nanowire template based on sacrificial $Co_2(OH)_2CO_3$. Self-supported FeS_2/C nanotubes exhibited improved cycling performance and significant high-rate capability, delivering capacities of 735 mA h g^{-1} at 0.25C and 482 mA h g^{-1} at 1.5C shown in Fig. 3, surpassing those of pristine FeS_2 reported in previous studies. The architecture of the composite nanotube arrays contributed positively to electrochemical enhancement by leveraging the benefits of a sizeable electrode–electrolyte surface area, improved electrical conductivity, adequate strain accommodation, and increased structural stability.[117]

Nanostructured composite cathode materials that facilitate solid-state lithium-ion batteries were found to have sustained high energy and high-rate performance throughout cycling. The particle size of titanium sulfide (TiS_2) was minimized through planetary ball-milling in order to improve the efficacy of nanostructured composite cathodes. The enhanced use of active materials and rapid kinetics achieved through the reduction of the size of TiS_2 leading to a high reversible battery capacity at both conditions *i.e.*, room and raised temperatures. Using nano-sized TiS_2 in high-power solid-state batteries resulted in a power density above 1000 W kg^{-1} for more than 50 cycles, reaching a peak power density surpassing 1400 W kg^{-1}.[118] Table

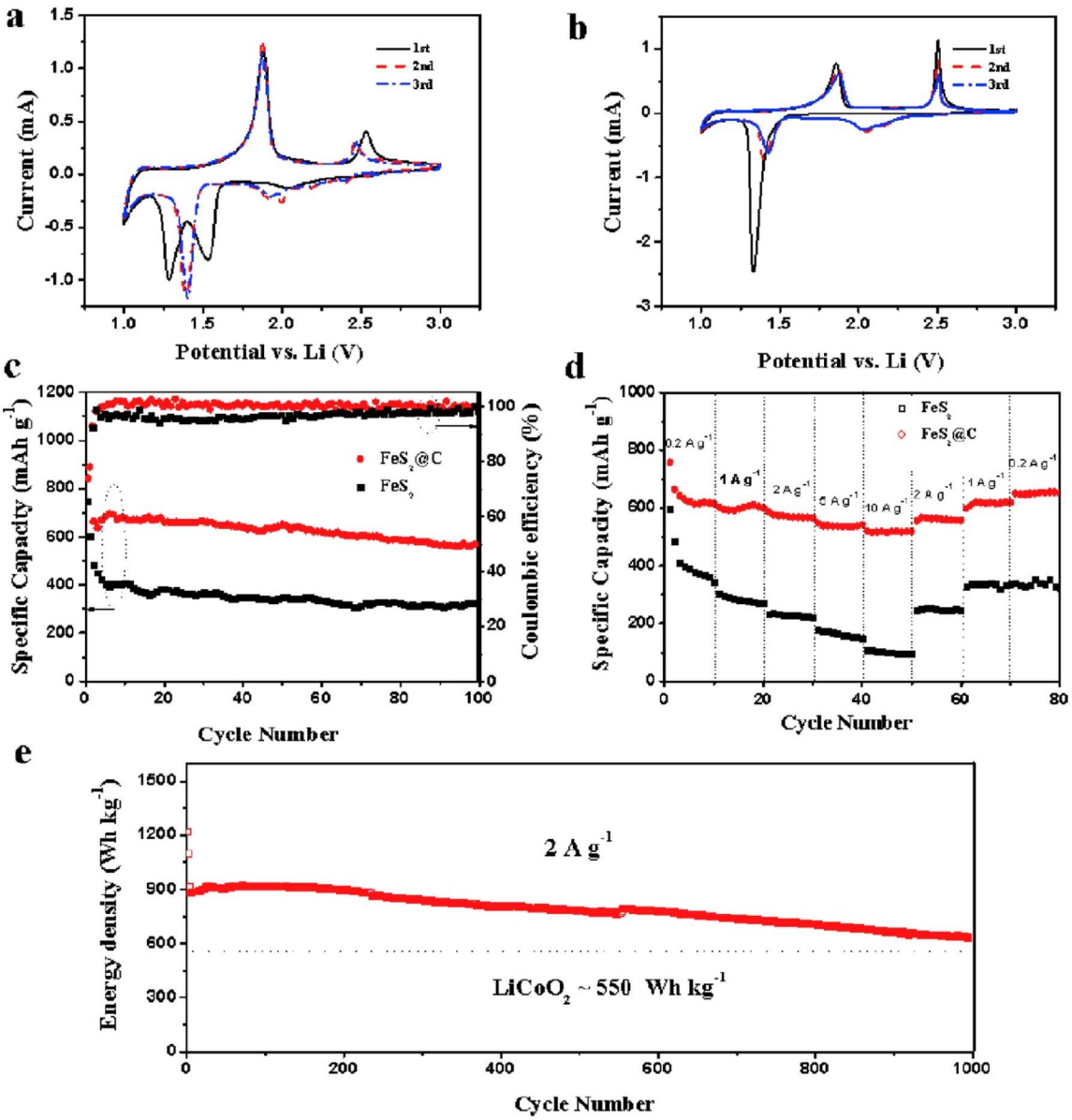

Fig. 3 Electrochemical comparison of FeS_2@C and FeS_2 cells: cyclic voltammogram of the (a) FeS_2@C and (b) FeS_2 cells at a scan rate of 0.1 mV s^{-1} within a voltage range of 1.0 and 3.0 V *vs.* Li/Li^+; (c) cycling stability and the respective coulombic efficiencies of FeS_2@C and FeS_2 cells at a current density of 0.1 A g^{-1} overs 100 cycles; (d) rate capabilities of FeS_2@C and FeS_2 cells at varying current densities from 0.2 A g^{-1} to 10 A g^{-1}; (e) discharge energy density of the FeS_2@C cell at a current density of 2 A g^{-1} *vs.* cycle number shown alongside the theoretical discharge energy density of $LiCoO_2$ cathode (550 W h kg^{-1} based on the mass of LCO). This figure has been adapted from ref. 116 with permission from Elsevier, copyright 2016.

3 enlists some transition metal sulphides used as cathode materials in LIBs.

2.5 Nickel-rich cathode materials

The performance of lithium-ion batteries is heavily influenced by the choice of cathode materials, which significantly impact energy density, cycle life, and overall cost. Among various cathode chemistries, high nickel-rich layered oxides, such as $LiNi_{1-x}M_xO_2$ (where M represents Co, Mn, and Al), have garnered considerable attention due to their impressive specific capacity exceeding 200 mA h g^{-1}, lower cost compared to cobalt-rich alternatives, and their ability to fulfil the energy requirements of grid storage and electric vehicles (EVs). These high nickel-rich cathodes typically derive from layered transition metal oxides based on the α-$NaFeO_2$ structure, which crystallizes in the $R\bar{3}m$ space group. The redox processes involving $Ni^{2+}/Ni^{3+}/Ni^{4+}$ are crucial for capacity generation, although cation mixing often occurs due to the similar ionic radii of Li^+ and Ni^{2+}, which can obstruct lithium ion diffusion and reduce capacity rates. In this context, manganese and aluminium serve as stabilizers—Mn^{4+} enhances structural integrity while Al^{3+} contributes to thermal stability—whereas cobalt plays a vital

Table 3 Transition metal sulfides as cathode materials for LIBs

Cathode material	Method of preparation	Structure	Reversible capacity (mA h g^{-1})	Cycle number	Coulombic efficiency (%)	Ref.
Defect-rich FeS_2 nanoflowers	Self-assembly method	Nanoflowers	841	3000	>95	119
FeS/N–C	Simple pyrolysis method	Nanoflowers	729	500	>95	120
S/FeS_2–C cathode	Template synthesis followed by carbon coating, calcination and sulfidation	Yolk–shell morphology	761.2	350	>90	121
Lamellar iron sulfide with interlayer solvated cations	Solvothermal decomposition	Lamellar structure	450	50	>90	122
Hierarchical FeS_2/C nanospheres	Controllable solvothermal method	Nanospheres	676	100	>85	123
$LiNi_{0.8}Co_{0.1}Mn_{0.1}O_2$ layered oxide cathode with LiS and NaS	Wet chemical treatment	Layered structure having surface passivation	181	100	>70	124
NiS_2/Ketjen black@S composites	Solvothermal method followed by wet chemical precipitation	Cubic pyrite NiS_2 nanospheres uniformly dispersed in composite matrix	461	500	99.1	125
Li_2S	Electrochemical activation process	Stable crystal lattice structure	1052	400	50–90	126
S/sulfide composite cathode	Slurry coating process	Solid film	1169	30	Good coulombic efficiency	127
$Fe_{0.34}Co_{0.33}Ni_{0.33}S_2$	Hydrothermal method	Hollow nanotubes assembled by nanoparticles	1350	300	>95	128
Li_2S	Coating lithium sulfide with polymerizable electrolyte additive	Particles coated with layer of electrolyte additive	1052	100	99.5	129
FeS_2	Use of chelating type binders in a carbonate-based electrolyte	Particles stabilized by chelating type binders	527.3	300	>95	130
Lithium rich layered titanium sulfides	Chemical lithiation of TiS_2	Layered structure	265	60	Good coulombic efficiency	131
Vacancy rich titanium sulfide trapped in a hollow carbon nano cage	Template-free arc-discharge method	Nanoparticles with abundant sulfur vacancies	1118.8	200	96.71	132
Lithium rich Li_2TiS_3	High energy ball-milling method	Nanoscale cubic rock-salt	423.2	100	112.2 during first cycle	133
Titanium disulfide with sulphur cluster vacancies			650	300	Good coulombic efficiency	134
VS_2	Hydrothermal synthesis	Hierarchical spheres composed of nanosheets with porous structure	215	100	>98	135
VS_2–VO_2@S	Hydrothermal and high temperature calcination method	Heterostructures	588.9	500	~60	136
Amorphous titanium polysulfide composites	High energy ball milling followed by liquid phase synthesis	Amorphous structure	507.4	100	40–50	137
Li_2S@graphene	Burning Li foils in CS_2 vapours	Nanoparticles encapsulated by a few layers of graphene	1160	100	Good coulombic efficiency	138

role in improving conductivity and maintaining structural robustness.[139,140]

The synthesis methods for nickel-rich cathodes significantly influence their properties. Various techniques have been developed to control particle morphology, size distribution, and chemical uniformity. Among these, the solid-state method stands out as a traditional approach where metal oxide or carbonate precursors are mechanically blended and subsequently calcined at elevated temperatures. While this method is cost-effective and scalable, it often leads to inferior chemical homogeneity.[141] Co-precipitation, commonly used in industrial applications, involves the lithiation and calcination of transition metal hydroxides or carbonates precipitated under controlled conditions, ensuring high purity and uniform particle size.[142] The sol–gel technique combines metal salts with organic chelators, such as citric acid, to form a gel that is later sintered, resulting in small, uniform particles and precise stoichiometric control.[143] Additionally, hydrothermal and single-crystal synthesis methods utilize high-pressure crystallization to yield single-crystal particles with minimal grain boundaries.[144]

Recent studies have focused on two important members of this family, $LiNi_{0.8}Co_{0.1}Mn_{0.1}O_2$ (NCM811) and $LiNi_{0.85}Co_{0.1}Al_{0.05}O_2$ (NCA8515), to overcome issues with thermal instability, transition metal dissolution, and structural degradation. A thorough investigation was conducted to shed light on the structural and electrochemical distinctions between NCM811 and NCA8515. NCA8515 demonstrated superior cycling stability over NCM811 despite having a more significant nickel concentration. NCM only kept 44% of its initial capacity after 500 cycles at 55 °C, whereas NCA kept 57%. NCA demonstrated better structural retention with reduced voltage decay (0.2427 V) than NCM (0.2794 V). According to first-principles calculations, the Al–O bonds in NCA8515 (2.8354 eV) are stronger than the Mn–O bonds in NCM811 (2.7976 eV). Weaker bonds in NCM encourage the movement of transition metals, the creation of oxygen vacancies, and structural collapse. These results underscore the importance of bonding stability and the selection of dopants in determining the longevity and safety of cathodes.[145]

High nickel-rich cathodes show potential; but their commercial viability is limited by a number of significant issues. Anisotropic volume variations during cycling, particularly in the H2 → H3 phase transition, create mechanical stress that leads to particle cracking. Electrolyte infiltration through these cracks speed up adverse side reactions and degradation. To lessen this problem, single-crystal particles or coatings like LiO_3 have been suggested.[146] At elevated voltages exceeding 4.3 V, particularly under high-temperature conditions, nickel and manganese are likely to leach into the electrolyte. This accelerates capacity fading by contaminating the solid electrolyte interphase (SEI) and depleting active material. Cation mixing is another issue that reduces ionic conductivity and overall battery performance by blocking lithium diffusion channels caused by Ni^{2+} migration into Li^{2+} sites. It has been demonstrated that Rb^+ or Na^+ doping increases the Li-layer gap, resolving this problem.[147] Exothermic reactions brought on by oxygen leakage at high temperatures (>200 °C) as a result of broken metal–oxygen bonds can result in thermal runaway. The thermal decomposition threshold is raised when magnesium and aluminium are co-doped.

Researchers have employed various material design strategies to overcome the aforementioned issues. One such approach is ion-doping, specifically cationic doping with Al^{3+}, which enhances structural stability and strengthens oxygen bonds. Another promising dopant, V^{5+}, contributes to the stabilization of the layered structure. Additionally, anion doping with F^- reinforces metal–oxygen interactions, substitutes for oxygen, and consequently mitigates thermal instability and oxygen loss.[148] Coating the surface with inorganic materials or polymers can serve as an effective strategy. Substances such as Li_2ZrO_3 and La_4NiLiO_8 create protective coatings that inhibit nickel dissolution and lower interfacial resistance.[149,150] Polyacrylic acid (PAA) and its associated polymers serve as effective barriers against moisture and carbon dioxide.[151,152] Excellent performance has been demonstrated by core–shell designs with a high-Ni core that provides substantial capacity, and a manganese-rich shell, which enhances stability. A full-gradient NCM has been shown to retain 90% capacity after 1000 charge–discharge cycles.

Future efforts should focus on the development of advanced multi-element coatings, *in situ* characterization techniques, and the integration of solid-state batteries to bridge the divide between laboratory achievements and commercial implementation. The use of multiple dopants, such as Al–Mg–F, may yield synergistic advantages in both performance and stability.[148] Advanced materials that offer both conductivity and protective features, including PEDOT and self-healing polymers, can deliver significant benefits. Real-time monitoring techniques can uncover dynamic structural changes during operation. Additionally, by pairing solid electrolytes like sulfides or oxides with high-nickel cathodes, it is possible to mitigate the degradation associated with liquid electrolytes, thereby enabling safer high-voltage operations.[153–156]

3. Commonly used anode materials in LIBs

A dense surface film forms on the electrode when Li comes into contact with polar aprotic solvents commonly found in electrolytes. This film impedes proper passivation, crucial for protecting the electrode's surface.[157–159] Lithium dendrites begin forming as the battery undergoes multiple charge and discharge cycles, posing a significant issue. These dendrites can penetrate the separator between the anode and cathode, creating severe safety risks and causing a substantial loss of lithium over time. Graphite remains the most commonly used anode material in LIBs. However, its relatively low capacitance restricts its energy storage potential, which lags meeting the growing demand for batteries with high performance. As a result, researchers are exploring alternative anode materials to improve battery performance.

For a lithium battery to maintain thermodynamic stability, the energy difference between the LUMO and the HOMO of the electrolyte must be greater than the voltage difference between

the anode and cathode. Specifically, the potential energy of the anode must be lower than the LUMO of the electrolyte, and the cathode's potential energy must be higher than that of the HOMO. This ensures the electrolyte's stability during operation, helping to prolong the battery's lifespan and reduce degradation over time.[160] In simpler terms, selecting suitable electrode materials is essential to ensure they do not destabilize the electrolyte, which would otherwise reduce the battery's performance and lifespan.

3.1 Intercalation-type anode materials

Oxides of TMs and other materials with 2D or 3D layered structures have been studied for their capability to intercalate and deintercalate Li^+ ions into their crystal structure, just like graphite as shown in Fig. 4. These materials are interesting because they can absorb and release lithium ions without damaging or destroying their crystal structure. This property is crucial because it makes them suitable for applications like LIBs, where maintaining the material's integrity throughout the charging and discharging cycles is essential.

3.1.1 Graphite intercalation compounds (GICs). The formation of GICs entails the introduction of atomic or molecular layers of different chemical species between the graphite's carbon layers. The covalent bonds between the carbon atoms within the layers, along with van der Waals forces maintain the structural integrity of the layers.[161] Numerous GICs have been investigated since their initial synthesis in 1841, with a diverse array of intercalants, including acidic oxides, metal chlorides, fluorides, alkali metals, bromides, metal oxides, oxyhalides, and strong acids, among many others. These compounds have been extensively explored for their unique structural, electronic, and optical properties, with applications in conductivity, superconductivity, catalysis, hydrogen storage, displays, and polarizers.[162]

GICs with lithium-ion storage intercalants, such as oxides of metals and chlorides of metal, show potential as leading anode materials for LIBs, offering significantly better cycling stability than other alternatives. $FeCl_3$–GIC was prepared using the melt-salt method with flake natural graphite (FNG) as the host material, and it was chosen as a model.[141] $FeCl_3$ molecules were intercalated uniformly into the graphite layers to form $FeCl_3$–GIC, which was tested in a half-cell comprising the Li/$FeCl_3$–GIC. In the first cycle, the material delivered 665 mA h g^{-1} discharge and 506 mA h g^{-1} charge, reaching 76% coulombic efficiency. A reversible capacity amounting to 506 mA h g^{-1} was consistently maintained in the following cycles, far surpassing the graphite's theoretical capacity. The exceptional efficiency of $FeCl_3$–GIC arises due to its unique structure. The intercalated $FeCl_3$ sandwiched between graphene layers offered a barrier for volume changes during the lithiation process. Additionally, the graphene layers boost electrical conductivity, while the expanded interlayer spacing promotes rapid lithium-ion diffusion. The redox reaction of $FeCl_3$ occurred in a favourable potential range (0.8–1.2 V *vs.* Li/Li^+), offering stability during high-rate discharge processes. Furthermore, $FeCl_3$–GIC demonstrated robust cycling performance, sustaining a reversible 480 mA h g^{-1} capacity with complete retention over 400 cycles at a current density of 100 mA g^{-1}.[163]

3.2 TMOs as anode materials

TMOs are promising anode materials for LIBs. Compared to commercial graphite with a limited theoretical capacity, TMOs offer comparatively higher capacities because of the ability of TM ions to undergo multiple valence state changes.[164,165] Besides their high capacity, TMOs present advantages such as cost-effectiveness, safe operating potentials, and the ease of synthesizing nanosized materials with varied structures. These benefits have spurred substantial research into developing

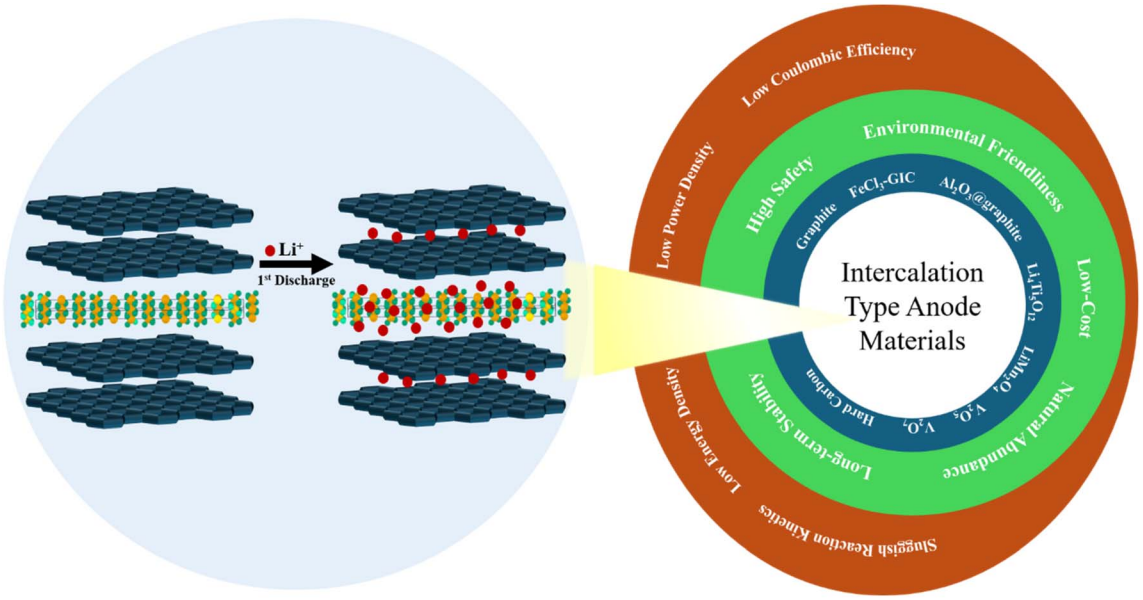

Fig. 4 Intercalation type anode materials with the schematic illustration of the intercalation mechanism for LIBs.

Table 4 TMOs as anode materials for LIBs

Anode material	Method of preparation	Structure	Reversible capacity (mA h g^{-1})	Cycle number	Coulombic efficiency (%)	Ref.
Co_3O_4 nanoparticles	Thermal decomposition of MOF precursor	Cubic spinel structure	913	60	68	169
Janus-structured nanocomposites with Fe_3O_4 nanoparticles and polydopamine on each side of graphene oxide sheets	Langmuir Schaefer technique	Super lattice like out of plane section of the multi-layered nanocomposites	639	1800	>95	170
$(CoNiZnFeMnLi)_3O_4$	Solid phase method	Spinel structure	605	100	65.22	171
Fe_3O_4@C/rGO composites	*In situ* plantation	Lamellar structure	849	120	79.19	172
Phosphorous doped graphene framework with porous Fe_2O_3 nano framework	Thermal treatment	Hierarchical structure	1051	100	74.6	173
MnO_2@HCN (hollow carbon nanospheres)	Chemical reduction method	Core–shell porous structure	604	200	Good coulombic efficiency	174
MnO@N-doped hollow carbon nanotubes	Self-template method	Pea-pod like configuration	966.7	300	62.7	175
Fe_3O_4 with partially reduced graphene oxide	Facile redox deposition method	Hybrid structure	2136	100	Good coulombic efficiency	176
Mesoporous α-Fe_2O_3 hierarchical tubes	Salt impregnation followed by air calcination	Mesoporous structure	880.7	800	67.9	177
$(CrMnFeNiCu)_3O_4$	Hydrothermal method	Spinel structure	913	250	99	178
$SnFe_2O_4$/rGO composites	One pot solvothermal method	Inverse spinel structure with face-centred cubic lattice	1010	300	80	179
SnO_2/Co_3O_4/rGO composites	Chemical precipitation followed by calcination and hydrothermal treatment	Nanocubes anchored onto rGO sheets	727	100	63.4	180
SnO_2/CSC/rGO composites	Co-precipitation method	Nanoparticles anchored on graphene sheets	410.5	100	70.87	181
SnO_x/TiO_2@N-doped carbon	Mild reduction reaction	Hierarchical microspheres	826.3	300	72.3	182
SnO_2/TiO_2 composites	Pulsed-laser deposition	Films with nanostructures	809.3	100	Good coulombic efficiency	183
SnO_2/ZnO@PPy hollow nanotubes	Electrospinning method	Hollow nanotubes	626.1	100	61.12	184
SnO_2 nanoparticles decorated three-dimensional carbon network	Internally NaCl template directing and freeze drying followed by pyrolysis	3D hierarchical honeycomb like carbon network	798	1000	62.5	185
SnO_2 quantum dots in a C and GO network	Solid-state ball-milling followed by water-phase self-assembly	Hierarchical network of C and GO having QD in it	1156	350	58.8	186
SnO_2 embedded rGO composites	CTAB assisted hydrothermal method followed by reduction	Particles embedded in sheet configuration	598	200	64.8	187
Sn/SnO_2/N-carbon doped superstructures	Facile electrospray carbonization strategy	Nanoparticles embedded in a matrix configuration	747.9	200	73.6	188
Carbon coated $TiNb_2O_7$	Soft-template synthesis followed by hydrothermal carbon coating process	Monoclinic crystallographic structure	2136	100	98	189

Table 4 (*Contd.*)

Anode material	Method of preparation	Structure	Reversible capacity (mA h g^{-1})	Cycle number	Coulombic efficiency (%)	Ref.
Co_3O_4@nitrogen doped graphitic carbon cabalistic oxide/MXene	Reduction under inert conditions followed by subsequent oxidation	2D nanosheets	830	500	67.6	190
$(Fe_{2.5}Ti_{0.5})_{1.04}O_4$/C/MXene	Solvothermal self-assembly followed by ultrasound hybridizing followed by high-temperature annealing	2D layered architecture	757.2	800	76.45	191
Mentha aquatic-derived graphitic C TiO_2	Biogenic single precursor approach	Hybrid structure	597	1000	>99	192
Mg^{2+} and Bi^{3+} doped lithium titanium oxide	Ball milling assisted solid-state method	Spinel cubic structure	200	50	67.9	193
Ni–NiO–MoO_2/rGO composites	*In situ* construction of nanostructures	Heterostructures having nanosheets with nano holes	910	220	98	194
Ni and NiO nanocomposites	Direct pyrolysis of a Ni oxalate precursor	Porous prismatic morphology	633.7	100	78.5	195
NiO–Ni foam	Freeze casting followed by thermal oxidation	Porous Ni foam with uniform NiO layer on the surface	550	50	70.9	196
PEDOT/MnO_2 coated on porous carbon nanofibers	Electrospinning followed by carbonization and electrodeposition	Electrode having crosslinked and rough surface	1191	20	>90	197
$(FeNiCrMnZn)_3O_4$	Ball milling followed by calcination	Hexagonal space group $R\bar{3}m$	386.7	185	67.9	198

advanced materials used as anodes for LIBs.[166,167] However, a significant challenge with TMOs is their poor cycle stability. During the lithiation (insertion of Li ions) and delithiation (removal of Li ions) processes, the material experiences repeated and considerable volume changes that disrupt the contact between the counter electrode and active material. This decreases battery performance and efficiency over time.[168] Table 4 represents several TMOs utilized as anode materials for LIBs.

Layered vanadium oxides, including LiV_3O_8, V_2O_5, VO_2, and V_6O_{13}, are highly valued as intercalation-type electrode materials because they can undergo multiple valence changes from V^{5+} to V^{2+}. These materials feature unique layered or tunnel-like structures that accommodate numerous Li^+ ions with minimal lattice strain, making them particularly attractive for battery applications.[199] Despite their advantages, vanadium oxides have high redox potentials, exceeding 2.5 V, making them unsuitable anodes. Recently, co-precipitation was used to synthesise 40–50 nm $Cu_3V_2O_8$ NPs. Despite of having discharge capacity of 462 mA h g^{-1} for the initial 10 cycles, these NPs reached 773 mA h g^{-1} after 50 cycles. The reversible production and breakdown of SEI film may improve Li storage at the contact. With 218 mA h g^{-1} discharge capacity at 1000 mA g^{-1} current density, the $Cu_3V_2O_8$ NPs anode performed well. Li storage was examined using *ex situ* XRD, which demonstrated that $Cu_3V_2O_8$ disintegrates into Cu metal and Li_3VO_4 at 0.01 V. Li_3VO_4 hosts lithium ions in following cycles *via* intercalation. This revolutionary "*in situ*" electrochemical compositing provides crucial insights for creating LIB anode materials.[200]

3.3 Lepidocrocite-type layered titanate structures

Layered titanates have attracted considerable attention in technology due to their advantageous physical characteristics, ability for ion exchange, and potential for electrochemical intercalation. Recent studies indicate that various layered titanates can facilitate reversible reduction intercalation with lithium and sodium ions. Some of these materials, with theoretical capacities exceeding 200 mA h g^{-1}, are capable of inserting alkali metal cations at shallow potentials, in some cases below 0.5 V. A high-capacity, reversible titanate anode could advance sodium-ion battery (SIB) technology, as graphite anodes that are commonly used in LIBs are not well-suited for intercalation of sodium due to larger size than Li ions. Although hard carbon materials have demonstrated high reversible sodium capacities, legitimate safety concerns are associated with their use. In contrast, titanates offer additional advantages, including higher densities (~3.5 g cm^{-3}) than graphite (2.25 g cm^{-3}) and other carbon-based electrode materials. This enhances energy density in both lithium-ion and sodium-ion systems, providing a safer alternative. Moreover, titanium's affordability, non-toxicity, and wide availability make these materials especially appealing for industrial uses, especially in industrial scale batteries for EVs and grid applications. The crystal structures of trititanate and lepidocrocite titanate are shown in Fig. 5.

The investigation of the electrochemical properties of lepidocrocite-type titanates, specifically those derived from $K_{0.8}Ti_{1.73}Li_{0.27}O_4$ demonstrates improved performance upon substituting potassium ions with sodium. This ion exchange results in a higher capacitance in both sodium and lithium half-cells, while preserving the overall structure of the titanate. However, it is noteworthy that the symmetry of the lattice is modified, as sodium occupies different positions within the crystal framework. Sodium's smaller ionic size allows more alkali metal cations to be inserted during discharge, enhancing reversible capacity in both types of cells. Lithium insertion occurs in lithium cells at 0.8 V *versus*. Li^+/Li, while Na

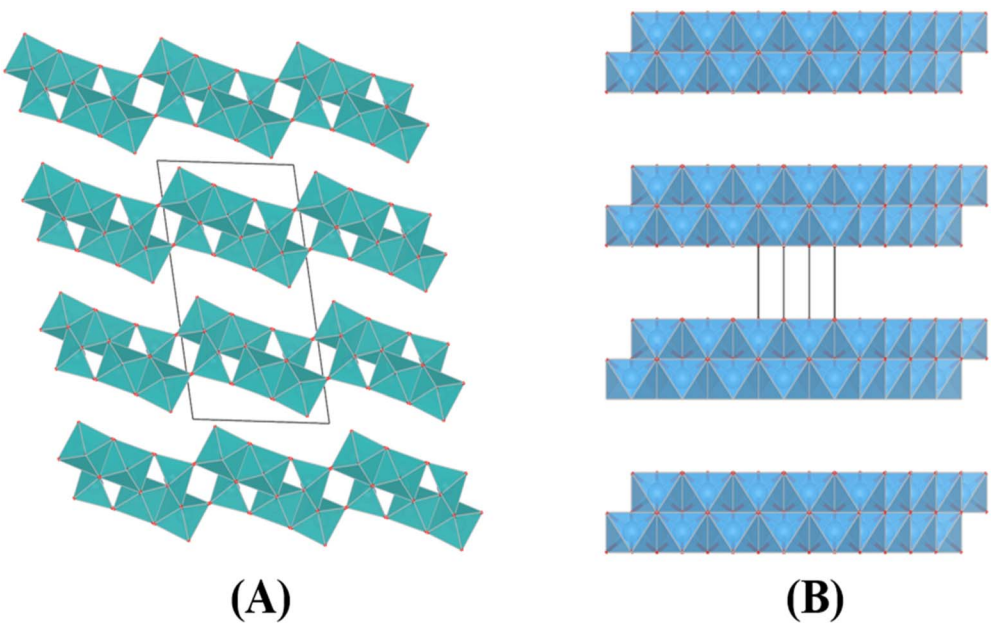

Fig. 5 Structure models of (A) trititanate and (B) lepidocrocite titanate. The unit cells are indicated in lines. This figure has been reproduced from ref. 201.

intercalation occurs at 0.5 V *versus*. Na^+/Na in sodium cells. The voltage profiles for both cells are sloping, indicating single-phase processes. Synchrotron XRD confirms the formation of a lithiated lepidocrocite structure during lithium discharge, with minimal volume change. The study demonstrates that lepidocrocite titanates can be tailored for application as anode materials in both LIBs and SIBs through compositional adjustments and ion exchange processes.[202]

3.4 Alloy-type anode materials

Certain elements such as Si and Sb, Sn, Zn, In, Bi, and Cd,[203,204] are known to form Li alloys. These alloys are considered promising anode materials as shown in Fig. 6.

Lithium alloying and dealloying reactions typically occur at lower potentials (≤1.0 V *vs.* Li), which ensures reversible capacity during lithium cycling. Silver–tin composite alloys are emerging anode materials. With the appropriate composition, the Ag–Sn composite system showed a high capacity and long cycle life, even though the system did not form the typical active/inactive composite structure since all components were active towards lithium. Efforts were made to elucidate the reaction mechanism of the composite alloys containing Li and to investigate the improved cycling performance by analysing the structural alterations during Li insertion and desertion. With optimized compositions and morphological structure, the $Ag_{52}Sn_{48}$ and $Ag_{46}Sn_{54}$ composite electrodes delivered approximately 800 mA h g^{-1}, maintaining a reversible over 350 mA h g^{-1} capacity for over 50 cycles. The $Ag_{52}Sn_{48}$ electrode preserved a reversible capacity of around 200 mA h g^{-1} even after 300 cycles. Structural changes in the $Ag_{52}Sn_{48}$ electrode during Li charge/discharge were analyzed using XRD. The results revealed that the composite alloy undergoes changes to form a ternary lithium inserted phase upon lithium insertion and restores to a structure containing β-Sn, Ag_3Sn, and residual Ag_2LiSn phases after Li extraction. The improved cycle life is attributed to its composite structure and the formation of ternary lithium inserted phase formed during the initial cycle. However, the residual Ag_2LiSn has been reported to likely contribute towards increasing the irreversible capacity loss.[205]

Silicon is also used in LIBs because of its higher lithium storage capacity of 4200 mA h g^{-1} and lower potential for lithium insertion.[206] The challenge faced with Si-based anodes is the substantial volume expansion—up to 400%—during lithium-ion insertion. This expansion can lead to cracking and fragmentation of the Si structure, resulting in capacity loss. To seek the solution to this issue, researchers have turned to various nano-shaped silicon materials like Si nanowires, nanoparticles, and nanotubes, which can better handle the volume fluctuations during charging and discharging cycles.[207] Among these, nanowire core–shell structures have gained particular interest. They can be engineered to ensure an efficient electrical pathway. At the same time, the outer shell,

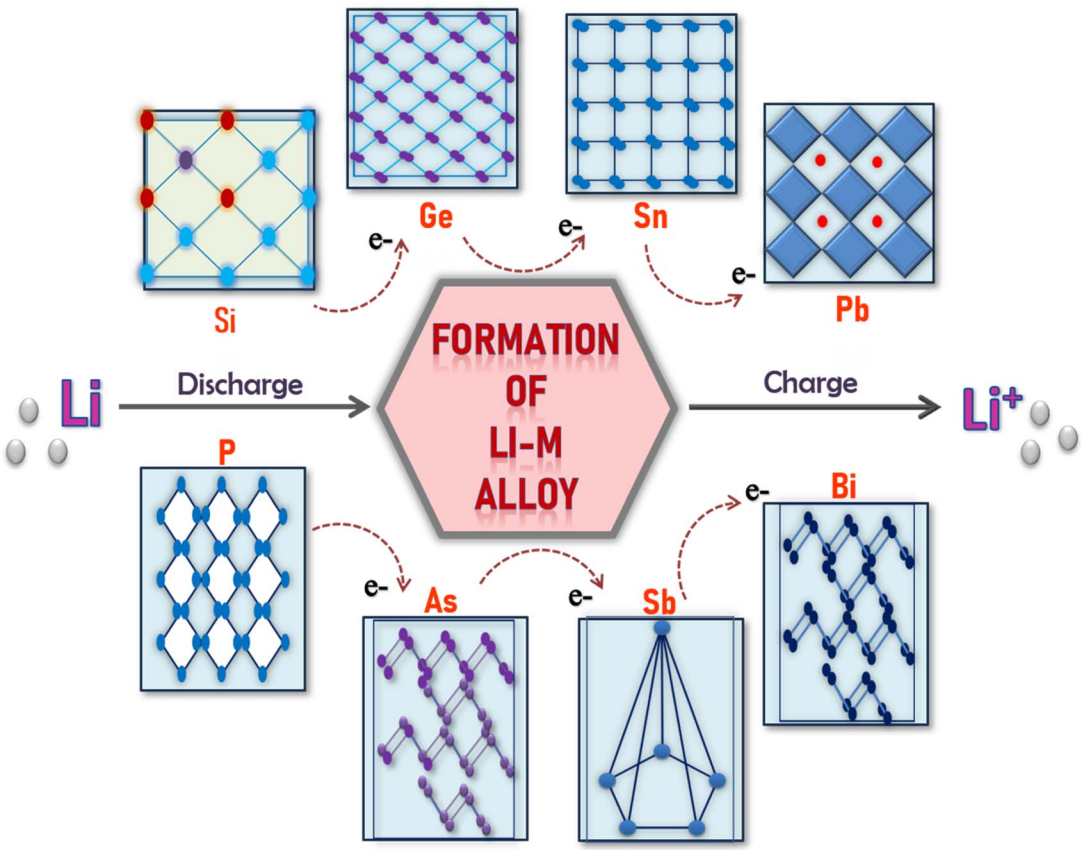

Fig. 6 Pictorial illustration of metals that can form an alloy with lithium.

typically a thin Si layer, provides a large surface area to facilitate faster lithium-ion insertion. Moreover, using carbon nanofibers (CNF) as the core in a heterogeneous core–shell structure instead of C–Si further improves the battery's performance and stability.[208,209]

A recent development involves an alloy-forming method, where researchers transformed the alloy formed from hollow Si–Cu nanotubes to amorphous core–shell nanowires formed from functionalized Si core with CuO shell. Applying a simple hydrogen annealing process reduced the CuO cores and diffused into the a-Si shell, forming the alloy nanotubes. These hollow nanotubes offer high capacity, self-conductive properties, and excellent mechanical support for the anode. This innovative structure achieved a high capacitance after 1000 cycles at 3.4 A g^{-1} (or 20 A g^{-1}), retaining a capacity of approx. 84% (or 88%) without requiring a conductive agent. Notably, the structure endured high-speed charging rates of 70 A g^{-1} for 35 cycles (equivalent to a full charge in 30 seconds) while retaining 88% of its capacity. This Si–Cu alloy nanotube design represents a breakthrough in unlocking the full potential of silicon-based LIBs.[210]

Since the initial examination in the 1970s and 1980s, Li storage metals went on to see a significant surge in interest, especially from 1995 onwards. This is primarily due to the discovery that the cycling stability of these metals significantly improves when they are used in alloys or nano-dispersed composites. Most research in this area has focused on metals like tin, aluminium, and silicon, as well as their various compounds. Some other metals such as antimony and bismuth have also been promising, as shown by early studies in 1975, followed by thermodynamic and kinetic research and more recent cycling studies.[211,212] Pure antimony and bismuth tend to have poor stability, often showing capacity losses after just a few cycles. This has been demonstrated in several studies. One notable improvement is using skinny Bi films, which offer better stability but are only a few micrometres thick. However, these films' practical use in whole cells is limited because their thinness restricts the total capacity that can be achieved.[213] The performance of these metals can be significantly enhanced by forming alloys. Among antimony-containing alloys, the one that has shown the highest stability and cycling capacity so far is tin–antimony (SnSb). This alloy has also been studied in various forms, such as a multi-phase alloy (Sn/SnSb), as a single-phase intermetallic compound, and in more recent times, as a composite combined with carbon nanotubes or mesocarbon microbeads. Other notable tin alloys include indium–antimony, cobalt–antimony, and $CoFe_3Sb_{12}$, though these represent only a small selection of the materials being explored for better cycling performance and stability.[214]

Sn/SnSb, Sn/SnSb/Bi and Sn/Bi multi-phase materials were prepared using $NaBH_4$ or Zn employed as a reducing agent and tested as potential anode materials for lithium-ion batteries through galvanostatic cycling. $NaBH_4$ produced more stable and finer materials, while Zn resulted in purer materials that exhibited lower irreversible capacity. The reversible capacities observed were approximately 600 mA h g^{-1}, 500 mA h g^{-1} and 350–400 mA h g^{-1} for Sn/SnSb, Sn/SnSb/Bi and Sn/Bi respectively. This difference in stability is partly due to the influence of intermetallic phases as the material undergoes the lithiation process.[215]

3.5 Conversion type anode materials

Some materials function as anodes through a redox or "conversion" reaction with lithium. This conversion reaction is not only limited to oxides but applies to other materials like fluorides, sulfides, and nitrides. Usually, Li_2O is electrochemically inactive and does not decompose into metal and oxygen. Lithium can cycle within the material at suitable voltages for the metal, enabling large, stable reversible capacities over multiple charge–discharge cycles. Nanotechnology has helped to develop materials that have been evaluated for lithium cycling *via* different pathways.[216] In this regard some key challenges must be overcome for conversion materials to be considered for potential commercialization, including voltage hysteresis, extended sloping regions in the discharge profile ascribed to redox reactions, poor cycling stability, rate capability, and notable loss of capacity within the first cycle.[217]

Voltage hysteresis, which refers to the variation in voltage during charge and discharge cycles, can reduce the overall efficiency of the battery. The sloping regions, as observed in the discharge profile, indicate that the voltage gradually decreases over time, making it harder to maintain a stable and predictable energy output. Inconsistent cycling stability means the material's performance degrades over repeated charging and discharging cycles, while rate instability indicates the material's inability to handle high charging or discharging speeds. Lastly, the capacity fading during the first cycle can significantly reduce the overall capacity of the battery, making it less efficient in the long term. Addressing these issues is critical for successfully commercializing conversion materials in LIBs.[218] Fig. 7 represents the comparative analysis of theoretical capacities of different metals when used as anode. Extensive research into alternative anode materials for LIBs has resulted in an improved understanding of materials chemistry and electrochemistry and, hence, has provided new insights over the past decade.[216]

3.6 Transition metal sulfides as anodes

3.6.1 Cu-based sulfides. Cu_2S and CuS nanorods have been found to demonstrate stable reversibility when Li is inserted and extracted during the cycles and show excellent rate capability. These electrodes retain reasonable capacitance as well at outstanding current densities (3200 mA g^{-1}), regardless of the rate. While, at high current rates, the CuS electrode retained over 370 mA h g^{-1}, and the Cu_2S one retained its discharge capacity at 260 mA h g^{-1}. After 100 cycles, the CuS and Cu_2S electrodes achieved 472 and 313 mA h g^{-1} discharge capacities, preserving 92% and 96% of the starting capacity at 100 mA g^{-1}. The simplicity of production and their improved electrochemical characteristics make them suitable negative electrodes for future LIBs.[219] Zhou *et al.* developed CuS nanorods measuring lesser than 10 nm employing a straightforward sol–gel method, eliminating the need for post-heating treatment.

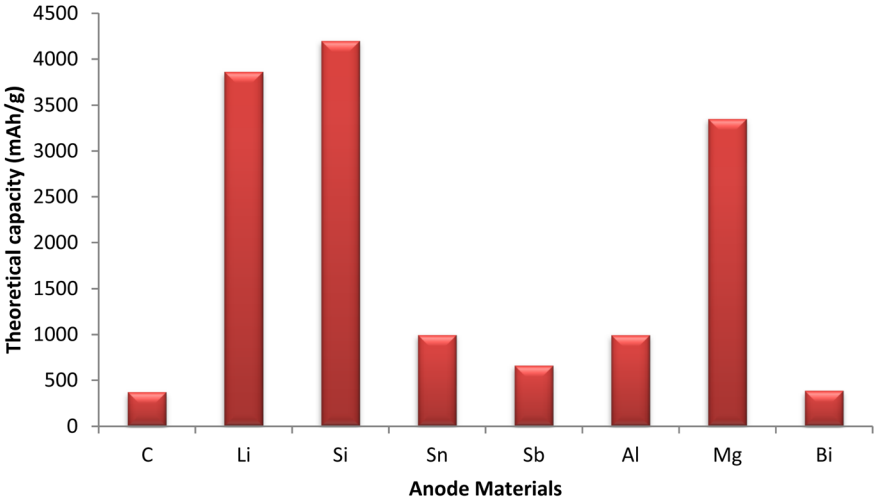

Fig. 7 Comparative analysis of theoretical capacities of different metals when used as anode.

These as-synthesized nanorods showed a hexagonal covellite CuS structure, which is responsible for demonstrating a significant reversible capacity, cyclic stability, and high coulombic efficiency.[220]

Carbon materials like CNTs, graphene, and rGO demonstrate various chemical and physical benefits, such as exceptional electronic conductivity, outstanding mechanical strength, and superior structural flexibility. As a result of this, incorporating carbon materials enhances electrochemical performance to cope the challenges of volume change and inadequate electronic conduction in metal sulfides. By using a one-pot hydrothermal approach, Tao and colleagues synthesized a CuS/graphene composite that demonstrated enhanced cyclability and reversible capacity as compared to the pristine CuS. The composite maintained approximately 296 mA h g^{-1} after 25 cycles at 50 mA g^{-1}.[221] Likewise, Yuan *et al.* prepared CuS/rGO composite as an anode for LIBs. The composite exhibited outstanding electrochemical lithium storage capacities when ether- and carbonate-based electrolytes were employed. At current densities of 100 mA g^{-1}, the two electrolytes demonstrated a reversible capacity of 422 and 390 mA h g^{-1} following 70 cycles. Following 200 charge/discharge cycles at 500 mA g^{-1}, the composite demonstrated a discharge capacity of 390 mA h g^{-1} in the ether-based electrolyte, achieving a capacity retention of 96.7%, as illustrated in Fig. 8.

The impressive electrochemical characteristics of the electrode was due to the synergistic interaction between the rGO and nanoflowers CuS.[222] CuS/graphene was reported to be synthesized as an anode *via* a microwave irradiation method that used a one-pot strategy carried out at room temperature conditions. As compared to the pure CuS, the CuS/graphene provided a notably improved reversible capacity and enhanced stability during Li ion charge/discharge cycles.[223] In the same vein, CNTs are known for their effective conductive network that boosts the electrochemical characteristics. Wang *et al.*[223] employed a straightforward microwave-assisted pathway to produce CuS nanospheres with CNTs interconnected to it. This composite material exhibited strong electrochemical performance. Following 450 cycles, the different percentage compositions of CuS/CNT, *i.e.*, CuS/0.1CNT and CuS/0.5CNT, exhibited discharge capacities of over 437 and 569 mA h g^{-1} at a rate of 400 mA g^{-1}, surpassing performance of controlled samples. Moreover, it was observed that the $CuS/_{0.5}CNT$ retained a capacity of approximately 400 mA h g^{-1} at 6400 mA g^{-1}. Inner electron transport, as well as reaction kinetics, are enhanced by the conducting network of CNTs, leading to higher reversible capacities and rate capabilities. Thus, by utilizing the favourable characteristics of rGO, such as its superior conductivity and mechanical strength, issues related to inadequate electronic conductivity and expanded lattice structure of Li_2S have been effectively addressed. A considerable amount of effort has been dedicated, and numerous strategies have been suggested to develop these materials.

Zhao and co-workers introduced a unique self-templating thermolysis approach, to synthesize Cu_2S hollow spheres with various shell coatings, utilizing the core's thermal decomposition characteristics and the shell's protective attributes. The method is different from conventional wet processing techniques. This synthetic approach has been applied to three distinct coatings, which include carbon, TiO_2, and MoS_2, resulting in the preparation of their respective hollow spheres, which were subsequently employed as efficient anodes for LIBs, demonstrating outstanding cycling stability. The electrochemical performance of $Cu_{2-x}S$@C was meticulously examined.[224] The $Cu_{2-x}S$@C electrode demonstrated boosted electrocatalytic performance compared to pure $Cu_{2-x}S$ and delivered a discharge capacity of 309 and 277 mA h g^{-1} following 300 cycles.[225]

3.6.2 Co-based sulfides. Various cobalt sulfides, including Co_9S_8, CoS, Co_3S_4, and CoS_2, have been tested as anodes. Yan *et al.* reported CoS_2 to achieve a 1st discharge capacity of 1280 mA h g^{-1} at 50 mA g^{-1}.[226] Jiao with his co-workers synthesized CoS_2 hollow spheres through a solvothermal

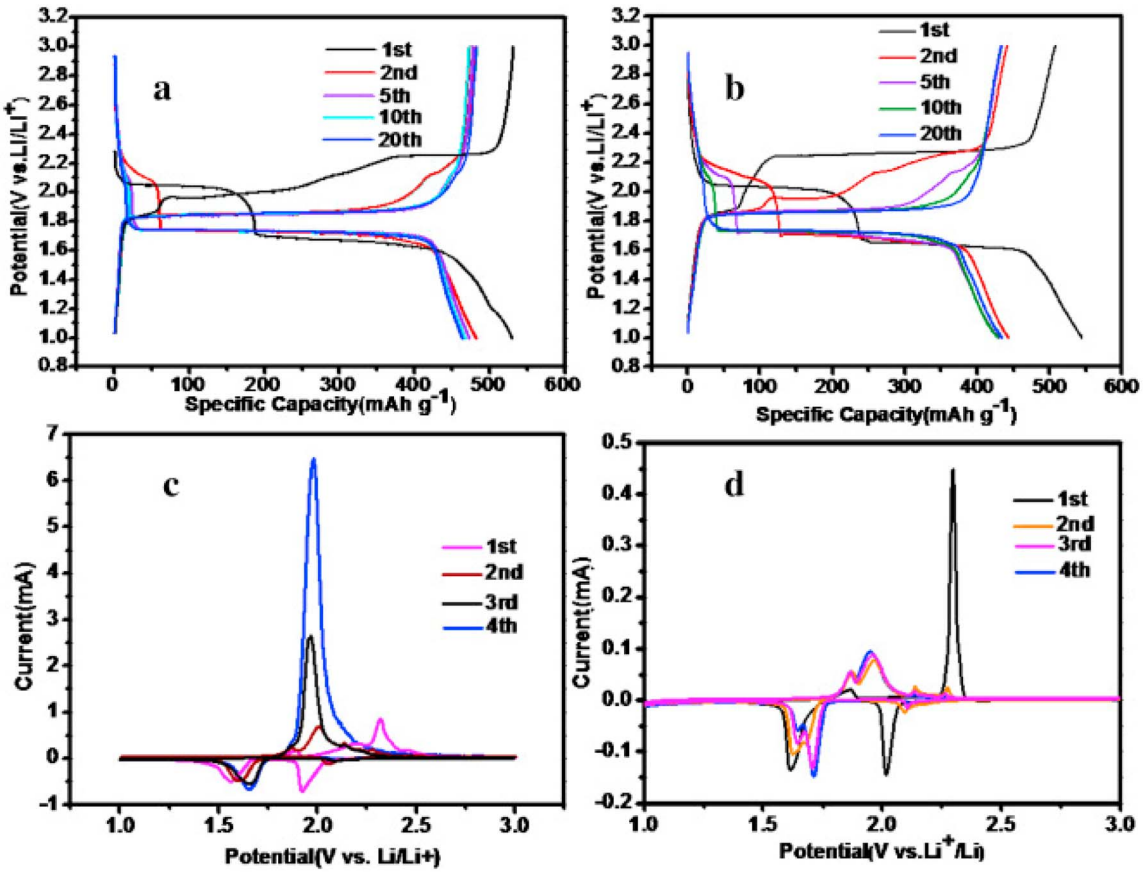

Fig. 8 Charge/discharge profiles of (a) copper sulfide and (b) CuS/rGO at a current density of 100 mA g^{-1}. Cyclic voltammetric curves of (c) CuS and (d) CuS/rGO between a *V* range of 1.0–3.0 V. This figure has been adapted from ref. 222 with permission from Elsevier, copyright 2016.

method and found these to exhibit a discharge capacity of 1210 mA h g^{-1} with good cycling stability, suggesting its potential for long-term applications as an anode material for LIBs.[227] Likewise, the electrocatalytic properties of Co_9S_8 nanotubes indicated a reasonable discharge capacity, suggesting its potential use as an electrode material for LIBs.[228] Numerous investigations into the application of Co_9S_8 in LIBs have been published. Numerous strategies have been implemented to increase conductivity, manage mechanical stress, and optimize the electrochemical activity of Co_9S_8. A simple NaCl method was employed to create 3D Co_9S_8@CNNs anchored in carbon nanosheet networks to enhance conductivity and electrochemical activity. By integrating the benefits of porous and nanoscale structures, 3D Co_9S_8@CNNs inhibited the clustering of nanostructures, offered a wealth of electrochemically active sites. Consequently, the synthesized 3D networks demonstrated exceptional electrochemical performance when employed as anodes.[229]

Hollow cobalt sulfide carbon nanocages showed excellent mechanical flexibility and significant structural stability, resulting in outstanding Li-ion storage capabilities. Operating between a *V* range of 1.0–3.0 V, it showed an energy density of 707 W h kg^{-1}, reasonable rate capabilities, and reversible capacities. Furthermore, it demonstrated stable cycling performance at 1C, showing approximately 26% capacity loss after an extensive 150 cycles, maintaining capacity retention of 365 mA h g^{-1}.[204] Qu *et al.*, presented a synthetic pathway for CoS NPs incorporated into Co_9S_8@C through carbonization followed by a sulfidation process. The material demonstrated improved rate stability and high capacity with a C_s of 1565 mA h g^{-1} at 0.1C (Fig. 9). Moreover, the battery demonstrated a consistent reversible capacity of 606 mA h g^{-1} above 300 cycles at 1C.[230]

A 1D MWCNT@a-C@Co_9S_8 nanocomposite with amorphous layer acting as a linker between the MWCNTs and Co_9S_8 was assessed as an anode for LIBs. It was found to exhibit notable advantages in higher capacity and longevity, outperforming MWCNTs@Co_9S_8 composite and pristine Co_9S_8. The reversible capacity remained at 662 mA h g^{-1} after 120 cycles conducted at 1 A g^{-1} current density. This nanocomposite's effective synthesis and outstanding performance provided many opportunities for exploring other sulfides as innovative anodes for LIBs.[231] Liu *et al.*, synthesized Co_9S_8/GNS and evaluated its performance as an anode for LIBs. In comparison to bulk material, the as-prepared nanocomposites showed better electrocatalytic performance, cyclic durability with a reversible capacity of 1480 mA h g^{-1}. The meticulously designed structure of Co_9S_8/GNS nanocomposite enhanced its electrochemical characteristics.[232] The incorporation of C materials facilitated the reduction of Co_9S_8 nanoparticle clustering by providing

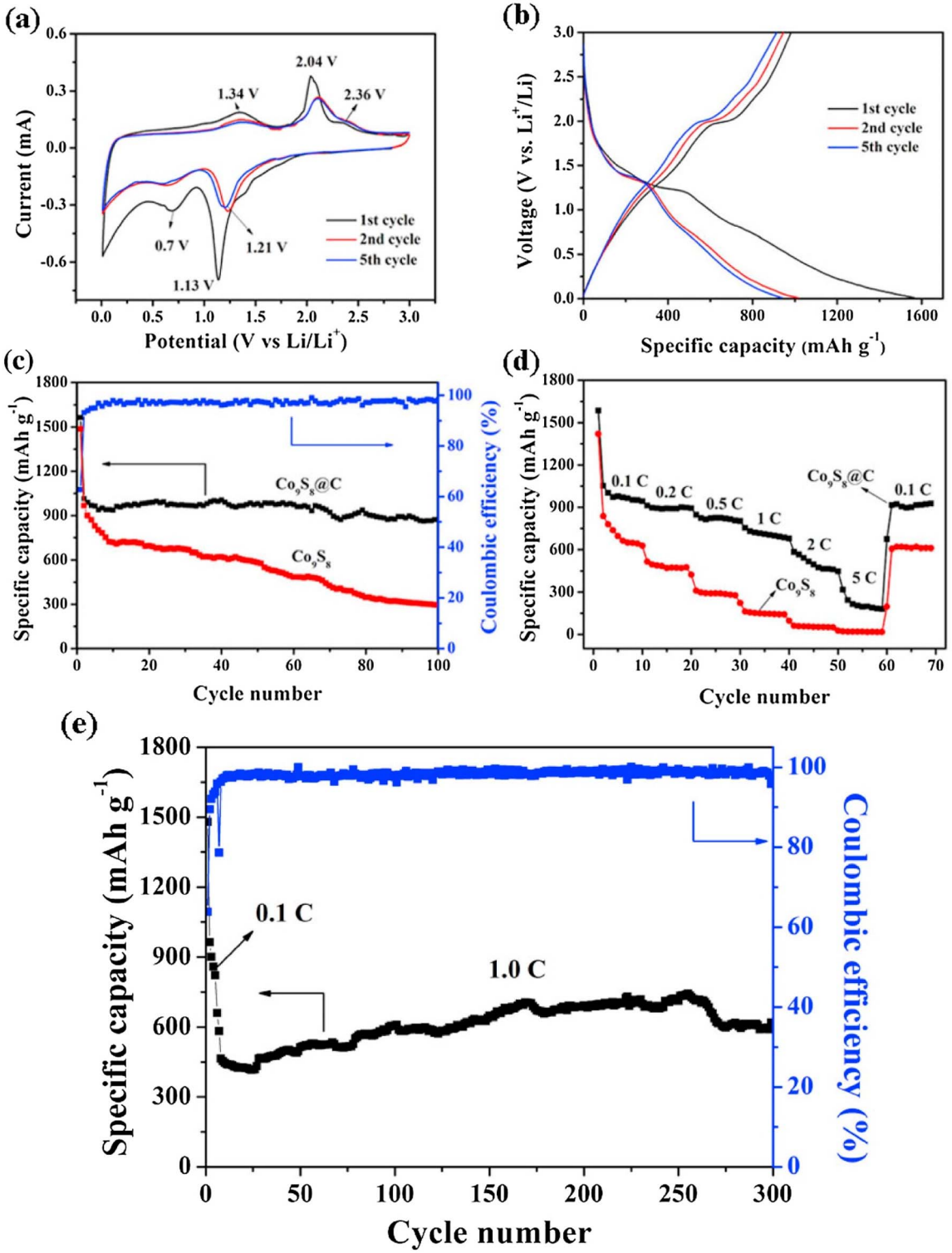

Fig. 9 (a) Cyclic voltammetric curves of Co_9S_8@C nanocomposite obtained at 0.1 mV s^{-1} within *V* of 0.01 and 3 V. At 0.1C (b) charge/discharge curves for Co_9S_8@C nanocomposite at different cycles and (c) cycling performance along with the coulombic efficiency of Co_9S_8@C in comparison to pristine Co_9S_8. (d) Comparison of Co_9S_8@C nanocomposite electrode rate performance at different current densities with reference to pure Co_9S_8. (e) The measured cycling performance and associated coulombic efficiency of the Co_9S_8@C nanocomposite. This figure has been adapted from ref. 230 with permission from Elsevier, copyright 2016.

abundant active sites and efficiently handling mechanical stress during the cycling of Li-ion batteries. To enhance the electrochemical characteristics of carbon materials, heteroatoms were introduced into their structures. Fang *et al.* synthesized Co_9S_8 nanoparticles incorporated within nitrogen-rich hollow carbon shells and demonstrated outstanding lithium storage

capabilities at elevated charge/discharge rates. The outstanding battery performance resulted from the hollow structures combined with the nitrogen-rich carbon encapsulation.[233]

A notable capacity recovery occurred during this cycling process, linked to increased capacitance achieved through successive electro-chemical milling. The formation of a carbon shell on the hollow nanospheres improved the reversible capacities at higher rates, achieving approximately 896 mA h g^{-1} up to 800 cycles at 2 A g^{-1}. The outstanding Li-ion storage capabilities highlighted the significant potential of sulfides as anodes with high capacity, rapid charge rates, and extended lifespan.[234] The CNTs incorporated TMSs show potential for use as anode materials for LIBs. However, their mechanisms and electrochemical performance are not yet fully understood. Developing high-performance materials from these composites requires an in-depth knowledge of their mechanism at the nanoscale. Wang *et al.* synthesized CoS/CNTs nanocomposites using a solvothermal method and probed their potential as an anode material for LIBs. The findings indicated that the material demonstrated robust cyclic stability and maintained a discharge rate of 780 mA h g^{-1} following 50 cycles at 100 mA g^{-1}. The outstanding electrochemical performance was attributed to the effective integration of the hybrid structure and enhanced electron transport facilitated by CNTs. The CoS/CNTs nanocomposites exhibited remarkable rate capabilities and superior performance, positioning them as effective anode materials for LIBs.[235] Tan *et al.* developed CoS NFs–rGO electrodes, which demonstrated a discharge capacity of 939 mA h g^{-1} after the 100th cycle at a current rate of 100 mA g^{-1}, while sustaining a coulombic efficiency greater than 98%.[236]

The self-assembled interweaving CoS_2/CNTs/graphene (CCG) was synthesized through the hydrothermal method. The architecture of CCG employed 1D CNTs and 2D graphene nanosheets to establish a conductive and porous network that mitigated the CoS_2 aggregation. CCG functioned as the anode material for lithium-ion batteries, exhibiting superior performance relative to uncoated CoS_2. It attained an initial discharge capacity of 993 mA h g^{-1} at a current rate of 100 mA g^{-1}, along with a rated capacity of 212 mA h g^{-1} at 200 mA g^{-1}.[237] A novel nanocomposite with durable hollow frameworks made of N-doped CNTs and highly active CoS_2 nanoparticles enhanced Li storage capacity as a LIB anode. The material had a capacitance of 937 mA h g^{-1} at 1 A g^{-1} and a cycle life of over 160 cycles.[238] CoS_2 nanoparticles, self-assembled and wrapped by CoS_2 QDs anchored onto graphene nanosheets, were synthesized through hydrothermal reaction. The composite demonstrated exceptional electrochemical performance. It has 1048 mA h g^{-1} reversible capacitance and 831 mA h g^{-1} capacity after 300 cycles at 1 A g^{-1} current density. The rated capacity reaches 411 mA h g^{-1} at a current density of 10 A g^{-1}, marking it as the highest among CoS_2-based materials under these elevated current density conditions. The exceptional performance was attributed to the distinctive structure featuring CoS_2 nanoparticles uniformly enveloped by graphene nanosheets rich in CoS_2 quantum dots.[239] A hierarchical structure of CoS_2/G was reported as an outstanding material for Li-ion batteries. The CoS_2/G electrode material showed a remarkable rate capability of around 398 mA h g^{-1} at a current density of 500 mA g^{-1}. The initial characterization of the material was achieved through X-ray absorption spectroscopy, revealing that CoS_2/G was transformed into metallic Co and LiS_2 upon discharge to 0.01 V.[240]

Guo *et al.*, employing the solvothermal technique, graphene nanosheets (GNs) were systematically arranged in layers around monodisperse CoS_2 nanocages. The adaptable GNs within the multilayer composite incorporate monodisperse CoS_2 nanocages, facilitated buffer volume changes, and prevented agglomeration throughout electrochemical cycling. Monodisperse nanocages exhibited resilience to volume fluctuations, facilitated a reduction in lithium diffusion, and maintained a non-agglomerated state. The sample exhibited an impressive capacity of 800 mA h g^{-1} after 150 cycles at a rate of 100 mA g^{-1}, and a capacity of 697 mA h g^{-1} following 300 cycles at 500 mA g^{-1}, alongside commendable capacity retention and outstanding rate capability, making it a promising candidate for use as an anode in Li-ion batteries.[241] Similarly, the CoS_2/rGO nanocomposite also functions as a highly efficient anode material for LIBs. It demonstrates high efficiency with a reversible capacity retention of 640 mA h g^{-1} after 50 cycles at 100 mA g^{-1}.[242] A successful alcoholysis approach was used to synthesize hollow CoS_2@C nanosheet aggregates for LIB anodes. The sample had a good rate capacity and consistent capacity of 720 mA h g^{-1} following 200 cycles. The aggregates' nano-scaled CoS_2 nanosheets ensured the electrode's high capacity and quick Li-ion diffusion.[243] Wang and co-workers synthesized ultra-small CoS_2 NPs in N-rich carbon, demonstrating encouraging Li-ion storage capabilities with minimal capacity loss at elevated charge/discharge rates. When the current density increased to 2500 mA g^{-1}, a reversible capacity of 410 mA h g^{-1} was attained. The remarkable and consistent performance was credited to the synergistic interaction between the NPs and N-rich carbon shells.[244] Similar hollow spheres with a different synthesis method were reported by Zhang *et al.*[238]

3.6.3 Mo-based sulfides. Molybdenum disulfide (MoS_2) possesses a layered architecture, with a plane of molybdenum atoms interposed between layers of sulfide ions. The bulk MoS_2 comprises stacked monolayers interconnected by weak van der Waals forces. Due to the facile intercalation and extraction of Li^+ ions from these layered structures, it has been widely investigated as an electrode material for LIBs.[245] Lou and his co-workers synthesized Mo-glycerate solid spheres and transformed them into hierarchical MoS_2 nanospheres *via* sulfidation. Due to their hollow interior and distinctive ultrathin subunits, the synthesized MoS_2 hollow nanospheres demonstrated remarkable efficiency as an anode material for LIBs. MoS_2 exhibited a noteworthy capacity of around 1100 mA h g^{-1} at a current density of 0.5 A g^{-1}, demonstrating excellent rate retention and extended cycle life.[246]

MoS_2 has drawn the attention of researchers in the domain of electrochemical energy storage. Yu *et al.* synthesized N-doped carbon shells, incorporated them in MoS_2 nanosheets, and referred to them as C@MoS_2 nanoboxes. Adding N-doped carbon shells increased the hybrid structure's conductivity and prevented MoS_2 nanosheet aggregation. Ultrathin MoS_2

nanosheets increase electrochemical reaction active sites. As an anode material for LIBs, these C@MoS_2 nanoboxes showed a capacitance of 1000 mA h g^{-1}, excellent cyclic stability for up to 200 cycles, and good rate performance.[247] Recent studies indicated that, alongside the atomic composition and arrangement, the dimensions significantly influence the properties and performances of specific materials. Recently, a significant focus has been on the extensive study of 2D graphene. The graphene displays distinctive characteristics not found in bulk graphite, including mechanical strength and optical properties. The 2D TM dichalcogenides, characterized by their layered structure akin to graphene, have garnered considerable interest. Research on 2D monolayer or few-layer MoS_2 has been undertaken for energy-related applications due to its unique properties and layered architecture, which include batteries, fuel cells, and photoelectrochemical systems.[248]

3.6.4 Fe-based sulphides as anodes in LIBs. Iron sulfides have attracted considerable attention for use in LIBs. Pyrite possesses several advantages, including a high theoretical energy density of approximately 1313 W h kg^{-1}, commendable thermal stability, affordability, natural abundance, and non-toxic properties. In contrast to other metal sulfides, pyrite has been utilized effectively in Li–FeS_2 batteries for an extended period. Furthermore, the potential for developing commercial

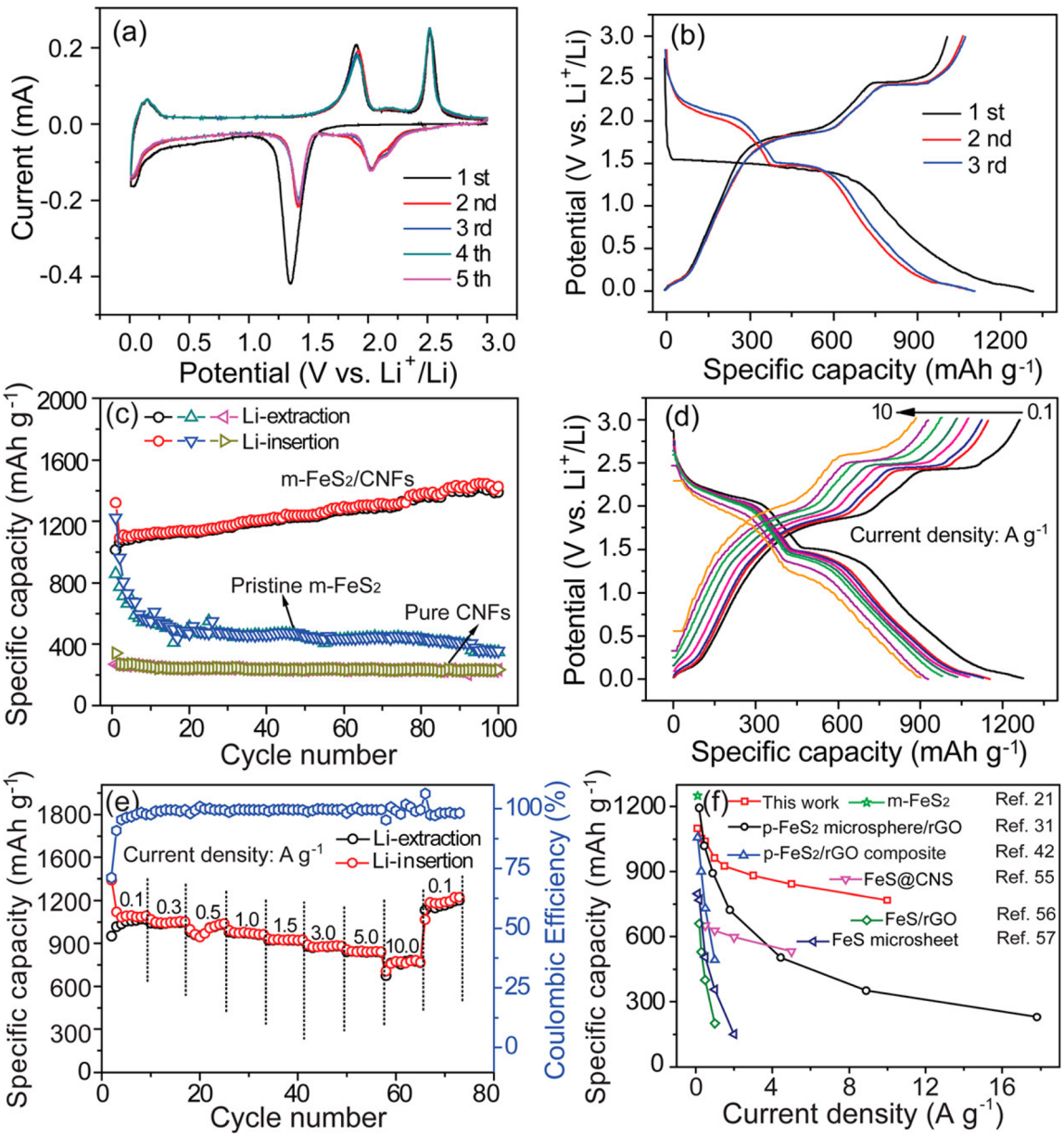

Fig. 10 (a) CV curves of m-FeS_2/CNFs at 0.1 mV s^{-1}. (b) The discharge/charge curves for m-FeS_2/CNFs at 0.1 A g^{-1}. (c) Comparison of the cycling performance of pure m-FeS_2, pure CNFs, and m-FeS_2/CNFs composite at 0.1 A g^{-1}. (d and e) Rate capabilities of m-FeS_2/CNFs composite anode material at different current densities within a voltage range of 0.01–3 V. (f) The specific capacities comparison of the m-FeS_2/CNFs composite electrode with FeS electrodes reported in the literature for lithium-ion batteries. This figure has been adapted from ref. 251 with permission from the American Chemical Society, copyright 2017.

FeS_2-based LIBs appears more promising than alternative metal sulfides.[249,250] Marcasite-FeS_2 exhibited stronger bond Fe–S bonds and reduced S–S interactions; it is likely to be a more effective electrode material than pyrite-FeS_2. Fan *et al.* developed a hierarchical composite of m-FeS_2 and carbon nanofibers (m-FeS_2/CNFs) featuring a grape-cluster architecture through hydrothermal synthesis, showcasing exceptional performance as an electrode material for lithium-ion batteries. It achieved a reversible capacity of 1399.5 mA h g^{-1} following 100 cycles at 100 mA g^{-1} at 10 A g (Fig. 10). The hierarchical m-FeS_2 microspheres, constructed from small FeS_2 nanoparticles within the m-FeS_2/CNF composite, transformed into a mimosa with open leaves during Li^+ insertion and reverted upon removal.[251]

Lee and co-workers synthesized FeS_2/rGO using a solvothermal process demonstrating remarkable performance, particularly under high current densities. Impedance measurements indicated that functionalizing FeS_2 with rGO markedly reduces the charge transfer resistance and enhances its structural stability. The as-synthesized material demonstrated a capacity of 970 mA h g^{-1} at a current rate of 890 mA g^{-1} following 300 cycles. LIB showed a capacity of 380 mA h g^{-1} at exceptionally high current density of 8900 mA g^{-1} after undergoing 2000 cycles.[252] FeS_2 nanocrystals were synthesized within carbon capsules by Xu *et al.* within pre-pared hierarchical porous carbon. The high-performance composite, featuring micro-porous shells and interconnected macro-porous carbon capsules, demonstrated exceptional ionic and electrical conductivities and a practical buffering effect on the volume changes of FeS_2. FeS_2@HPC demonstrated a notable C_s of 907 mA h g^{-1} during the initial cycle thereby maintaining a capacity of 720 mA h g^{-1} following 100 cycles at a rate of 1C.[253]

3.6.5 Other transition metal-based sulphides in LIBs. 1D nanostructures exhibit distinct properties that render them advantageous for utilization as active materials for LIBs. Initially, the 1D structure facilitates adapts to volume changes associated with lithium charge/discharge cycles in a specific direction. Additionally, the gaps between the adjacent structures can serve as channels for electrolytes, facilitating their diffusion into the electrode, thus extending the lifespan of batteries. Furthermore, the 1D nanostructure arrays offer large surface-to-volume ratio when compared with bulk materials and enhance the availability of active sites and facilitate fast diffusion of Li^+ ions.[254] In addition to previously discussed materials, other TM sulphides, particularly 2D materials like TiS_2, WS_2, and VS_2, are being considered as favourable anodes for LIBs. TiS_2 is recognized for its exceptional electronic and ionic conductivity, that makes it ideal for energy applications. Leveraging the rapid Li^+ diffusion rates, TiS_2 is primarily investigated for its applications in high-power batteries.[255] For the successful implementation of solid-state LIBs in future EVs, it is crucial to fabricate electrodes that are stable and deliver high energy density and power outputs. To tackle these problems, Sun *et al.* reported that TiS_2 anode in the "Water in salt" electrolyte has high electrochemical reversibility. The electrochemical reversibility of TiS_2 was much improved, and the hydrolysis side reaction was effectively controlled in the aqueous electrolyte by using the "Water in salt" electrolyte. Combined with a $LiMn_2O_4$ cathode, the $LiMn_2O_4$/TiS_2 fuel cell exhibited a notable energy density of 78 W h kg^{-1} at 1.7 V and commendable performance.[256] WS_2 is a layered TM dichalcogenide stacked in 2D. The material exhibited an identical crystal structure to MoS_2, characterized by S–W–S layers held together by van der Waals interactions, and is highly favoured for Li^+ ion intercalation, signifying its potential use in energy storage devices. The semiconducting characteristics of WS_2, combined with the insulating properties of discharge products Li_2S, result in sluggish kinetics. Consequently, numerous initiatives have been undertaken to enhance electric conductivity.[257]

Liu *et al.* reported WS_2 nanoflowers@rGO in which rGO served as a cross-link, thereby enabling a 3D conductive network while also safeguarding from the effects of volume changes in WS_2 that occur during charge discharges cycles. The distinctive configuration of the nano-composite facilitated improved ion and electron diffusion while simultaneously bolstering electrode stability, resulting in a high-capacity anode for LIBs. The WS_2–NF@rGO achieved a C_s of 730 mA h g^{-1} following 150 cycles at 100 mA g^{-1} current density while sustaining a capacity exceeding 260 mA h g^{-1} at 2 A g^{-1}.[258] A WS_2 nanosheet@ carbon fibre cloth (CFC) composite have shown promise for developing advanced flexible anodes in LIBs. The presence of a metallic phase in WS_2 allowed the 1T@2H WS_2@CFC electrode to achieve a specific capacity of 1130 mA h g^{-1} after 200 cycles at a current density of 0.1 A g^{-1}, along with an impressive rate capability of 510 mA h g^{-1} after 800 cycles at 2 A g^{-1}, while experiencing a minimal initial discharge capacity loss of 12.64%. Furthermore, the integrated capacitive charge storage within the 1T@2H WS_2@CFC electrode was examined, revealing its advantages for rapid charge storage and sustained cyclability over extended periods.[259]

The multi-layered nanostructured WS_2, combined with enhanced electronic conductivity and volume accommodating effect of CMK-3, resulted in a material that exhibited optimal discharge capacity, enhanced rate capability, and improved cyclability when compared with pristine WS_2. The material exhibited a capacitance of 720 mA h g^{-1} over 100 cycles when tested for LIBs at a current density of 100 mA g^{-1}. This remarkable performance highlighted the immense potential of the WS_2@CMK-3 nanocomposite.[260] The successful integration of graphene sheets with CNF remains an elusive goal. To address this, Fan and co-workers presented a novel and straightforward method for preparing flexible graphene CNF (GCNF) membranes, wrapping the CNF with conductive graphene sheets, significantly enhancing electrical conductivity. Carbonization of the resulting hybrid membranes made of GO and electro-spun polyacrylonitrile (oPAN) NFs was the only demanding step in that approach. Hierarchical WS_2/GCNF hybrid membranes were fabricated using a highly conductive GCNF membrane as a template, featuring multi-layered WS_2 nanosheets grown uniformly onto a NFs, serving as efficient anode for LIBs. The WS_2/GCNF nanocomposite membrane exhibited a large specific surface area, extensive porous structure, notable electrical conductivity, and robust material strength. These characteristics facilitated rapid Li^+ diffusion, efficient electron transfer, and enhanced stability. The

optimized WS_2/GNF composite membrane demonstrated an initial charge capacity of 1128.2 mA h g^{-1} at a current rate of 0.1 A g^{-1}, along with notable cyclic stability, and marinating 95% of its capacity after 100 charge/discharge cycles.[261]

A simple solvothermal approach, followed by freeze-drying and then post-annealing, was used to synthesize a hybrid nanoarchitecture aerogel with a 3D scaffold structure made out of organized microchannels and CNTs–reduced graphene oxide (rGO). The 3D-ordered microchannel structures facilitated effective electronic transport and offered superior ionic conductive pathways, improving the performance of the material. The WS_2/CNT–rGO aerogel nanostructure achieved a C_s of 749 mA h g^{-1} at a current density of 100 mA g^{-1}, and a coulombic efficiency of 53.4% in the first cycle.[262] An intercalation-transformation approach was used to successfully synthesize a multilayer-cake WS_2/C nanocomposite. This process involved sandwiching a few layers of WS_2 and carbon in an alternating sequence, which demonstrated promising performance, due to enhanced chare transport properties of the interlayer carbon and its distinctive "regular" and "alternate" architecture. The nanocomposite exhibited an impressive capacity of 829.4 mA h g^{-1} at a current rate of 0.3 A g^{-1} following 140 cycles, maintaining a stable capacity of approximately 326.8 mA h g^{-1} even at a higher current density of 8.0 A g^{-1}.[263]

Fang *et al.* presented a straightforward one-pot method for synthesizing hierarchical VS_2/graphene nanosheets (VS_2/GNS) composites. The composite's structure featured 50 nm thick VS_2 sheets uniformly distributed onto graphene whereby the composite demonstrated optimal rate capability and cyclability, maintaining 181.1 mA h g^{-1} even after 200 cycles at 0.2C. Comprehensive investigations indicated that VS_2/GNS nanocomposite demonstrated commendable reversible performance, delivering a C_s of 528 mA h g^{-1} following 100 cycles at 200 mA g^{-1}. The electrochemical performance of the composite serving as an anode is ascribed to the synergistic effect between VS_2 and GNS, which facilitates rapid electron transport between the two, as well as supports facile diffusion of Li-ions within the electrode structure. Furthermore, GNS offered a structural framework that supported the growth of 2D VS_2 nanosheets, that results in alleviating the effects of volume changes, thereby enhancing cyclic stability. These composites showed potential as electrode materials for the upcoming generations of rechargeable batteries.[264]

VS_4 showed promise as an anode material due to its distinct chain-like structure, elevated levels of sulfur, and unique electrochemical behaviour. Here, amorphous carbon coated with MWCNTs served as the basis for the VS_4 nanoparticles generated *via* a solvothermal process. The unique structure allows modified CNTs to improve charge transportation within the composite and externally, a feat that was challenging to accomplish with alternative structures. The composite outperformed the numerous TM sulfides in terms of cyclic stability and rate capability owing to these enhancements in charge transfer. The reversible capacity achieved was 922 mA h g^{-1} following 100 cycles at a rate of 0.5 A g^{-1}. A 1000 cycle at 2 or 5 A g^{-1} didn't affect the 576 or 401 mA h g^{-1} capacity (Fig. 11).[265]

Jang *et al.* introduced a colloidal method for synthesizing ultrathin ZrS_2 nanodiscs, which were approximately 1.6 nm thick and comprised of two S–Zr–S unit cells. The S–Zr–S layers within individual discs were connected through weak van der Waal forces, allowing each UT-ZrS_2 disc to create spaces serving as host sites for Li-ion intercalation. The UT-ZrS_2, due to its nanosized particles, resulted in a 230% increase in discharge capacity and significant enhancement in stability compared to its bulk counterpart. The impact of nanosized UT-ZrS_2 was particularly substantial during charge/discharge cycles, with an observed average recovery of 88% in reversible capacity for UT-ZrS_2 discs with a width of 20 nm.[266]

Osaka and co-workers synthesized SnS_2 nanoparticles, which achieved a 620 mA h g^{-1} of discharge capacity and reduced degradation of the electrode. The findings suggested that increasing the surface area enhanced Li-ion intercalation–deintercalation within the active material while at the same time reducing the stress during the cycles that improved the electrochemical pathways and, thus, electrode kinetics.[267] Liu *et al.* proposed a flowerlike SnS_2 structure synthesized *via* a solvothermal process. The investigation focused on the impact of synthetic parameters, such as the choice of electrolyte and thiourea concentration, on the morphology of the resulting products. The material demonstrated superior electrochemical properties. The flower-like SnS_2 structures achieved a higher reversible capacity of approximately 502 mA h g^{-1} and exhibited more stable cyclic retention by the 50th cycle compared to SnS_2 nanoplates.[268] 3D SnS_2 microspheres were produced using the facile hydrothermal method and used as an anode material. These SnS_2 microspheres, formed through the self-assembly of layered nanosheets, demonstrated boosted Li^+ storage capacity with a stable cycle life and retained an optimal discharge capacity following 100 charge/discharge cycles. Their exceptional performance was attributed to the distinctive 3D hierarchical architectures of these SnS_2 microspheres.[269] Hollow microspheres of SnS_2 and 3D nanoflakes-based SnS_2 hollow microspheres were hydrothermally synthesized and exhibited improved performance as an anode material.[270] A gram-scale and template-free solvothermal route was used to synthesize ultra-long SnS_2 nanobelts with a production yield of up to approximately 98%. The SnS_2 nanobelts thus produced outperformed the graphite anode when its C_s (640 mA h g^{-1}) and cyclic stability were compared, which was 560 mA h g^{-1} after 50 cycles.[271]

Crystalline SnS_2 nanosheets were made *via* a one-step solvothermal method and integrated into negative electrodes for LIBs. Compounds of SnS_2 synthesized in ethylene glycol displayed a nanosheet morphology with an approximate thickness of 2 nm and demonstrated remarkable capacity retention of around 95% following 50 cycles at 0.5C.[272] Zhai *et al.* synthesized ultra-thin hexagonal SnS_2 nanosheets through a straightforward hydrothermal reaction, demonstrating a reasonably enhanced reversible capacity with an optimal cyclic stability, achieving an impressive capacity retention of 96% following 50 cycles.[273] Liu *et al.* used a straightforward chemical bath deposition method to fabricate SnS_2 nanowall (NW) arrays onto the copper foils. The NW arrays demonstrated enhanced Li ion

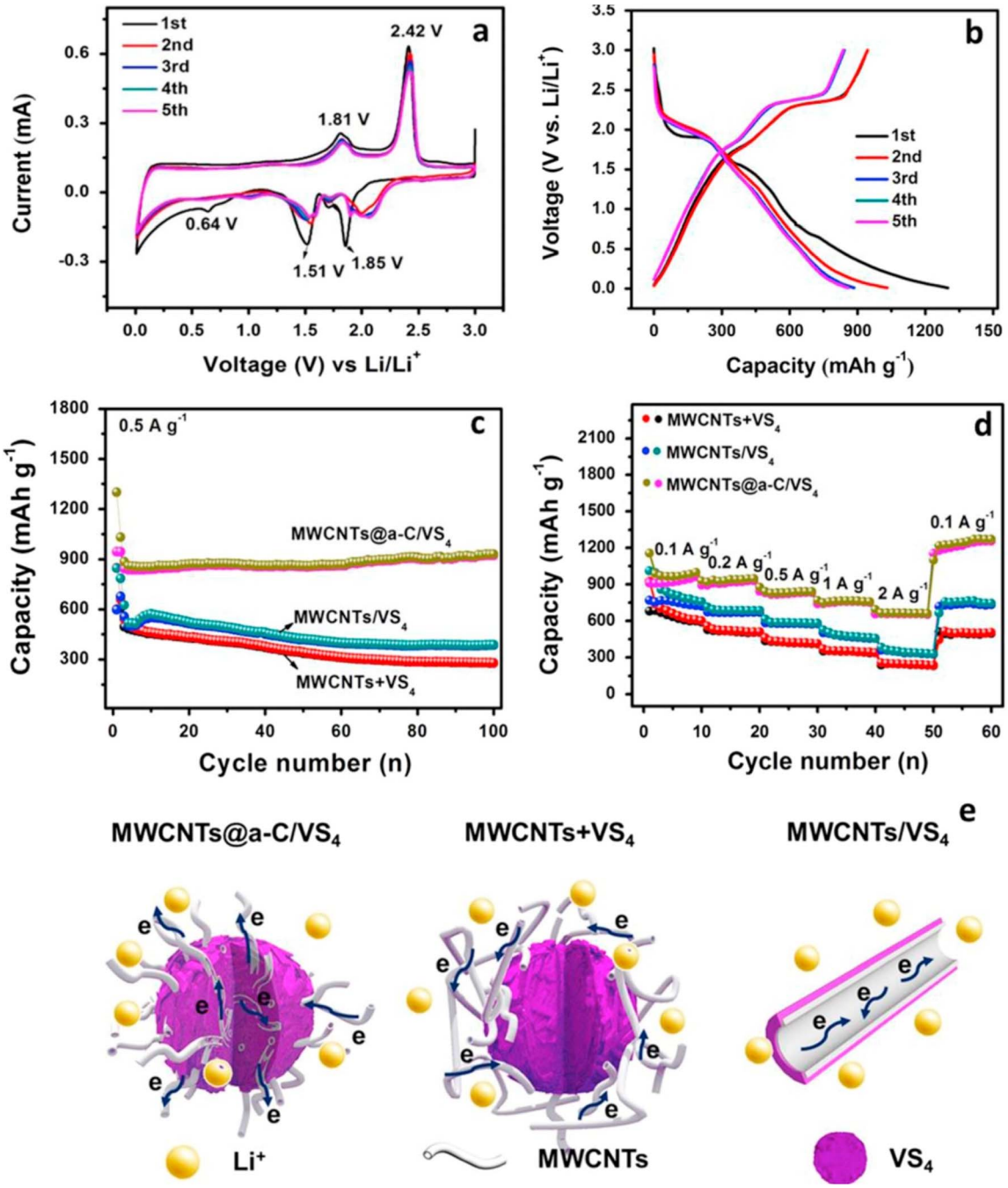

Fig. 11 (a) Cyclic voltammograms (b) discharge/charge profiles of MWCNTs@a-C/VS_4 (c) cycling stability at a current density of 0.5 A g^{-1} (d) rate capability comparison among MWCNTs@a-C/VS_4, MWCNTs + VS_4, and MWCNTs/VS_4 (e) schematic diagram depicting the electron and charge transfer mechanisms for the three composite types (MWCNTs@a-C/VS_4, MWCNTs + VS_4 and MWCNTs/VS_4). This figure has been adapted from ref. 265 with permission from Elsevier, copyright 2017.

storage capacities when employed as an anode material. At 0.3C, the NW arrays delivered a C_s of 700 mA h g^{-1} following 40 cycles and maintained a steady 400 mA h g^{-1} capacity as it is subjected to a high rate of 1.2C.[274] Similarly, Zhong *et al.* was successful in synthesizing layered SnS_2 nanosheets directly onto the Sn foil with improved electrochemical performance for LIBs.[275] Other than nanosheets, NPs of tin sulfides (SnS and SnS_2) were also synthesized hydrothermally and resulted in superior electrochemical performance and long cyclic life. However, their discharge capacities still need to be improved.[276] Du *et al.* proposed commercial scale synthesis of 2D SnS_2 nanoplates, which resulted in notable electrochemical behaviour and capacity retention following 30 cycles.[277]

MWCNTs and carbon in metallic nanocomposites can significantly enhance the electrochemical properties. Carbon-coated SnS_2 NPs were synthesized by Kim *et al.*[278] *via*

Table 5 Transition metal sulfides-based anode materials for LIBs

Anode material	Method of preparation	Structure	Reversible capacity (mA h g^{-1})	Cycle number	Coulombic efficiency (%)	Ref.
rGO@NiS composites	Solvothermal synthesis	Particles uniformly distributed in 3D network	1328.7	120	69.1	282
$NiTi_2S_4$ ternary sulfide	High energy mechanical milling	Nanoparticles with monoclinic crystal structure	635	50	89	283
α/γ-MnS embedded in N-doped layered carbon	One-step annealing process	Nanosheets	1042	1000	67.6	284
Nickel cobalt manganese sulfide/C composite	Gas sulfidation process	Metal sulfides embedded in C matrix	900.4	200	70.1	285
Ni_3S_2/Ni@VCMN	Plasma-assisted chemical vapour deposition	Polycrystalline Ni_3S_2 nanostructures capping Ni nanoparticles forming a "broccoli like" morphology	1113	100	92.8	286
$Ni_3S_2/Ti_3C_2T_x$/C	One-step solvothermal reaction	Nanoparticles supported on sheets	1150.8	400	58.9	287
Ni_3S_2@PPy	One-step reflux method	Nanoparticles grown on foam	396.5	100	84.6	288
Nanostructured polycrystalline Ni_3S_2	Powder vapour transport technique	Flower shaped nanostructures	931	30	98–99	289
Ni-doped Ni_3S_2 nanoflakes intertexture grown on GO	Two step solvothermal reaction	Nanoflakes	741.8	120	94.77	290
$Ni_3S_2/NiSe_2$ hollow spheres	*In situ* gas phase selenization method	Hollow spheres	709	200	Good coulombic efficiency	291
Ni_3S_2@Ni foam	Facile hydrothermal method	3-D porous structure		400	98.3	292
Petal-like Ni_3S_2 nanosheets on 3D carbon nanotube foams	One-pot solvothermal method	Petal-like nanosheets on 3D nanotube foams	968.2	900	40.3	293
Ni_3S_2 functionalized V_2O_3 nanospheres	One-step solvothermal method	Nanocrystals with nanospheres	550	100	Good coulombic efficiency	294
$Ni_9S_8/Ni_3S_2/NiS_{1.03}$ particles with homogenous bonds to 3D rGO sheets	Facile hydrothermal method followed by freeze drying and calcination	Particles supported on sheets	826.3	1000	100	295
VS_2/rGO composites	Solvothermal method	Honey comb like structure	737	150	80.57	296
VS_2 nanosheets/graphene composites	Solvothermal method	Monodispersed porous bowl shaped nanosheets	889	500	≈60	297
3D VS_2/rGO heterostructure	*In situ* assembly of nanosheets	Heterostructure	644.02	140	Good coulombic efficiency	298
Hierarchical composite of VS_2/CNTs/C	Solvothermal method	3D hierarchical structure	1075	900	~40	299
VS_2@C/TiO_2	Electrospinning carbonization followed by hydrothermal method	Branch leaf structure	324.2	200	~100	300
Vertically aligned VS_2 on graphene	Scalable solvothermal and post annealing process	3D heterostructure	989	1000	64	301
Vanadium sulfide decorated at C network	Slurry-coating method	3D porous conductive network	188	2500	~40	302
CoS_2–MnS@C	Thermal decomposition or pyrolysis	Nanoparticles on C matrix	814	100	55	303

Table 5 (*Contd.*)

Anode material	Method of preparation	Structure	Reversible capacity (mA h g^{-1})	Cycle number	Coulombic efficiency (%)	Ref.
CoS_2–MnS@rGO	Thermal decomposition or pyrolysis	Nanoparticles on rGO matrix	1324	100	58	303
CoS_2–MnS@CNTs	Thermal decomposition or pyrolysis	Nanoparticles on CNTs matrix	1017	100	55	303
α-MnS nanoparticles anchored on holey graphene	*Ex situ* strategy	Nanoparticles anchored on holey graphene sheets	870.5	200	66	304
MnS–MoS_2 heterostructure	One-step solvothermal method	Particles embedded on matrix	1246.2	500	40–50	305
α-MnS@axial multichannel carbon nanofibers	Electro bowling spinning technique	Nanoparticles embedded in axial multichannel nanofibers	772	200	72.9	306
Mn_2SnS_4@ZnS@Nitrogen doped carbon	Dual modification method	Nanocubes coated with ZnS and encapsulated in NC shell	1508.6	500	77.8	307
Mn–Sn bimetallic sulfides doped C nanorods	Simple solvothermal method	Heterostructures	719.6	1000	70.9	308
Hierarchical MoS_2@αMnS nanocomposites	One-pot hydrothermal method	Nanosheets wrapped by nanoparticles forming a rose like morphology	1498	120	78.1	309

a solvothermal process, resulting in a significant electrochemical response. Huang and co-workers successfully synthesized Porous 3D SnS_2 nanoflowers incorporating acetylene black by using a facile solvothermal route aided by PEG. The material displayed a boosted cyclic stability and rate capability, achieving an average reversible capacity of up to 525 mA h g^{-1} at a high current rate over 70 cycles. The electrochemical performance results dues to the synergistic effect of acetylene black and the distinctive structure of SnS_2. Acetylene black enhanced the electron transfer and stabilized the electrode structure by mitigating the impact of volume changes. In addition to that, the porous architecture of SnS_2 contributed to stabilizing the electrode structure and enhanced the shuttling of Li^+ ions.[279] Kang *et al.* focused on 3D MWCNTs/SnS_2 heterostructured electrodes, which exhibited remarkable rate capabilities at high rates. The significance of MWCNTs was extensively examined to trace the roots of the improved rate capabilities.[280] Graphene nanocomposites loaded with SnS_2 NPs were synthesized hydrothermally. The electrochemical characterizations indicated a significant reversible capacity exceeding 800 mA h g^{-1} at 0.1C and maintained 200 mA h g^{-1} at a 5C rate.[281] Ji *et al.* concluded that graphene–SnS_2 nanocomposites demonstrated superior performance in LIBs as anode materials. Some of the recent transition metal sulfide-based anode materials for LIBs are listed in Table 5.[281]

3.7 Soft and hard-carbon anodes

Hard carbon (HC) is attracting interest as a potential anode material for next-generation LIBs because of its distinctive microstructure and improved electrochemical properties. In contrast to graphite, hard carbon exhibits a non-graphitizable nature characterized by a disordered structure. This structure encompasses defects, micropores, and expanded interlayer spacing, all of which enhance lithium-ion storage capacity and facilitate quicker ion diffusion. Nonetheless, obstacles such as low initial coulombic efficiency (ICE), significant irreversible capacity, and voltage hysteresis hinder its potential for commercial application.[310] Curved, randomly orientated graphitic sheets with short-range order but no long-range order make up hard carbon. Li^+ intercalation is facilitated by the increased interlayer gap (0.37–0.42 nm), and more Li^+ storage sites are provided by the defects and functional groups of the structure. Hard carbon can outperform graphite in terms of low-temperature performance (down to −50 °C) and larger capacity (up to 1000 mA h g^{-1}), all while minimizing electrode expansion during cycling, which enhances safety. However, irreversible Li^+ consumption during SEI generation and pore trapping is the reason for its low ICE (≤80%). Remaining hydrogen-terminated aromatic fragments that bind Li^+ ions cause voltage hysteresis.[311]

Hard carbons utilize three primary mechanisms for Li^+ storage: the filling of nanopores, adsorption at defect sites and functional groups, and intercalation within graphitic nanodomains. These mechanisms are supported by Raman, XRD, and SAXS, providing evidence for Li^+ absorption in nanopores and the reversible structural changes that occur during this

process. Hard carbons are classified according to their predecessors, which include compounds generated from biomass, pitch, and resin. High purity and adjustable porosity are features of resin-based carbons, which have capacities of up to 1294 mA h g^{-1}. Pitch-based carbons, which are derived from petroleum pitch or pre-oxidized coal tar, normally have capacities of about 829 mA h g^{-1}. With their high carbon yield and heteroatom doping, biomass-derived carbons—such as those found in cellulose, lignin, and starch—offer sustainable alternatives.[312,313] Heteroatom doping (such as nitrogen, phosphorus, and sulphur) is one optimization technique for hard carbons that enhances capacity and interlayer spacing. Graphitization is avoided by pre-oxidizing precursors, and pore engineering guarantees closed pores for Li^+ storage that do not allow electrolyte penetration. Prelithiation makes up for the early loss of Li^+, and controlled pyrolysis temperatures balance porosity and crystallinity. By mixing hard and soft carbon, hybrid designs seek to increase capacity and ICE.[314]

Future studies should concentrate on using sophisticated characterization techniques (*e.g.*, TEM, NMR) to understand Li^+ storage dynamics, optimizing precursor materials for fine microstructure control, and investigating hybrid designs with metal oxides for better volumetric energy density. The best heteroatom configurations can be predicted with the use of computational modelling. Reducing manufacturing costs by using biomass and resolving challenges with consistency and purity will be crucial for industrial scaling. Hard carbons can also be used in rapid-charging applications for grid storage systems and electric vehicles by increasing low-voltage capacity and utilizing fast Li^+ diffusion. Conclusively, hard carbon may prove to be a more effective anode material than graphite for high-energy, rapid-charging LIBs. Although there are still obstacles to overcome, improvements in pore design, doping, and precursor selection may enable it to reach its maximum potential and become an essential part of energy storage systems of the future.[315]

Soft carbon, a form of carbon material with a somewhat organized structure, can change into graphite when heated to high temperatures, usually above 2500 °C. Soft carbon is better suited for various energy storage applications compared to hard carbon due to its ability to allow for varying levels of graphitization. Its disordered structure and capacity to adjust the degree of graphitization render it ideal for use in sodium-ion and potassium-ion batteries, enhancing its effectiveness in energy storage solutions.[316] A key feature of soft carbon is its controllable graphitization, which enhances electronic conductivity while potentially reducing interlayer spacing and influencing ion diffusion. With a broader interlayer spacing than graphite, soft carbon allows for more rapid intercalation and deintercalation of lithium ions. Additionally, by manipulating the material's shape to create nanostructures, its stability and surface area can be improved. The incorporation of defects and heteroatom doping, such as nitrogen or sulfur, further enhances the Li^+ storage capacity by generating more active sites.[317]

Soft carbon can store lithium through two main processes: adsorption and intercalation. Li^+ ions adsorb onto defect sites and heteroatoms, adding to the capacity and accelerating the kinetics. They also intercalate into the graphitic domains, a reversible process that could expand volume. In nanostructured or doped soft carbon, hybrid mechanisms that combine intercalation and adsorption are frequently seen. These mechanisms provide enhanced performance, including decreased diffusion barriers and metallic conductivity. For LIBs, soft carbon offers a number of benefits, such as superior rate capability because of faster Li^+ diffusion, structural stability that can adapt to volume variations during cycling, and customization through doping and graphitization changes. There are still issues, though, like permanent capacity loss in the early cycles, which can be lessened with pre-lithiation techniques. Its low-temperature performance and the high expense of accurate synthesis are further obstacles to its widespread application.[318] Future soft carbon research should focus on advanced characterization techniques to better understand its storage mechanisms and optimize synthesis procedures. Hybrid materials that combine high-capacity and soft carbon materials with specially designed electrolytes may improve its performance. In conclusion, soft carbon is a promising anode material for LIBs because of its special qualities. Additional developments in design and manufacturing may unlock its full potential for high-performance energy storage applications.

4. Future electrode materials

The development of lithium-ion batteries depends heavily on high-energy-density cathode materials. Lithium and manganese rich (LMR) materials ($(xLi_2MnO_3 \cdot (1-x)LiMO_2)$, where M = Ni, Co, Mn) and Ni-rich NCM/NCA (*e.g.*, NCM811) are among the high-voltage cathodes that are attracting interest. These materials are appealing for next-generation batteries because of their high energy density and capacity (more than 250 mA h g^{-1}). Voltage decay, structural instability, and electrolyte breakdown at high voltages are still major problems, though. Recent advancements have aimed to enhance these materials *via* doping and surface coatings, which aid in structural stabilization.

Sulfur cathodes offer a cost-effective solution with a remarkably high theoretical capacity of 1675 mA h g^{-1}. Despite these benefits, shuttle effect of polysulfides (Li_2S_n) results in a short cycle life. Strategies like employing interlayers, porous carbon hosts, and catalysts (such metal oxides) to speed up polysulfide conversion have been investigated in order to overcome this. Advanced electrolytes with localised high-concentration techniques are also being developed to enhance cycle stability and performance.[319] Oxygen (O_2) cathodes are lightweight and have the highest potential energy density (3500 W h kg^{-1}). Nevertheless, they encounter difficulties such electrolyte instability, adverse responses, and low reversibility. To improve the stability and performance of oxygen-based cathodes, recent studies have concentrated on protecting lithium anodes and creating stable catalysts like RuO_2.[320]

Silicon and lithium metal are particularly promising anode materials. Despite having a very high capacity of 3579 mA h g^{-1} for $Li_{15}Si_4$, silicon confronts many difficulties because of its

enormous volume expansion (more than 300%), which causes electrode pulverization. Nanostructuring (like Si nanoparticles or porous Si) and composite designs (like Si–graphite mixes) are being investigated as ways to get around this. Commercial applications of silicon already exist; for example, Tesla's "Silicon Oxide" anodes blend silicon with graphite to enhance performance.[321] The maximum theoretical capacity of 3860 mA h g^{-1} and the lowest potential of −3.04 V are provided by lithium metal. However, problems including endless volume change, unstable solid electrolyte interphase (SEI), and dendritic development make it difficult to employ. The creation of 3D porous carbon hosts for regulated deposition, synthetic SEI layers with polymer coatings, and solid-state electrolytes inhibiting dendritic growth are some ways to lessen these issues. For next-generation batteries like Li–S and Li–O_2, where its large capacity can greatly improve energy storage, lithium metal is especially promising.[322]

The future of high-energy-density batteries depends on resolving a number of important issues. Understanding material behaviour and enhancing performance will require multi-scale research that blends theoretical modelling (density functional theory and phase-field modelling) with experimental methods. With continuous efforts to create materials that can tolerate high current densities without degrading, fast-charging capabilities are another area of focus. Widespread adoption will also need finding economical ways to close the gap between lab-scale breakthroughs and industrial-scale production.[323,324]

5. Environmental impact of LIBs production and disposal

LIBs, which have emerged as a key component of contemporary technology, power electric vehicles and portable electronics. Although these batteries are essential for allowing clean energy solutions and lowering carbon emissions while in use, there is rising concern about the environmental impact of their manufacture, disposal, and recycling. To produce LIBs, raw materials including lithium, cobalt, nickel, and graphite must be extracted, which can significantly affect the environment. Soil erosion, water pollution, and habitat destruction are all consequences of mining these resources, especially in areas with lax environmental standards. For instance, lithium extraction in Chile's Atacama Desert uses much water, endangering nearby water sources. The Democratic Republic of the Congo is the primary mining location for cobalt, which is associated with both environmental degradation and human rights abuses. The manufacture of LIBs uses a lot of energy, greatly increasing their carbon footprint. Cathode manufacturing is one of the most carbon dioxide-intensive steps in the production process, particularly when materials like lithium cobalt oxide are utilized. High emissions of greenhouse gases are the result of this. Depending on the battery type and manufacturing process, the cumulative energy demand for LIB manufacturing is estimated to be between 316 MJ kW^{-1} h^{-1} and 2318 MJ kW^{-1} h^{-1}. Lithium hexafluorophosphate and ethylene carbonate are two solvents used in this production process that can emit toxic chemicals as they break down, further polluting the environment.[325,326]

Though LIBs offer significant environmental benefits, particularly when employed in electric vehicles powered by renewable energy, they also present certain negative effects. The overall environmental impact largely hinges on the energy source utilized for charging; however, the integration of LIBs in electric vehicles contributes to a reduction in emissions. The environmental benefit of LIBs is lessened in areas where coal or other fossil fuels are used extensively to generate electricity because coal power is a significant source of greenhouse gas emissions. Furthermore, there are possible health dangers associated with electromagnetic radiation (EMR) from LIB-powered gadgets such as computers and cell phones. Long-term EMR exposure has been connected to a number of health problems, such as heart disease, brain tumours, and sleep disorders. The extensive usage of LIB-powered devices underscores the necessity for continued research into potential health hazards linked with continuous exposure to EMR, even though these effects are still being studied.[327,328]

When LIBs approach the end of their life cycle, their impact on the environment becomes increasingly apparent. It is anticipated that the quantity of used LIBs will rise in tandem with the growing demand for portable devices and electric cars. An estimated 11.5 million tons of LIB trash will be produced worldwide by 2030. Because these batteries contain hazardous elements, including cobalt, nickel, and lithium, that can poison water supplies and seep into the soil, improper disposal poses serious environmental dangers. The hazardous elements in LIBs may be discharged into the environment if they are disposed of inappropriately, either by unlawful dumping or incineration. For instance, plants and soil creatures are poisoned by cobalt and lithium, which impacts soil health and biodiversity. Hydrofluoric acid (HF), a very hazardous chemical that can have serious adverse effects on the environment and human health, can be released when the electrolytes in LIBs break down. The hazardous chemicals released by wasted LIBs that are allowed to decompose in landfills have the potential to contaminate soil and groundwater, causing long-term environmental harm. When LIBs are improperly disposed of in open spaces, the batteries may catch fire, further releasing hazardous gases like HF and raising the possibility of air and soil contamination.[329]

A key strategy for mitigating the adverse environmental impacts of LIBs is their recycling. This process enables the recovery of essential metals such as cobalt, nickel, and lithium found in LIBs, thereby reducing the ecological costs associated with resource extraction. Additionally, recycling diminishes the need for energy-intensive and environmentally detrimental raw material mining. By incorporating recycled materials, the overall environmental footprint of manufacturing new batteries can be significantly reduced. Fig. 12 illustrates the environmental impacts associated with LIBs.

5.1 Recycling of LIBs

Recycling presents a sustainable approach to reclaim valuable materials, reduce reliance on new resources, and lessen

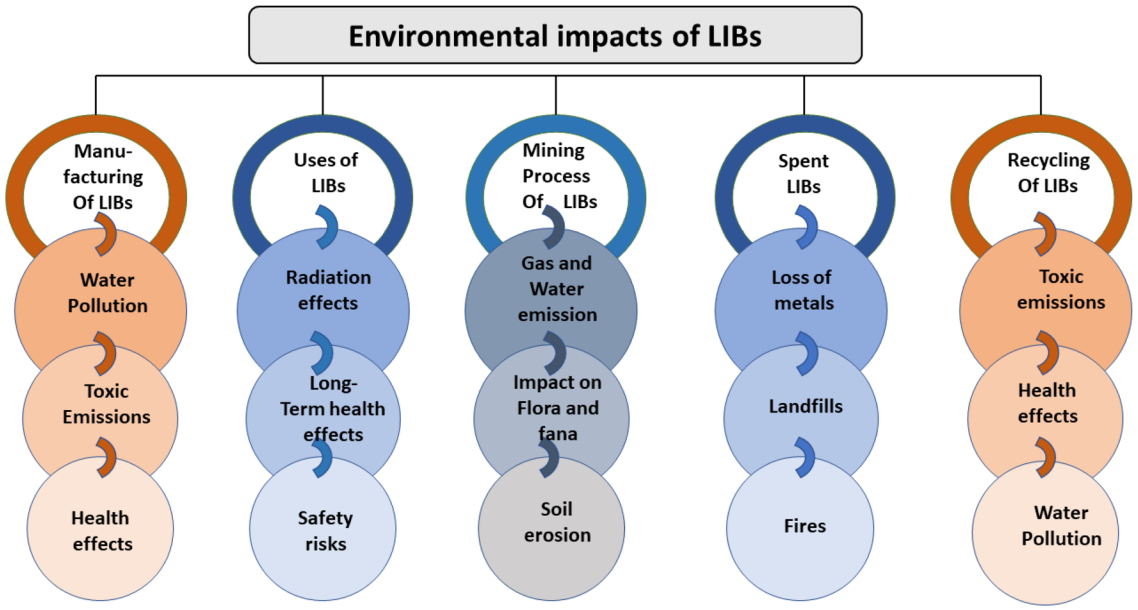

Fig. 12 Environmental impacts of LIBs.

environmental effects. The recycling process involves several steps: collection, discharging, dismantling, material separation, and metal recovery. Depending on the chemistry of the batteries and the materials being targeted, three primary recycling methods are utilized: hydrometallurgy, pyrometallurgy, and the developing method of solvometallurgy. These methods are often paired with specialized techniques aimed at recovering specific components of the batteries.[330,331] Hydrometallurgy is a method that includes leaching battery materials using aqueous solutions, followed by the separation and purification of metal ions. It is the most established and commonly used technique for recycling LIBs due to its relatively low energy consumption and the capacity to produce high-purity battery-grade materials. The procedure generally utilizes leachants, including sulfuric, hydrochloric, or organic acids like citric acid, often combined with reducing agents such as hydrogen peroxide to improve the metal dissolution process. After leaching, valuable metals are extracted through methods such as precipitation, solvent extraction, or electrochemical techniques. Hydrometallurgy is particularly effective in recovering lithium, cobalt, and nickel from various cathode materials, including $LiCoO_2$, nickel–manganese–cobalt, and lithium manganese oxide. Recent improvements have increased leaching efficiency by optimizing temperature, solid-to-liquid ratio, and pH. The process produces minimal secondary waste and presents opportunities for solvent reuse, although chemical handling and effluent treatment are still significant concerns.[332,333]

Solvometallurgy utilizes non-aqueous solvents for metal extraction and has emerged as an environmentally friendly alternative to conventional aqueous hydrometallurgy. A significant advancement in this field is the utilization of deep eutectic solvents (DES). These solvents are formed by combining a hydrogen bond donor (HBD) with a hydrogen bond acceptor (HBA), resulting in a liquid that exhibits unique solvation properties at comparatively low temperatures. Common examples of DES include combinations of choline chloride with urea or ethylene glycol. These solvents are eco-friendly, non-volatile, and relatively straightforward to produce. DES can effectively leach metals from cathodes like NMC and LCO, although their efficiency is generally lower than that of mineral acids due to their lesser acidity. Nevertheless, their effectiveness can be improved by adding more acidic HBDs, such as *p*-toluenesulfonic acid or citric acid. Leaching typically takes place with moderate heating, and this process can be integrated with electrochemical metal recovery.[334,335]

Pyrometallurgy employs elevated temperatures to process LIBs for the recovery of metals, utilizing methods such as smelting or roasting. During this process, organic binders and electrolytes are decomposed, and metal oxides are reduced to alloyed forms that can be refined further. Also, this approach is very tolerant to battery chemistries and formats, so it works very well with mixed or unsorted waste. That enables scaling and automation potential and has led to lots of commercial operations, in particular by companies like Umicore and Glencore. Nonetheless, pyrometallurgy is energy demanding and can release dangerous gases. This often results in the loss of lithium and graphite, with additional hydrometallurgical processes needed for complete materials recovery. Newer techniques such as salt-assisted roasting and microwave-assisted reduction aim to improve lithium extraction and minimize its environmental cost.[336]

The diverse materials utilized in LIBs have led to the creation of specialized recycling methods aimed at specific components, enhancing both efficiency and the recovery of value. Graphite, a common component of LIB anodes, is increasingly being recovered by supercritical fluid extraction, water-based separation, or thermal treatment. Recycling graphite is essential for lowering mining pressures and promoting circular supply

chains, despite its lesser economic value than cathode metals. Cathode materials are the primary focus because of their high value. Pyrometallurgical and hydrometallurgical methods are the primary approaches in this domain. However, emerging alternatives such as phytomining, which employs plants for metal extraction, and bioleaching, which utilizes microorganisms to dissolve metals, offer low-impact solutions. These innovative techniques demonstrate potential for selective and energy-efficient recovery, although further research is still required to fully understand their capabilities. Lithium salts and organic solvents, two electrolyte components that are frequently lost during high-temperature processing, are receiving more attention for recovery. Electrolyte recovery can be achieved through methods such as liquid–liquid extraction and supercritical CO_2. Additionally, the use of green solvents for the recovery of binder components, such as polyvinylidene fluoride (PVDF), enhances the sustainability of the overall process.[337,338]

Despite technological progress, the recycling of LIBs continues to encounter significant challenges. The diversity in cell designs and chemical compositions complicates automated disassembly and the establishment of standardized processing methods. Additionally, fluctuating prices of metals and elevated processing costs undermine the economic viability of recycling initiatives. Stringent environmental regulations are necessary due to the potential for hazardous waste and emissions from certain procedures. In many regions, ineffective collection methods and a lack of consumer awareness further impede the supply of feedstock. Variations in global e-waste legislation also affect investment and implementation in recycling efforts. To address these challenges, collaboration among manufacturers, recyclers, and policymakers is essential. Implementing extended producer responsibility regulations and designing batteries with recycling in mind could catalyze systemic change.[339] Integrating various technologies to achieve high recovery rates with minimal environmental impact is key to the future of LIB recycling. Hybrid methods that combine hydrometallurgy for purification and pyrometallurgy for bulk processing are becoming more popular. With further study, it is also anticipated that solvometallurgical processes employing DES and other environmentally friendly solvents would expand. Emerging technologies for improving recycling efficiency include blockchain for material tracking, machine learning for sorting, and automation for battery disassembly. Additionally, battery producers increasingly focus on closed-loop recycling, which involves reusing recovered materials in new batteries. The transformation of LIB recycling from a specialized sector into a widely accepted pillar of the circular economy would require investments in infrastructure, public–private collaborations, and standardized rules. A circular, zero-waste battery economy is attainable with coordinated innovation, policy, and industry cooperation activities.[340,341]

5.2 Safety concerns

LIBs have received the utmost attention in meeting the energy demands of the electronic automobile industries. However, at the same time, they have safety issues because of combustible materials. Fires and explosions of lithium-ion batteries have caused global concerns because they can lead to severe harm and damage. For example, in 2020, a Tesla ignited and detonated on the highway following a collision. Such incidents can cause severe harm and damage not only to the environment but also to human life. So, safety issues can never be neglected while discussing the role of a material in battery performance. The main reasons of battery thermal runaway, which leads to fires and explosions, are mechanical damage, electrical faults, excessive heat, and internal short circuits. Mechanical abuse means when the battery is crushed or hit. It leads to direct contact between the electrodes, resulting in short circuiting and fire explosion.[342] Electrical abuse includes external short circuit (because of touching of wires with each other) and overcharging.[343] Thermal abuse is because of exposure of the battery to high temperature for a sufficient length of time, leading to dangerous chemical reactions. Internal short circuit occurs because of malfunctioning inside the battery, causing direct contact between the opposite electrodes.[344]

The main components of the batteries that are prone to combustion are electrodes, electrolyte and separators. Substances mostly used as cathodes are transition metal oxides and transition metal sulfides[345] while carbon, nano-carbon, alloy materials and metal oxides are used as anodes.[346,347] So, while choosing materials for cathodes and anodes, safety issues should also be considered.

Anodes, though a key component of the battery, are prone to failures because of several reasons, which can lead to thermal runaway or combustion. Due to overcharging, lithium deposition on the surface of the anode occurs, which causes dendrite formation leading to short circuit and combustion.[348] High temperature causes decomposition of the solid electrolyte interface, which triggers unwanted chemical reactions leading to thermal runaway.[349] Li-ion movement can cause mechanical stress on the anode material, leading to cracks in the material and deformation. Loss of anode material also occurs because of electric shock, which occurs when the anode materials lose contact with other battery components, leading to increased resistance.

Various strategies are being adopted to enhance the safety of electrode materials. The key role here is of the solid electrolyte interface present on the surface of the anode. This SEI layer directly or indirectly affects the safety of lithium-ion batteries. If this layer is unstable, it can lead to dangerous side reactions, leading to thermal runaway or failure of the battery. So, one of the possible solutions to improve safety is to create an artificial SEI layer. It can be done by coating the anode with some heat-resistant material. It can be an Al_2O_3 layer or a polymer with a high value of the thermal expansion coefficient. Another way to create this layer is by adding certain additives in the electrolyte. These additives help build the SEI layer. However, one problem with the SEI layer is that it may improve safety, but at the same time, it reduces battery capacity. So future research should aim to devise ways to develop SEI layer which not only improves the safety but also does not provide harm to the energy storage capacity.[350]

Cathode materials can also cause safety issues because of thermal instability, heat accumulation and structural collapse. At high temperatures, chemical reactions occur between the cathode and the electrolyte, which produces heat. Once heat is produced, it cannot escape easily, so accumulation of heat occurs, which causes damage to the battery. Moreover, removing lithium ions from the cathode weakens the cathode's structure, reducing the battery's capacity and its life span. Various modifications are being adopted to improve the safety issues of cathode materials. These include doping and surface/structure modification. Doping can prevent structural collapse and reduce oxygen release and thermal instability by suppressing unwanted phase transition and reducing voltage degradation. Surface modification or coating prevents side reactions which reduce oxygen release. Cathodes with core–shell morphology minimize abrupt structural changes leading to stress-induced cracks preventing side reactions and increasing thermal stability. Single-crystal cathodes are also being made which are resistant to oxygen release and enhance thermal stability. These and many other innovations can improve the safety of cathode materials by making them thermally stable and resistant to unwanted side-reactions. However, it has also been found that cathode materials that improve safety lower the energy density. For example, LFP is the safest but has the lowest energy density.[351] So, future research should aim to make cathode materials that balance safety and energy density.[350] Fig. 13 illustrates the safety issues in Li-ion batteries.

5.3 Future batteries

The hunt for effective, sustainable, and scalable energy storage technologies has been sparked by the exponential rise in the world's energy consumption and the pressing need to slow down climate change. LIBs, which power everything from smartphones to electric vehicles, have long dominated the technological scene. However, issues like scarce lithium supplies, exorbitant prices, safety worries, and environmental effects are driving a big change in the battery sector.[352] This shift directs scientific research and industry attention towards sodium-ion batteries (SIBs), solid-state batteries (SSBs), and other future battery technologies to achieve more excellent performance, sustainability, and cost-effectiveness.[353] Like lithium-ion batteries, Na^+ move between the anode and cathode during charging and discharging in sodium-ion batteries. However, regarding raw material availability and cost, using sodium—an element significantly more abundant and equally distributed than lithium—offers a decisive advantage. Because of this, SIBs are especially appealing for integrating renewable energy sources and grid-scale storage. Unlike LIBs, which require more expensive copper for the anode, SIBs are compatible with aluminium current collectors for both electrodes. This significantly lowers the battery's weight and total production cost.[354]

Despite these benefits, SIBs still have technical issues, especially with material stability and energy density. Because sodium ions are heavier and bigger than lithium ions, their energy density is lower and their ionic diffusion is slower. The longevity of batteries is further limited by the structural deterioration that cathode and anode materials frequently experience from repeated cycles of charging and discharging. The creation of suitable electrolytes that guarantee safe and effective ion transport represents another major challenge.[355] Researchers have investigated a range of cathode and anode materials in order to address these issues. Although they have large capacities, Layered Transition Metal Oxides (LTMOs) such as Na_xTMO_2 have phase instability as a drawback for cathodes. Despite problems with crystal water and flaws, Prussian Blue

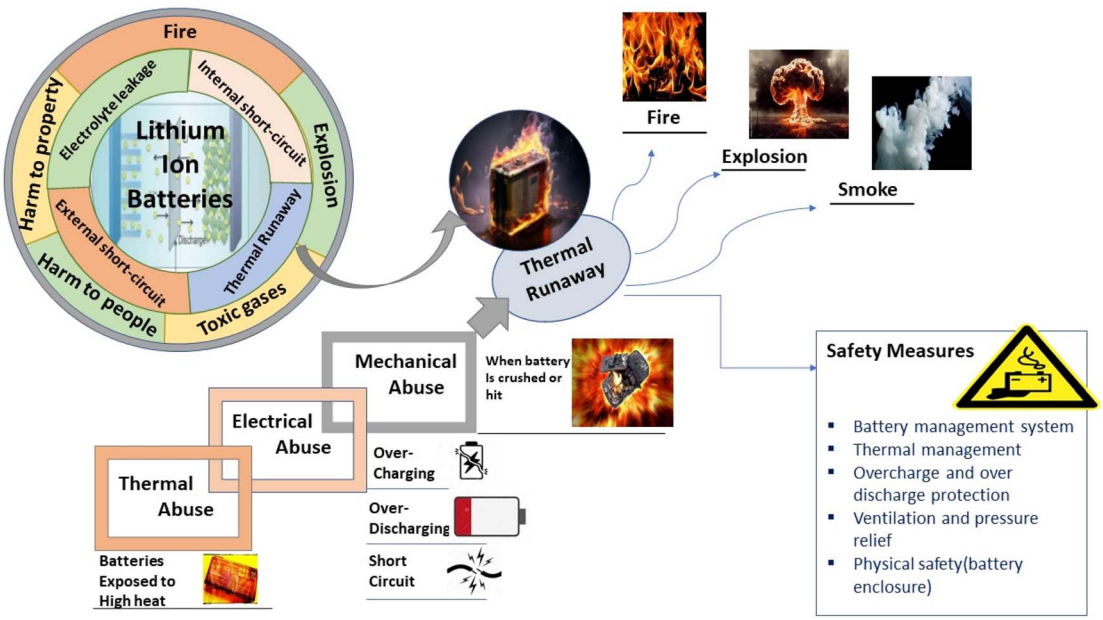

Fig. 13 Safety issues associated with Li-ion batteries.

Analogues (PBAs) have an open structure that facilitates Na^+ diffusion. Despite their reputation for structural stability, polyanionic compounds like $Na_3V_2(PO_4)_3$ have relatively low energy densities. Hard carbon has become the most promising material on the anode side because of its consistent performance, extended cycle life, and high capacity. Other options, such as titanium-based compounds (such as $Na_2Ti_3O_7$), provide safer voltage profiles but necessitate additional cycling stability improvements. Despite being environmentally beneficial and sustainable, organic materials are hampered by problems with solubility in traditional electrolytes. SIBs are best suited for uses like stationary energy storage systems, renewable energy grids, and low-speed electric cars where cost, safety, and resource sustainability considerations outweigh the necessity for a very high energy density.[356]

With the promise of improved safety, energy density, and cycle life, the idea of all-solid-state batteries (ASSBs), which substitute solid-state electrolytes (SSEs) for flammable liquid electrolytes, is gaining popularity. All-Solid-State Sodium Batteries (ASSBs) combine the inherent safety and compactness of solid-state designs with sodium's cost-effectiveness and resource advantages in sodium-ion chemistry. ASSBs solve several classic battery safety issues, including thermal runaway and electrolyte leakage. They also encourage the adoption of metallic sodium anodes, which have far greater capacities than traditional anode materials in theory. This creates opportunities to increase significantly the gadget lifetime and energy density.[357] However, ASSB development is still in its early phases and confronts significant engineering and scientific obstacles. One of the primary problems is that many solid electrolytes have limited ionic conductivity at normal temperature, which reduces the effectiveness of charge and discharge. Furthermore, poor contact and excessive interfacial resistance frequently plague the interface between solid electrodes and solid electrolytes, reducing battery performance and cycle life. Because many SSEs are brittle and prone to cracking under stress, particularly while cycling, mechanical instability is another issue.[358]

Research on ASSBs has focused on three primary types of solid-state electrolytes: oxide-based electrolytes, sulfide-based electrolytes, and polymer-based electrolytes. The production of batteries is made more difficult by oxide-based electrolytes, such as NASICON and β-alumina, which are known for their great mechanical strength and chemical stability but frequently need high-temperature sintering. Sulfide-based electrolytes, such as Na_3PS_4, have strong ionic conductivities but are also moisture-sensitive and can emit harmful gases when exposed. Polymer-based electrolytes are versatile and easy to produce but often display poorer ionic conductivities and limited heat stability. Notwithstanding these problems, ASSBs are seen to be perfect for uses requiring high performance and safety, like defence technology, aerospace systems, and high-end electric cars. To get around the drawbacks of individual components and strike the ideal balance between flexibility, conductivity, and stability, hybrid solid electrolytes—made up of a blend of polymers and ceramics—are also being created.[359]

Innovative ideas that go beyond conventional notions influence the direction of battery technology. Anode-free sodium batteries (AFSBs) are one such idea that represents a daring new design paradigm. These solutions save battery weight, volume, and production complexity by eliminating the requirement for a pre-installed anode. During charging, sodium is instead plated straight onto the current collector. To guarantee safe and effective functioning, however, problems, including uneven sodium deposition and dendritic formation, must be resolved. An additional potential approach is the use of metal–organic framework-derived anodes, which improve the electrochemical performance of SIBs by providing high porosity and conductivity. These materials can be designed for good ion transport and structural stability and show excellent tunability. Hybrid solid electrolytes are also becoming more popular to close the gap between solid-state and conventional liquid-based batteries. These systems offer a compromise that overcomes the mechanical and interfacial limitations of traditional SSEs by combining the flexibility of polymers with the high conductivity of ceramics. Furthermore, the discovery, optimization, and scaling of battery materials and systems are entirely transformed by the combination of artificial intelligence, machine learning, and autonomous research platforms like the Battery Interface Genome-Materials Acceleration Platform (BIG-MAP). Researchers can now see battery degradation, interface reactions, and ion dynamics in previously unheard-of detail thanks to methods like *operando* spectroscopy, real-time sensing, and digital twinning.[360,361] The shift from lithium-ion to next-generation battery technologies signifies a paradigm shift in our understanding of energy storage, striking a balance between sustainability and performance, innovation and pragmatism, and advancement and environmental responsibility. The future of batteries promises to be not only more efficient but also safer, cleaner, and more widely available, thanks to ongoing research and global collaboration.[360–364]

6. Conclusions, challenges and future prospects

Lithium-ion batteries have revolutionized energy storage, particularly in the realms of electric vehicles and renewable energy, due to their superior characteristics over conventional technologies. Investigating nanomaterials, alternative organic compounds, and innovative metal alloys presents considerable potential for enhancing the performance of both cathodes and anodes. With continued innovation, the next generation of LIBs hold great promise to meet the growing global energy demands and contribute to sustainable, high-efficiency energy storage solutions. Significant research efforts are focused on improving these systems' safety, longevity, and performance. A promising development area is solid-state batteries, which address the hazards associated with liquid electrolytes that can lead to fire risks. These batteries provide higher energy densities and increased lifespans but are still under development. Recycling and second-life usage of LIBs are also of great concern to the inter-operability and compatibility of electric power trains.

Indeed, effective mechanisms for recycling minimize the flow of material waste back into the natural environment and the need to mine for raw materials. In the same way, reusing batteries used in EVs for less demanding roles, such as energy storage for renewable power systems, will also help give batteries a longer life and make the whole process more sustainable. There are future possibilities for LIBs in terms of battery materials. Alternative materials for graphite are being investigated – lithium–sulfur or silicon anodes that, for instance, can have higher capacities and longer-cycle life. Emerging advances in nanotechnology and manufacturing techniques can help herald affordable ways to produce high-performance batteries. In conclusion, LIBs face tough challenges; however, the research and the resulting technological innovations point to a bright future. Safety, sustainability, and performance enhancements will be decisive factors in addressing the demand for energy storage applications, such as consumer electronics, EVs, and renewable power systems. They will remain in use in the future and can even become an essential tool for managing energy storage and usage.

The key issue of LIBs is the safety. Their high energy density leads to rapid heating. In certain circumstances, damage or improper use of these batteries may result in fires or explosions. Consequently, addressing these safety issues necessitates advanced electronic systems to monitor and control battery temperature and voltage and the design of complex and intricate battery packs. Another issue of concern is the depletion of raw materials and their environmental consequences, particularly concerning lithium, cobalt, and nickel. The extraction and processing of these resources are expected to result in environmental challenges and ethical concerns, including the employment of child labour in cobalt mining. With the increasing use of Li-ion batteries, the stress on these ingredients increases, calling for a focus on green sourcing and recycling. The constantly diminishing performance is another challenge. As mentioned, LIBs degrade with each charge cycle due to phenomena such as the formation of layers of SEI and lithium plating. This deterioration shortens battery lifespan and impacts the efficiency of electronic devices and vehicles reliant on these batteries. Addressing this issue necessitates advancements in materials and battery management strategies.

Data availability

Data are available within the manuscript in the form of figures and tables. No primary research results, software or code have been included and no new data were generated or analyzed as part of this review.

Conflicts of interest

Authors declare no conflict of interest.

References

1 N. Sarfraz, N. Kanwal, M. Ali, K. Ali, A. Hasnain, M. Ashraf, M. Ayaz, J. Ifthikar, S. Ali and A. Hendi, Materials advancements in solid-state inorganic electrolytes for highly anticipated all solid Li-ion batteries, *Energy Storage Mater.*, 2024, 103619.
2 S. Kaushik, T. Mehta, P. Chand, S. Sharma and G. Kumar, Recent advancements in cathode materials for high-performance Li-ion batteries: Progress and prospects, *J. Energy Storage*, 2024, **97**, 112818.
3 M. Winter, B. Barnett and K. Xu, Before Li ion batteries, *Chem. Rev.*, 2018, **118**(23), 11433–11456.
4 H. Zhao, J. Li, Q. Zhao, X. Huang, S. Jia, J. Ma and Y. Ren, Si-based anodes: advances and challenges in Li-ion batteries for enhanced stability, *Electrochem. Energy Rev.*, 2024, **7**(1), 11.
5 N. Khan, C. A. Ooi, A. Alturki, M. Amir and T. Alharbi, A critical review of battery cell balancing techniques, optimal design, converter topologies, and performance evaluation for optimizing storage system in electric vehicles, *Energy Rep.*, 2024, **11**, 4999–5032.
6 R. Yudhistira, D. Khatiwada and F. Sanchez, A comparative life cycle assessment of lithium-ion and lead-acid batteries for grid energy storage, *J. Cleaner Prod.*, 2022, **358**, 131999.
7 J. Li, Y. Peng, Q. Wang and H. Liu, Status and prospects of research on lithium-ion battery parameter identification, *Batteries*, 2024, **10**(6), 194.
8 L. G. Chagas, S. Jeong, I. Hasa and S. Passerini, Ionic liquid-based electrolytes for sodium-ion batteries: tuning properties to enhance the electrochemical performance of manganese-based layered oxide cathode, *ACS Appl. Mater. Interfaces*, 2019, **11**(25), 22278–22289.
9 M. Chen, L. L. Shao, X.-Q. Wang, X. Qian, Z. Y. Yuan, L. X. Fang, A. X. Ding, X. W. Lv and Y. N. Wang, Controlled synthesis of highly active nonstoichiometric tin phosphide/carbon composites for electrocatalysis and electrochemical energy storage applications, *ACS Sustain. Chem. Eng.*, 2022, **10**(4), 1482–1498.
10 M. Bamdezh and G. Molaeimanesh, The path from conventional battery thermal management systems to hybrid battery thermal management systems for electric vehicles, opportunities and challenges, *J. Energy Storage*, 2024, **100**, 113160.
11 X. W. Lin, Y. B. Li, W. T. Wu, Z. F. Zhou and B. Chen, Advances on two-phase heat transfer for lithium-ion battery thermal management, *Renewable Sustainable Energy Rev.*, 2024, **189**, 114052.
12 R. Chen, C. L. A. Leung and C. Huang, Exploring the properties of disordered rocksalt battery cathode materials by advanced characterization, *Adv. Funct. Mater.*, 2024, 2308165.
13 Q. Li, H. Wang, Y. Wang, G. Sun, Z. Li, Y. Zhang, H. Shao, Y. Jiang, Y. Tang and R. Liang, Critical Review of Emerging Pre-metallization Technologies for Rechargeable Metal-Ion Batteries, *Small*, 2024, **20**(6), 2306262.
14 H. Zhao, H. Zuo, J. Wang and S. Jiao, Practical application of graphite in lithium-ion batteries: Modification, composite, and sustainable recycling, *J. Energy Storage*, 2024, **98**, 113125.

15 Y. Liu, H. Shi and Z.-S. Wu, Recent status, key strategies and challenging perspectives of fast-charging graphite anodes for lithium-ion batteries, *Energy Environ. Sci.*, 2023, **16**(11), 4834–4871.
16 A. Celadon, H. Sun, S. Sun and G. Zhang, Batteries for electric vehicles: Technical advancements, environmental challenges, and market perspectives, *SusMat*, 2024, **4**(5), e234.
17 F. N. U. Khan, M. G. Rasul, A. Sayem and N. K. Mandal, Design and optimization of lithium-ion battery as an efficient energy storage device for electric vehicles: A comprehensive review, *J. Energy Storage*, 2023, **71**, 108033.
18 B. Cui, Z. Xiao, S. Cui, S. Liu, X. Gao and G. Li, Safety Issues and Improvement Measures of Ni-Rich Layered Oxide Cathode Materials for Li-Ion Batteries, *Electrochem. Energy Rev.*, 2024, **7**(1), 27.
19 X. Hu, F. Gao, Y. Xiao, D. Wang, Z. Gao, Z. Huang, S. Ren, N. Jiang and S. Wu, Advancements in the safety of Lithium-Ion Battery: The trigger, consequence and mitigation method of thermal runaway, *Chem. Eng. J.*, 2024, 148450.
20 A. K. Azad, A. M. Abdalla, P. I. I. Kumarasinghe, S. Nourean, A. T. Azad, J. Ma, C. Jiang, M. M. K. Dawood, B. Wei and C. N. K. Patabendige, Developments and key challenges in micro/nanostructured binary transition metal oxides for lithium-ion battery anodes, *J. Energy Storage*, 2024, **84**, 110850.
21 I. M. Nwachukwu, A. C. Nwanya, A. Alshoaibi, C. Awada, A. Ekwealor and F. I. Ezema, Recent progress in green synthesized transition metal-based oxides in lithium-ion batteries as energy storage devices, *Curr. Opin. Electrochem.*, 2023, **39**, 101250.
22 K. Su, P. Chi, T. Paul, C. Chung, W. Chen, Y. Su, P. Wu, C. Su and M. Wu, Lithiation and delithiation induced magnetic switching and electrochemical studies in α-LiFeO2 based Li ion battery, *Mater. Today Phys.*, 2021, **18**, 100373.
23 Y. Chu, Y. Mu, L. Zou, J. Cheng, S. Xi, Q. Pan, M. Han, H. Wang, Q. Li and F. Zheng, Synergistic structure of LiFeO2 and Fe2O3 layers with electrostatic shielding effect to suppress surface lattice oxygen release of Ni-rich cathode, *Chem. Eng. J.*, 2023, **465**, 142750.
24 Y. Hu, H. Zhao, M. Tan, J. Liu, X. Shu, M. Zhang, S. Liu, Q. Ran, H. Li and X. Liu, Synthesis of α-LiFeO2/Graphene nanocomposite via layer by layer self-assembly strategy for lithium-ion batteries with excellent electrochemical performance, *J. Mater. Sci. Technol.*, 2020, **55**, 173–181.
25 Y. R. Xing, H. Lu, Y. H. Si, K. Bai, S. M. Yu and Y. J. Zhao, Temperature-controlled direct dry synthesis of Co-Ni free cathode materials 0.7 $Li_2MnO_3\cdot$ 0.3 $LiFeO_2$ for lithium-ion batteries, *J. Alloys Compd.*, 2022, **915**, 165392.
26 Y. Hu and X. Liu, A novel method for preparing α-LiFeO2 nanorods for high-performance lithium-ion batteries, *Ionics*, 2020, **26**(2), 1057–1061.
27 J. Liao, C. Wang, J. Liu, G. Shan, X. Huo, P. Sun, N. Nie, J. Zhang and W. Li, Fe Dopants Intensify the Electrochemical Performance of $LiNi_{0.60}Mn_{0.40}O_2$ Cathode Materials, *Ind. Eng. Chem. Res.*, 2024, **63**(27), 11959–11970.
28 J. Lan, H. Hou, K. Meng, M. Feng and J. Li, The recovery of expired ferrous gluconate and spent Li foils into high performance straw-bundle-like α-LiFeO2/C cathode, *Electrochim. Acta*, 2021, **390**, 138827.
29 Z. Sun, Z. Zhang and H. Li, Templated synthesis of nano-LiCoO2 cathode for lithium-Ion batteries with enhanced rate capability, *Mater. Lett.*, 2021, **303**, 130570.
30 S. Takeno, T. Suematsu, R. Kunisaki, G. Hasegawa, K. Watanabe, N. Kuwata, K. Mitsuishi, T. Ohnishi, K. Takada and K. Suematsu, New insight into designing a thick-sintered cathode for Li-ion batteries: the impact of excess lithium in $LiCoO_2$ on its electrode performance, *J. Mater. Chem. A*, 2025, **13**(4), 2943–2949.
31 J. Lin, C. Zeng, L. Wang, Y. Pan, X. Lin, R. C. K. Reddy, Y. Cai and C. Y. Su, Self-standing MOF-derived LiCoO2 nanopolyhedron on Au-coated copper foam as advanced 3D cathodes for lithium-ion batteries, *Appl. Mater. Today*, 2020, **19**, 100565.
32 Z. Xiao, J. Liu, G. Fan, M. Yu, J. Liu, X. Gou, M. Yuan and F. Cheng, Lithium bis (oxalate) borate additive in the electrolyte to improve Li-rich layered oxide cathode materials, *Mater. Chem. Front.*, 2020, **4**(6), 1689–1696.
33 W. M. Seong and A. Manthiram, Complementary effects of Mg and Cu incorporation in stabilizing the cobalt-free LiNiO2 cathode for lithium-ion batteries, *ACS Appl. Mater. Interfaces*, 2020, **12**(39), 43653–43664.
34 R. A. Yuwono, F.-M. Wang, N. L. Wu, Y. C. Chen, H. Chen, J.-M. Chen, S. C. Haw, J. F. Lee, R. K. Xie and H. S. Sheu, Evaluation of $LiNiO_2$ with minimal cation mixing as a cathode for Li-ion batteries, *Chem. Eng. J.*, 2023, **456**, 141065.
35 J. Välikangas, P. Laine, M. Hietaniemi, T. Hu, P. Tynjälä and U. Lassi, Precipitation and calcination of high-capacity LiNiO2 cathode material for lithium-ion batteries, *Appl. Sci.*, 2020, **10**(24), 8988.
36 L. Mu, W. H. Kan, C. Kuai, Z. Yang, L. Li, C. J. Sun, S. Sainio, M. Avdeev, D. Nordlund and F. Lin, Structural and electrochemical impacts of Mg/Mn dual dopants on the $LiNiO_2$ cathode in Li-metal batteries, *ACS Appl. Mater. Interfaces*, 2020, **12**(11), 12874–12882.
37 Y. Zhang, H. Li, J. Liu, J. Liu, H. Ma and F. Cheng, Enhancing $LiNiO_2$ cathode materials by concentration-gradient yttrium modification for rechargeable lithium-ion batteries, *J. Energy Chem.*, 2021, **63**, 312–319.
38 Y. Wang, Y. Zhu and P. Gao, Synthesis and characterization of Nickel-rich layered LiNi1-xMnxO2 (x= 0.02, 0.05) cathodes for lithium-ion batteries, *Electrochim. Acta*, 2022, **427**, 140891.
39 S. Ober, A. Mesnier and A. Manthiram, Surface stabilization of cobalt-free LiNiO2 with niobium for lithium-ion batteries, *ACS Appl. Mater. Interfaces*, 2023, **15**(1), 1442–1451.
40 L. Shen, F. Du, Q. Zhou, T. Xu, Z. Fan, Y. Wen, J. Wang, J. Wu and J. Zheng, Cobalt-free nickel-rich cathode materials based on Al/Mg co-doping of LiNiO2 for lithium ion battery, *J. Colloid Interface Sci.*, 2023, **638**, 281–290.

41 Y. Chu, J. Zhou, W. Liu, F. Chu, J. Li and F. Wu, Cobalt-Free LiNiO2 with a Selenium Coating as a High-Energy Layered Cathode Material for Lithium-Ion Batteries, *Small Sci.*, 2023, **3**(7), 2300023.
42 G. Zhang, Y. Zhu, S. Lv, Z. Wang and P. Gao, Enhanced electrochemical performance of LiNiO2 cathode material by precursor preoxidation for lithium-ion batteries, *J. Alloys Compd.*, 2023, **953**, 170134.
43 C. Lee, J.-M. Choi, Y. Miyahara, I. Jeon, K. Miyazaki and T. Abe, Bifunctional Al2O3-Based Artificial Layers on LiNiO2 Cathodes for High-Energy-Density Aqueous Li-Ion Batteries, *Chem. Mater.*, 2023, **36**(2), 860–869.
44 J. Wu, J. Yang, J. Zheng, M. Wang, S. Li, B. Huang, Y. Li, Q. Zhu, Q. Chen and S. Xiao, Co-Doping of Al3+ and Ti4+ and Electrochemical Properties of LiNiO2 Cathode Materials for Lithium-Ion Batteries, *ChemSusChem*, 2023, **16**(19), e202300607.
45 Y. Tian, Y. Qiu, Z. Liu, X. Wei and H. Cao, LiMnO2@ rGO nanocomposites for high-performance lithium-ion battery cathodes, *Nanotechnology*, 2020, **32**(1), 015402.
46 N. H. Vu, V.-D. Dao, H. H. T. Vu, N. Van Noi, D. T. Tran, M. N. Ha and T.-D. Pham, Hydrothermal Synthesis of Li2MnO3-Stabilized LiMnO2 as a Cathode Material for Li-Ion Battery, *J. Nanomater.*, 2021, **2021**(1), 9312358.
47 Y. Sun, M. Guo, S. Shu, D. Ding, C. Wang, Y. Zhang and J. Yan, Preparation of Li2MnO3 nanowires with structural defects as high rate and high capacity cathodes for lithium-ion batteries, *Appl. Surf. Sci.*, 2022, **585**, 152605.
48 H. Liu, Y. Zhuang, X. Zhu and H. Xia, Tunable conversion to spinel–layered LiMnO2 via protonated Mn3O4 for ultrastable lithium-ion batteries, *Energy Fuels*, 2024, **38**(16), 15855–15860.
49 Y. Xia, Z. Fang, C. Lu, Z. Xiao, X. He, Y. Gan, H. Huang, G. Wang and W. Zhang, A Facile Pre-Lithiated Strategy towards High-Performance Li2Se-LiTiO2 Composite Cathode for Li-Se Batteries, *Nanomaterials*, 2022, **12**(5), 815.
50 W. Zhang, L. Xiao, J. Zheng, H. Chen, Y. Zhu and K. Xiang, Improving Electrochemical Performance and Structural Stability of $LiNi_{0.6}$ $Co_{0.2}$ $Mn_{0.2}$ O_2 via Nanoscale Coating with $LiTiO_2$, *JOM*, 2020, **72**, 2250–2259.
51 Y. Wang, X. Bai, Z. Luo and L. Fu, High specific capacity thermal battery cathodes $LiCu_2O_2$ and $LiCu_3O_3$ prepared by a simple solid phase sintering, *Front. Chem.*, 2020, **8**, 575787.
52 K. J. P. C. Mizushima, P. C. Jones, P. J. Wiseman and J. B. Goodenough, $LixCoO_2$ (0< x <-1): A new cathode material for batteries of high energy density, *Mater. Res. Bull.*, 1980, **15**(6), 783–789.
53 H. Ma, F. Wang, M. Shen, Y. Tong, H. Wang and H. Hu, Advances of $LiCoO_2$ in Cathode of Aqueous Lithium-Ion Batteries, *Small Methods*, 2024, **8**(6), 2300820.
54 Y. Tan, W. Chang, J. Cai, Y. Liu, X. Tan and C. Lai, Interface regulation strategies toward the challenges faced by cathode materials and solid electrolytes, *J. Mater. Sci.*, 2023, **58**(27), 10911–10942.
55 A. Yoshino, The birth of the lithium-ion battery, *Angew. Chem., Int. Ed.*, 2012, **51**(24), 5798–5800.
56 Z. Sun, J. Zhao, M. Zhu and J. Liu, Critical problems and modification strategies of realizing high-voltage LiCoO2 cathode from electrolyte engineering, *Adv. Energy Mater.*, 2024, **14**(8), 2303498.
57 R. Konar, S. Maiti, N. Shpigel and D. Aurbach, Reviewing failure mechanisms and modification strategies in stabilizing high-voltage LiCoO2 cathodes beyond 4.55 V, *Energy Storage Mater.*, 2023, 103001.
58 Y. Wang, C. Xu, X. Tian, S. Wang and Y. Zhao, Challenges and Modification Strategies of High-Voltage Cathode Materials for Li-ion Batteries, *Chin. J. Struct. Chem.*, 2023, 100167.
59 J. An, H. Zhang, Y. Wang, Z. Kong, W. Li, X. Gao, J. Song and Y. Yao, Application and prospects of interface engineering in energy storage and conversion of graphdiyne-based materials, *EcoEnergy*, 2024, **3**(1), 77–104.
60 M. Lv, R. Zhao, Z. Hu, J. Yang, X. Han, Y. Wang, C. Wu and Y. Bai, Binder Design Strategies for Cathode Materials in Advanced Secondary Batteries, *Energy Environ. Sci.*, 2024, **17**(14), 4871–4906.
61 C. Li, J. Jin, Z. Yuan, C. Zhang, L. Wu and C. Wang, A Review on Leaching of Spent Lithium Battery Cathode Materials Adopting Deep Eutectic Solvents, *ChemistryOpen*, 2024, e202400258.
62 M. Moin, M. Moin, S. Wang, A. W. Anwar, Z. Ahsan, A. Ali, Q. Lei, Y. Ma and G. Song, Recent developments in coating investigation of LiNixMnyCo1-x-yO2 cathode material with promising (Li, Ni) rich layered for future generation lithium-ion batteries, *J. Alloys Compd.*, 2024, 175710.
63 X. Ma, J. Wang, Z. Wang, L. Wang, H. Xu and X. He, Engineering strategies for high-voltage LiCoO2 based high-energy Li-ion batteries, *Electron*, 2024, e33.
64 Y. Lyu, X. Wu, K. Wang, Z. Feng, T. Cheng, Y. Liu, M. Wang, R. Chen, L. Xu and J. Zhou, An overview on the advances of LiCoO2 cathodes for lithium-ion batteries, *Adv. Energy Mater.*, 2021, **11**(2), 2000982.
65 P. Thakkar, S. Khatri, D. Dobariya, D. Patel, B. Dey and A. K. Singh, Advances in materials and machine learning techniques for energy storage devices: A comprehensive review, *J. Energy Storage*, 2024, **81**, 110452.
66 T. Wulandari, D. Fawcett, S. B. Majumder and G. E. Poinern, Lithium-based batteries, history, current status, challenges, and future perspectives, *Battery Energy*, 2023, **2**(6), 20230030.
67 W. Zhong, Z. Zeng, S. Cheng and J. Xie, Advancements in Prelithiation Technology: Transforming Batteries from Li-Shortage to Li-Rich Systems, *Adv. Funct. Mater.*, 2024, **34**(2), 2307860.
68 K. Ullah, N. Shah, R. Wadood, B. M. Khan and W. C. Oh, Recent trends in graphene based transition metal oxides as anode materials for rechargeable lithium-ion batteries, *Nano Trends*, 2023, **1**, 100004.
69 J. Ma, T. Liu, J. Ma, C. Zhang and J. Yang, Progress, Challenge, and Prospect of LiMnO2: An Adventure toward High-Energy and Low-Cost Li-Ion Batteries, *Adv. Sci.*, 2024, **11**(2), 2304938.

70 H. Yi, Y. Liang, Y. Qian, Y. Feng, Z. Li and X. Zhang, Low-cost Mn-based cathode materials for lithium-ion batteries, *Batteries*, 2023, **9**(5), 246.
71 H. Chen, X. Xia and J. Ma, Comprehensive Review of Li-Rich Mn-Based Layered Oxide Cathode Materials for Lithium-Ion Batteries: Theories, Challenges, Strategies and Perspectives, *ChemSusChem*, 2024, e202401120.
72 A. N. Banerjee and S. W. Joo, 'Beyond Li-Ion Technology'-A status review, *Nanotechnology*, 2024, **35**, 472001.
73 H. Du, Y. Wang, Y. Kang, Y. Zhao, Y. Tian, X. Wang, Y. Tan, Z. Liang, J. Wozny and T. Li, Side Reactions/Changes in Lithium-Ion Batteries: Mechanisms and Strategies for Creating Safer and Better Batteries, *Adv. Mater.*, 2024, 2401482.
74 S. Lee, Y. Cho, H. K. Song, K. T. Lee and J. Cho, Carbon-coated single-crystal LiMn 2 O 4 nanoparticle clusters as cathode material for high-energy and high-power lithium-ion batteries, *Angew. Chem., Int. Ed.*, 2012, **35**(51), 8748–8752.
75 M.-J. Lee, S. Lee, P. Oh, Y. Kim and J. Cho, High performance LiMn2O4 cathode materials grown with epitaxial layered nanostructure for Li-ion batteries, *Nano Lett.*, 2014, **14**(2), 993–999.
76 K. Akhmetova, F. Sultanov, A. Mentbayeva, N. Umirov, Z. Bakenov and B. Tatykayev, Advances in multi-element doping of LiFePO4 cathode material for capacity enhancement in Li-ion batteries, *J. Power Sources*, 2024, **624**, 235531.
77 Q. Zhang, Y. Zhou, Y. Tong, Y. Chi, R. Liu, C. Dai, Z. Li, Z. Cui, Y. Liang and Y. Tan, Reduced graphene oxide coating LiFePO4 composite cathodes for advanced lithium-ion battery applications, *Int. J. Mol. Sci.*, 2023, **24**(24), 17549.
78 M. Chen, F. M. Liu, S. S. Chen, Y.-J. Zhao, Y. Sun, C. S. Li, Z. Y. Yuan, X. Qian and R. Wan, In situ self-catalyzed formation of carbon nanotube wrapped and amorphous nanocarbon shell coated LiFePO4 microclew for high-power lithium ion batteries, *Carbon*, 2023, **203**, 661–670.
79 X. Qiu, C. Wang, L. Xie, L. Zhu, X. Cao and X. Ji, Challenges and perspectives towards direct regeneration of spent LiFePO4 cathode, *J. Power Sources*, 2024, **602**, 234365.
80 M. Shan, C. Dang, K. Meng, Y. Cao, X. Zhu, J. Zhang, G. Xu and M. Zhu, Recycling of LiFePO4 cathode materials: From laboratory scale to industrial production, *Mater. Today*, 2024, **73**, 130–150.
81 X. Shen, Z. Qin, P. He, X. Ren, Y. Li, F. Wu, Y. Cheng and Z. He, Refined Grain Enhancing Lithium-Ion Diffusion of LiFePO4 via Air Oxidation, *Coatings*, 2023, **13**(6), 1038.
82 h. Rostami, J. Valio, P. Tynjälä, U. Lassi and P. Suominen, Life Cycle of LiFePO4 Batteries: Production, Recycling, and Market Trends, *ChemPhysChem*, 2024, e202400459.
83 X.-Z. Liao, Z.-F. Ma, L. Wang, X.-M. Zhang, Y. Jiang and Y.-S. He, A novel synthesis route for LiFePO4/C cathode materials for lithium-ion batteries, *Electrochem. Solid-State Lett*, 2004, **7**(12), A522.
84 G. Wang, L. Yang, Y. Chen, J. Wang, S. Bewlay and H. Liu, An investigation of polypyrrole-LiFePO4 composite cathode materials for lithium-ion batteries, *Electrochim. Acta*, 2005, **50**(24), 4649–4654.
85 F. F. Bazito and R. M. Torresi, Cathodes for lithium ion batteries: the benefits of using nanostructured materials, *J. Braz. Chem. Soc.*, 2006, **17**, 627–642.
86 J. C. Arrebola, A. Caballero, M. Cruz, L. Hernán, J. Morales and E. R. Castellón, Crystallinity control of a nanostructured LiNi0. 5Mn1. 5O4 spinel via polymer-assisted synthesis: a method for improving its rate capability and performance in 5 V lithium batteries, *Adv. Funct. Mater.*, 2006, **16**(14), 1904–1912.
87 L. Zhou, D. Zhao and X. D. Lou, LiNi 0.5 Mn 1.5 O 4 hollow structures as high-performance cathodes for lithium-ion batteries, *Angew. Chem., Int. Ed.*, 2011, **1**(51), 239–241.
88 H. K. Liu, G. X. Wang, Z. Guo, J. Wang and K. Konstantinov, Nanomaterials for lithium-ion rechargeable batteries, *J. Nanosci. Nanotechnol.*, 2006, **6**(1), 1–15.
89 S. Ye, J. Lv, X. Gao, F. Wu and D. Song, Synthesis and electrochemical properties of LiMn2O4 spinel phase with nanostructure, *Electrochim. Acta*, 2004, **49**(9–10), 1623–1628.
90 P. G. Bruce, B. Scrosati and J. M. Tarascon, Nanomaterials for rechargeable lithium batteries, *Angew. Chem., Int. Ed.*, 2008, **47**(16), 2930–2946.
91 Y. Ren, A. R. Armstrong, F. Jiao and P. G. Bruce, Influence of size on the rate of mesoporous electrodes for lithium batteries, *J. Am. Chem. Soc.*, 2010, **132**(3), 996–1004.
92 K. Amine, I. Belharouak, Z. Chen, T. Tran, H. Yumoto, N. Ota, S.-T. Myung and Y.-K. Sun, Nanostructured anode material for high-power battery system in electric vehicles, *Adv. Mater.*, 2010, **22**(28), 3052.
93 S.-Y. Chung, J. T. Bloking and Y.-M. Chiang, Electronically conductive phospho-olivines as lithium storage electrodes, *Nat. Mater.*, 2002, **1**(2), 123–128.
94 X. Rui, X. Zhao, Z. Lu, H. Tan, D. Sim, H. H. Hng, R. Yazami, T. M. Lim and Q. Yan, Olivine-type nanosheets for lithium ion battery cathodes, *ACS Nano*, 2013, **7**(6), 5637–5646.
95 H.-S. Park, S.-J. Hwang and J.-H. Choy, Relationship between chemical bonding character and electrochemical performance in nickel-substituted lithium manganese oxides, *J. Phys. Chem. B*, 2001, **105**(21), 4860–4866.
96 D. Kovacheva, H. Gadjov, K. Petrov, S. Mandal, M. G. Lazarraga, L. Pascual, J. M. Amarilla, R. M. Rojas, P. Herrero and J. M. Rojo, Synthesizing nanocrystalline LiMn 2 O 4 by a combustion route, *J. Mater. Chem.*, 2002, **12**(4), 1184–1188.
97 L. Yu, H. Yang, X. Ai and Y. Cao, Structural and electrochemical characterization of nanocrystalline Li [Li0. 12Ni0. 32Mn0. 56] O2 synthesized by a polymer-pyrolysis route, *J. Phys. Chem. B*, 2005, **109**(3), 1148–1154.
98 A. S. Arico, P. Bruce, B. Scrosati, J.-M. Tarascon and W. Van Schalkwijk, Nanostructured materials for advanced energy conversion and storage devices, *Nat. Mater.*, 2005, **4**(5), 366–377.
99 P. Poizot, S. Laruelle, S. Grugeon, L. Dupont and J. Tarascon, Nano-sized transition-metal oxides as

negative-electrode materials for lithium-ion batteries, *Nature*, 2000, **407**(6803), 496–499.

100 K. T. Nam, D.-W. Kim, P. J. Yoo, C.-Y. Chiang, N. Meethong, P. T. Hammond, Y.-M. Chiang and A. M. Belcher, Virus-enabled synthesis and assembly of nanowires for lithium ion battery electrodes, *Science*, 2006, **312**(5775), 885–888.

101 N. Li, C. J. Patrissi, G. Che and C. R. Martin, Rate capabilities of nanostructured LiMn2 O 4 electrodes in aqueous electrolyte, *J. Electrochem. Soc.*, 2000, **147**(6), 2044.

102 A. M. Cao, J. S. Hu, H. P. Liang and L. J. Wan, Self-assembled vanadium pentoxide (V2O5) hollow microspheres from nanorods and their application in lithium-Ion batteries, *Angew. Chem., Int. Ed.*, 2005, **44**(28), 4391–4395.

103 A. R. Armstrong, G. Armstrong, J. Canales and P. G. Bruce, TiO2-B nanowires, *Angew. Chem., Int. Ed.*, 2004, **43**(17), 2286–2288.

104 J.-Y. Luo, H.-M. Xiong and Y.-Y. Xia, LiMn2O4 nanorods, nanothorn microspheres, and hollow nanospheres as enhanced cathode materials of lithium ion battery, *J. Phys. Chem. C*, 2008, **112**(31), 12051–12057.

105 S. J. Visco and L. C. DeJonghe, Ionic conductivity of organosulfur melts for advanced storage electrodes, *J. Electrochem. Soc.*, 1988, **135**(12), 2905.

106 M. Liu, S. J. Visco and L. C. De Jonghe, Electrochemical properties of organic disulfide/thiolate redox couples, *J. Electrochem. Soc.*, 1989, **136**(9), 2570.

107 S. J. Visco, C. C. Mailhe, L. C. De Jonghe and M. B. Armand, A novel class of organosulfur electrodes for energy storage, *J. Electrochem. Soc.*, 1989, **136**(3), 661.

108 T. Matsunaga, T. Kubota, T. Sugimoto and M. Satoh, High-performance lithium secondary batteries using cathode active materials of triquinoxalinylenes exhibiting six electron migration, *Chem. Lett.*, 2011, **40**(7), 750–752.

109 Z. Shadike, H. S. Lee, C. Tian, K. Sun, L. Song, E. Hu, I. Waluyo, A. Hunt, S. Ghose and Y. Hu, Synthesis and Characterization of a Molecularly Designed High-Performance Organodisulfide as Cathode Material for Lithium Batteries, *Adv. Energy Mater.*, 2019, **9**(21), 1900705.

110 J. Cheng, Y. Pan, J. Zhu, Z. Li, J. Pan and Z. Ma, Hybrid network CuS monolith cathode materials synthesized via facile in situ melt-diffusion for Li-ion batteries, *J. Power Sources*, 2014, **257**, 192–197.

111 C. Feng, L. Zhang, Z. Wang, X. Song, K. Sun, F. Wu and G. Liu, Synthesis of copper sulfide nanowire bundles in a mixed solvent as a cathode material for lithium-ion batteries, *J. Power Sources*, 2014, **269**, 550–555.

112 J. Wang, S. Ng, G. Wang, J. Chen, L. Zhao, Y. Chen and H. Liu, Synthesis and characterization of nanosize cobalt sulfide for rechargeable lithium batteries, *J. Power Sources*, 2006, **159**(1), 287–290.

113 R. Jin, J. Zhou, Y. Guan, H. Liu and G. Chen, Mesocrystal Co 9 S 8 hollow sphere anodes for high performance lithium ion batteries, *J. Mater. Chem. A*, 2014, **2**(33), 13241–13244.

114 S. C. Han, K.-W. Kim, H. J. Ahn, J. H. Ahn and J. Y. Lee, Charge–discharge mechanism of mechanically alloyed NiS used as a cathode in rechargeable lithium batteries, *J. Alloys Compd.*, 2003, **361**(1–2), 247–251.

115 P. Zhao, H. Cui, J. Luan, Z. Guo, Y. Zhou and H. Xue, Porous FeS2 nanoparticles wrapped by reduced graphene oxide as high-performance Lithium-ion battery cathodes, *Mater. Lett.*, 2017, **186**, 62–65.

116 F. Zhang, C. Wang, G. Huang, D. Yin and L. Wang, FeS2@ C nanowires derived from organic-inorganic hybrid nanowires for high-rate and long-life lithium-ion batteries, *J. Power Sources*, 2016, **328**, 56–64.

117 G. Pan, F. Cao, X. Xia and Y. Zhang, Exploring hierarchical FeS2/C composite nanotubes arrays as advanced cathode for lithium ion batteries, *J. Power Sources*, 2016, **332**, 383–388.

118 J. E. Trevey, C. R. Stoldt and S.-H. Lee, High power nanocomposite TiS2 cathodes for all-solid-state lithium batteries, *J. Electrochem. Soc.*, 2011, **158**(12), A1282.

119 Y. Xi, X. Ye, S. Duan, T. Li, J. Zhang, L. Jia, J. Yang, J. Wang, H. Liu and Q. Xiao, Iron vacancies and surface modulation of iron disulfide nanoflowers as a high power/energy density cathode for ultralong-life stable Li storage, *J. Mater. Chem. A*, 2020, **8**(29), 14769–14777.

120 R. Li, H. Shen, E. Pervaiz and M. Yang, Facile in situ nitrogen-doped carbon coated iron sulfide as green and efficient adsorbent for stable lithium–sulfur batteries, *Chem. Eng. J.*, 2021, **404**, 126462.

121 D. Xie, S. Mei, Y. Xu, T. Quan, E. Härk, Z. Kochovski and Y. Lu, Efficient Sulfur Host Based on Yolk-Shell Iron Oxide/Sulfide-Carbon Nanospindles for Lithium-Sulfur Batteries, *ChemSusChem*, 2021, **14**(5), 1404–1413.

122 N. E. Horwitz, E. V. Shevchenko, J. Park, E. Lee, J. Xie, B. Chen, Y. Zhong, A. S. Filatov and J. S. Anderson, Synthesis, modular composition, and electrochemical properties of lamellar iron sulfides, *J. Mater. Chem. A*, 2020, **8**(31), 15834–15844.

123 Q. Xiong, X. Teng, J. Lou, G. Pan, X. Xia, H. Chi, X. Lu, T. Yang and Z. Ji, Design of pyrite/carbon nanospheres as high-capacity cathode for lithium-ion batteries, *J. Energy Chem.*, 2020, **40**, 1–6.

124 S. H. Akella, S. Taragin, A. Mukherjee, O. Lidor-Shalev, H. Aviv, M. Zysler, D. Sharon and M. Noked, Tailoring nickel-rich LiNi0. 8Co0. 1Mn0. 1O2 layered oxide cathode materials with metal sulfides (M2S: M= Li, Na) for improved electrochemical properties, *J. Electrochem. Soc.*, 2021, **168**(8), 080543.

125 Y. Liang, C. Ma, Y. Wang, H. Yu, X. Shen, S. Yao, T. Li and S. Qin, Cubic pyrite nickel sulfide nanospheres decorated with Ketjen black@ sulfur composite for promoting polysulfides redox kinetics in lithium-sulfur batteries, *J. Alloys Compd.*, 2022, **907**, 164396.

126 H. Ye, M. Li, T. Liu, Y. Li and J. Lu, Activating Li2S as the lithium-containing cathode in lithium–sulfur batteries, *ACS Energy Lett.*, 2020, **5**(7), 2234–2245.

127 H. Yuan, H. X. Nan, C. Z. Zhao, G. L. Zhu, Y. Lu, X. B. Cheng, Q. B. Liu, C. X. He, J. Q. Huang and Q. Zhang, Slurry-coated sulfur/sulfide cathode with Li

metal anode for all-solid-state lithium-sulfur pouch cells, *Batteries Supercaps*, 2020, **3**(7), 596–603.

128 H. Guo, J. Hu, H. Yuan, N. Wu, Y. Li, G. Liu, N. Qin, K. Liao, Z. Li and W. Luo, Ternary transition metal sulfide as high real energy cathode for lithium–sulfur pouch cell under lean electrolyte conditions, *Small Methods*, 2022, **6**(2), 2101402.

129 C. Geng, W. Qu, Z. Han, L. Wang, W. Lv and Q. H. Yang, Superhigh coulombic efficiency lithium–sulfur batteries enabled by in situ coating lithium sulfide with polymerizable electrolyte additive, *Adv. Energy Mater.*, 2023, **13**(15), 2204246.

130 H. Liu, Z. Wu, H. Wang, X. Niu, H. Li and L. Wang, Chelating-Type Binders toward Stable Cycling and High-Safety Transition-Metal Sulfide-Based Lithium Batteries, *ACS Energy Lett.*, 2024, **9**(9), 4666–4672.

131 F. Flamary-Mespoulie, A. Boulineau, H. Martinez, M. R. Suchomel, C. Delmas, B. Pecquenard and F. Le Cras, Lithium-rich layered titanium sulfides: Cobalt-and Nickel-free high capacity cathode materials for lithium-ion batteries, *Energy Storage Mater.*, 2020, **26**, 213–222.

132 Y. Zhang, Y. Si, W. Guo, X. Li, S. Tang, Z. Zhang, X. Wang and Y. Fu, In situ synthesis of vacancy-rich titanium sulfide confined in a hollow carbon nanocage as an efficient sulfur host for lithium–sulfur batteries, *ACS Appl. Energy Mater.*, 2021, **4**(9), 10104–10113.

133 Y. Hu, Z. Sun, Z. Zhang, S. Liu, F. He, Y. Liu, Z. Zhuang and F. Liu, Lithium-Rich Li2TiS3 Cathode Enables High-Energy Sulfide All-Solid-State Lithium Batteries, *Adv. Energy Mater.*, 2023, **13**(5), 2202756.

134 J. Lu, F. Lian, Y. Zhang, N. Chen, Y. Li, F. Ding and X. Liu, Sulfide cluster vacancies inducing an electrochemical reversibility improvement of titanium disulfide electrode material, *J. Mater. Chem. A*, 2020, **8**(14), 6532–6538.

135 J. Wang, J. Okabe, Y. Komine, H. Notohara, K. Urita, I. Moriguchi and M. Wei, The optimized interface engineering of VS2 as cathodes for high performance all-solid-state lithium-ion battery, *Sci. China Technol. Sci.*, 2022, **65**(8), 1859–1866.

136 Y. Deng, W. Tang, Y. Zhu, J. Ma, M. Zhou, Y. Shi, P. Yan and R. Liu, Catalytic VS2–VO2 Heterostructure that Enables a Self-Supporting Li2S Cathode for Superior Lithium–Sulfur Batteries, *Small Methods*, 2023, **7**(6), 2300186.

137 W. Fan, M. Jiang, G. Liu, W. Weng, J. Yang and X. Yao, Amorphous Titanium Polysulfide Composites with Electronic/Ionic Conduction Networks for All-Solid-State Lithium Batteries, *ACS Appl. Mater. Interfaces*, 2022, **14**(15), 17594–17600.

138 B. Zhao, Z. Ren, G. Tan, Z. Li and J. Xie, Defects on Li2S@ graphene cathode improves the performance of lithium-sulfur battery, A theoretical study, *Acta Mater.*, 2022, **226**, 117632.

139 M. Jeong, H. Kim, W. Lee, S.-J. Ahn, E. Lee and W.-S. Yoon, Stabilizing effects of Al-doping on Ni-rich LiNi0. 80Co0. 15Mn0. 05O2 cathode for Li rechargeable batteries, *J. Power Sources*, 2020, **474**, 228592.

140 Y. Xia, J. Zheng, C. Wang and M. Gu, Designing principle for Ni-rich cathode materials with high energy density for practical applications, *Nano Energy*, 2018, **49**, 434–452.

141 W.-T. Lin, S.-T. Wang, M.-H. Li, C.-M. Huang and S.-W. Lin, A Study on Research and Development Strategies of Total Heat Exchanger Using Systematic Methods, *Adv. Mater. Res.*, 2012, **403–408**, 5299–5302.

142 H. Dong and G. M. Koenig, A review on synthesis and engineering of crystal precursors produced via coprecipitation for multicomponent lithium-ion battery cathode materials, *CrystEngComm*, 2020, **22**(9), 1514–1530.

143 W. Li, L. Yao, X. Zhang, W. Lang, J. Si, J. Yang and L. Li, The effect of chelating agent on synthesis and electrochemical properties of LiNi 0.6 Co 0.2 Mn 0.2 O 2, *SN Appl. Sci.*, 2020, **2**, 1–8.

144 A. Purwanto, C. S. Yudha, U. Ubaidillah, H. Widiyandari, T. Ogi and H. Haerudin, NCA cathode material: Synthesis methods and performance enhancement efforts, *Mater. Res. Express*, 2018, **5**(12), 122001.

145 B. Wang, F.-L. Zhang, X.-A. Zhou, P. Wang, J. Wang, H. Ding, H. Dong, W.-B. Liang, N.-S. Zhang and S.-Y. Li, Which of the nickel-rich NCM and NCA is structurally superior as a cathode material for lithium-ion batteries?, *J. Mater. Chem. A*, 2021, **9**(23), 13540–13551.

146 S. Yin, W. Deng, J. Chen, X. Gao, G. Zou, H. Hou and X. Ji, Fundamental and solutions of microcrack in Ni-rich layered oxide cathode materials of lithium-ion batteries, *Nano Energy*, 2021, **83**, 105854.

147 W. Huang, W. Zhuang, N. Li, M. Gao, W. Li, X. Xing and S. Lu, Nanoscale Y-doped ZrO2 modified LiNi0. 88Co0. 09Al0. 03O2 cathode material with enhanced electrochemical properties for lithium-ion batteries, *Solid State Ionics*, 2019, **343**, 115087.

148 Y.-Y. Wang, Y.-Y. Sun, S. Liu, G.-R. Li and X.-P. Gao, Na-doped LiNi0. 8Co0. 15Al0. 05O2 with excellent stability of both capacity and potential as cathode materials for Li-ion batteries, *ACS Appl. Energy Mater.*, 2018, **1**(8), 3881–3889.

149 G. Yang, K. Pan, Z. Yan, S. Yang, F. Peng, J. Liang, F. Lai, H. Wang, X. Zhang and Q. Li, Fully coating of Mg3B2O6 in nonaqueous solution on Ni-rich LiNi0. 8Co0. 1Mn0. 1O2 secondary particles to improve cycling stability of lithium-ion batteries, *Chem. Eng. J.*, 2023, **452**, 139405.

150 H. Hao, S. Xu, N. Jing, M. Wang, Z. Wang, L. Yang, J. Chen, G. Wang and G. Wang, Negative thermal expansion material: promising for improving electrochemical performance and safety of lithium-ion batteries, *J. Phys. Chem. Lett.*, 2021, **12**(26), 6134–6142.

151 S. Peng, X. Kong, J. Li, J. Zeng and J. Zhao, Alleviating the storage instability of LiNi0. 8Co0. 1Mn0. 1O2 cathode materials by surface modification with poly (acrylic acid), *ACS Sustain. Chem. Eng.*, 2021, **9**(22), 7466–7478.

152 Y. Han, S. Heng, Y. Wang, Q. Qu and H. Zheng, Anchoring interfacial nickel cations on single-crystal LiNi0. 8Co0. 1Mn0. 1O2 cathode surface via controllable electron transfer, *ACS Energy Lett.*, 2020, **5**(7), 2421–2433.

153 C. Xu, P. J. Reeves, Q. Jacquet and C. P. Grey, Phase behavior during electrochemical cycling of Ni-rich cathode materials for Li-ion batteries, *Adv. Energy Mater.*, 2021, **11**(7), 2003404.

154 B. You, Z. Wang, F. Shen, Y. Chang, W. Peng, X. Li, H. Guo, Q. Hu, C. Deng and S. Yang, Research progress of single-crystal nickel-rich cathode materials for lithium ion batteries, *Small Methods*, 2021, **5**(8), 2100234.

155 A. Butt, G. Ali, K. Tul Kubra, R. Sharif, A. Salman, M. Bashir and S. Jamil, Recent advances in enhanced performance of Ni-rich cathode materials for Li-ion batteries: a review, *Energy Technol.*, 2022, **10**(3), 2100775.

156 Y.-H. Luo, H.-X. Wei, L.-B. Tang, Y.-D. Huang, Z.-Y. Wang, Z.-J. He, C. Yan, J. Mao, K. Dai and J.-C. Zheng, Nickel-rich and cobalt-free layered oxide cathode materials for lithium ion batteries, *Energy Storage Mater.*, 2022, **50**, 274–307.

157 I. Nainville, A. Lemarchand and J.-P. Badiali, Passivation of a lithium anode: A simulation model, *Electrochim. Acta*, 1996, **41**(18), 2855–2863.

158 M. Chen, M.-Y. Zhao, K. Liu, F.-M. Liu, Z.-Y. Yuan, X. Qian, R. Wan, C.-S. Li and A.-X. Ding, Structural Reconstruction via Carbon Nanotube Spatially Confined Metal Catalysis: A Morphology-Controlled Approach to Convert Polycyclic Aromatic Hydrocarbon into Carbon Nanofibers for Highly Active Anodes in Li-Ion Batteries, *Inorg. Chem.*, 2025, **64**(7), 3594–3607.

159 M. Chen, F.-M. Liu, M.-Y. Zhao, X. Qian, Z.-Y. Yuan, R. Wan, C.-S. Li, X. Zhang and S. Wang, Controllable synthesis and growth mechanism of cracked cowpea-like NCNT encapsulated with Fe3N nanoparticles for high-performance anode material in lithium-ion batteries, *Carbon*, 2024, **230**, 119579.

160 P. Roy and S. K. Srivastava, Nanostructured anode materials for lithium ion batteries,*J. Mater. Chem. A*, 2015, **3**(6), 2454–2484.

161 M. S. Dresselhaus and G. Dresselhaus, Intercalation compounds of graphite, *Adv. Phys.*, 2002, **51**(1), 1–186.

162 E. Pollak, B. Geng, K.-J. Jeon, I. T. Lucas, T. J. Richardson, F. Wang and R. Kostecki, The interaction of Li+ with single-layer and few-layer graphene, *Nano Lett.*, 2010, **10**(9), 3386–3388.

163 F. Wang, J. Yi, Y. Wang, C. Wang, J. Wang and Y. Xia, Graphite Intercalation Compounds (GICs): A New Type of Promising Anode Material for Lithium-Ion Batteries, *Adv. Energy Mater.*, 2014, **4**(2), 1300600.

164 M. Chen, F.-M. Liu, S.-S. Chen, X. Qian, Y.-J. Zhao, Y. Sun, C.-S. Li, R. Wan and Z.-Y. Yuan, Low-temperature metal-catalyzed synthesis of encapsulated metal oxide nanoparticles in nitrogen-doped carbon nanotubes from carbon nitride as anodic materials of high-performance lithium-ion batteries, *New J. Chem.*, 2023, **47**(7), 3215–3221.

165 M. Chen, F.-M. Liu, H. Zhao, S.-S. Chen, X. Qian, Z.-Y. Yuan and R. Wan, In situ encapsulation of iron oxide nanoparticles into nitrogen-doped carbon nanotubes as anodic electrode materials of lithium ion batteries, *Phys. Chem. Chem. Phys.*, 2022, **24**(44), 27114–27120.

166 Z. Cai, L. Xu, M. Yan, C. Han, L. He, K. M. Hercule, C. Niu, Z. Yuan, W. Xu and L. Qu, Manganese oxide/carbon yolk–shell nanorod anodes for high capacity lithium batteries, *Nano Lett.*, 2015, **15**(1), 738–744.

167 F.-M. Liu, M.-Y. Zhao, S. Wang, M. Chen, X. Qian, Z.-Y. Yuan, Y. Sun, C.-S. Li and R. Wan, A new synthesis strategy for nitrogen-doped carbon nanofibers with cobalt oxide nanoparticles as anodic electrode materials for lithium ion batteries, *Chem. Commun.*, 2023, **59**(85), 12771–12774.

168 D. Aurbach, A. Nimberger, B. Markovsky, E. Levi, E. Sominski and A. Gedanken, Nanoparticles of SnO produced by sonochemistry as anode materials for rechargeable lithium batteries, *Chem. Mater.*, 2002, **14**(10), 4155–4163.

169 X. Tan, Y. Wu, X. Lin, A. Zeb, X. Xu, Y. Luo and J. Liu, Application of MOF-derived transition metal oxides and composites as anodes for lithium-ion batteries, *Inorg. Chem. Front.*, 2020, **7**(24), 4939–4955.

170 J. Jang, S. H. Song, H. Kim, J. Moon, H. Ahn, K.-I. Jo, J. Bang, H. Kim and J. Koo, Janus graphene oxide sheets with Fe3O4 nanoparticles and polydopamine as anodes for lithium-ion batteries, *ACS Appl. Mater. Interfaces*, 2021, **13**(12), 14786–14795.

171 K.-H. Tian, C.-Q. Duan, Q. Ma, X.-L. Li, Z.-Y. Wang, H.-Y. Sun, S.-H. Luo, D. Wang and Y.-G. Liu, High-entropy chemistry stabilizing spinel oxide (CoNiZnXMnLi) 3O4 (X= Fe, Cr) for high-performance anode of Li-ion batteries, *Rare Met.*, 2022, **41**(4), 1265–1275.

172 J.-L. Xu, X. Zhang, Y.-X. Miao, M.-X. Wen, W.-J. Yan, P. Lu, Z.-R. Wang and Q. Sun, In-situ plantation of Fe3O4@ C nanoparticles on reduced graphene oxide nanosheet as high-performance anode for lithium/sodium-ion batteries, *Appl. Surf. Sci.*, 2021, **546**, 149163.

173 J. Ma, Y. Kong, S. Liu, Y. Li, J. Jiang, Q. Zhou, Y. Huang and S. Han, Flexible phosphorus-doped graphene/metal–organic framework-derived porous Fe2O3 anode for lithium-ion battery, *ACS Appl. Energy Mater.*, 2020, **3**(12), 11900–11906.

174 Z. Cao, Y. Yang, J. Qin and Z. Su, A core-shell porous MnO2/Carbon nanosphere composite as the anode of lithium-ion batteries, *J. Power Sources*, 2021, **491**, 229577.

175 Y.-P. Liu, C.-X. Xu, W.-Q. Ren, L.-Y. Hu, W.-B. Fu, W. Wang, H. Yin, B.-H. He, Z.-H. Hou and L. Chen, Self-template synthesis of peapod-like MnO@ N-doped hollow carbon nanotubes as an advanced anode for lithium-ion batteries, *Rare Met.*, 2023, **42**(3), 929–939.

176 B. B. Kopuklu, A. Tasdemir, S. A. Gursel and A. Yurum, High stability graphene oxide aerogel supported ultrafine Fe3O4 particles with superior performance as a Li-ion battery anode, *Carbon*, 2021, **174**, 158–172.

177 G. Xu, G.-Y. Wang, X.-F. Zhang, Z.-P. Deng, L.-H. Huo and S. Gao, Biotemplate synthesis of mesoporous α-Fe2O3 hierarchical structure with assisted pseudocapacitive as an anode for long-life lithium ion batteries, *Ceram. Int.*, 2021, **47**(3), 3772–3779.

178 T. X. Nguyen, C.-C. Tsai, J. Patra, O. Clemens, J.-K. Chang and J.-M. Ting, Co-free high entropy spinel oxide anode with controlled morphology and crystallinity for outstanding charge/discharge performance in Lithium-ion batteries, *Chem. Eng. J.*, 2022, **430**, 132658.

179 Y.-H. Sun, M.-X. Huang, D.-C. Guan, G.-L. Zhang, J.-L. Wei, J.-M. Nan and F.-Y. Yi, Influence of the Sn (Fe)–C bonds content in SnFe2O4@ reduced graphene oxide composites on the electrochemical behavior of lithium-ion batteries, *J. Alloys Compd.*, 2021, **854**, 157297.

180 L. Chen, B. Tang, H. Li, B. Wang and B. Huang, Porous SnO2/Co3O4 nanocubes anchored onto reduced graphene oxide as a high-performance anode for lithium-ion batteries, *Solid State Ionics*, 2023, **396**, 116241.

181 M. Tu, L. Y. R. Jia, X. Kong, R. Zhang and B. Xu, Chitosan modulated engineer tin dioxide nanoparticles well dispersed by reduced graphene oxide for high and stable lithium-ion storage, *J. Colloid Interface Sci.*, 2023, **635**, 105–116.

182 H. Ying, T. Yang, S. Zhang, R. Guo, J. Wang and W.-Q. Han, Dual Immobilization of SnO x Nanoparticles by N-Doped Carbon and TiO2 for High-Performance Lithium-Ion Battery Anodes, *ACS Appl. Mater. Interfaces*, 2020, **12**(50), 55820–55829.

183 W. Wang, Y. Li, L. Li, L. Wang and K. Wang, SnO2/TiO2 nanocomposite prepared by pulsed laser deposition as anode material for flexible quasi-solid-state lithium-ion batteries, *Int. J. Electrochem. Sci.*, 2020, **15**(12), 11709–11722.

184 J. Zhang, L. Li, J. Chen, N. He, K. Yu and C. Liang, Controllable SnO2/ZnO@ PPy hollow nanotubes prepared by electrospinning technology used as anode for lithium ion battery, *J. Phys. Chem. Solids*, 2021, **150**, 109861.

185 H. Yu, Y. Zhang, L. Li, Z. Ding, Y. Chen, Q. Yuan, R. Sun, K. Li, C. Liu and J. Wu, SnO2 nanoparticles embedded in 3D hierarchical honeycomb-like carbonaceous network for high-performance lithium ion battery, *J. Alloys Compd.*, 2021, **858**, 157716.

186 B. Li, S. Bao, Q. Tan, R. Zhang, L. Shan, C. Wang, G. Wu and B. Xu, Engineering tin dioxide quantum dots in a hierarchical graphite and graphene oxide framework for lithium-ion storage, *J. Colloid Interface Sci.*, 2021, **600**, 649–659.

187 X. Li, Z. Zhao, Y. Deng, D. Ouyang, X. Yang, S. Chen and P. Liu, Interfacial engineering in SnO2-embedded graphene anode materials for high performance lithium-ion batteries, *Sci. Rep.*, 2024, **14**(1), 16751.

188 Z. Shen, X. Guo, H. Ding, D. Yu, Y. Chen, N. Li, H. Zhou, S. Zhang, J. Wu and H. Pang, Construction of ternary Sn/SnO2/nitrogen-doped carbon superstructures as anodes for advanced lithium-ion batteries, *Nano Res.*, 2024, **17**(11), 9721–9727.

189 H. Lyu, J. Li, T. Wang, B. P. Thapaliya, S. Men, C. J. Jafta, R. Tao, X.-G. Sun and S. Dai, Carbon coated porous titanium niobium oxides as anode materials of lithium-ion batteries for extreme fast charge applications, *ACS Appl. Energy Mater.*, 2020, **3**(6), 5657–5665.

190 H. G. Oh and S.-K. Park, Two-dimensional composite of Nitrogen-doped graphitic Carbon-coated cobaltosic oxide nanocrystals on MXene nanosheets as High-performance anode for Lithium-ion batteries, *Appl. Surf. Sci.*, 2021, **564**, 150415.

191 L. Wan, D. H. Chua, H. Sun, L. Chen, K. Wang, T. Lu and L. Pan, Construction of two-dimensional bimetal (Fe-Ti) oxide/carbon/MXene architecture from titanium carbide MXene for ultrahigh-rate lithium-ion storage, *J. Colloid Interface Sci.*, 2021, **588**, 147–156.

192 A. T. A. Ahmed, R. Soni, A. S. Ansari, C. Y. Lee, H.-S. Kim, H. Im and C. Bathula, Biowaste-derived graphitic carbon interfaced TiO2 as anode for lithium-ion battery, *Surf. Interfaces*, 2022, **35**, 102404.

193 N. Firdous, N. Arshad, N. Muzaffar and P. Norby, Effect of Mg+ 2 and Bi+ 3 co-doping on structural and electrochemical properties of lithium titanium oxide for use as anode material in lithium-ion battery, *J. Electroanal. Chem.*, 2020, **876**, 114515.

194 Y. Chen, H. Chen, F.-H. Du, X. Shen, Z. Ji, H. Zhou and A. Yuan, In-situ construction of nano-sized Ni-NiO-MoO2 heterostructures on holey reduced graphene oxide nanosheets as high-capacity lithium-ion battery anodes, *J. Alloys Compd.*, 2022, **926**, 166847.

195 M. Du, Q. Li and H. Pang, Oxalate-derived porous prismatic nickel/nickel oxide nanocomposites toward lithium-ion battery, *J. Colloid Interface Sci.*, 2020, **580**, 614–622.

196 Y. Song, J. Hwang, S. Lee, B. Thirumalraj, J.-H. Kim, P. Jenei, J. Gubicza and H. Choe, Synthesis of a high-capacity NiO/Ni foam anode for advanced lithium-ion batteries, *Adv. Eng. Mater.*, 2020, **22**(11), 2000351.

197 M. A. A. M. Abdah, M. Mokhtar, L. T. Khoon, K. Sopian, N. A. Dzulkurnain, A. Ahmad, Y. Sulaiman, F. Bella and M. S. Su'ait, Synthesis and electrochemical characterizations of poly (3, 4-ethylenedioxythiophene/manganese oxide coated on porous carbon nanofibers as a potential anode for lithium-ion batteries, *Energy Rep.*, 2021, **7**, 8677–8687.

198 B. Xiao, G. Wu, T. Wang, Z. Wei, Y. Sui, B. Shen, J. Qi, F. Wei, Q. Meng and Y. Ren, High entropy oxides (FeNiCrMnX) 3O4 (X= Zn, Mg) as anode materials for lithium ion batteries, *Ceram. Int.*, 2021, **47**(24), 33972–33977.

199 S. Yuan, Y. B. Liu, D. Xu, D. L. Ma, S. Wang, X. H. Yang, Z. Y. Cao and X. B. Zhang, Pure single-crystalline Na1. 1V3O7. 9 nanobelts as superior cathode materials for rechargeable sodium-ion batteries, *Adv. Sci.*, 2015, **2**(3), 1400018.

200 M. Li, Y. Gao, N. Chen, X. Meng, C. Wang, Y. Zhang, D. Zhang, Y. Wei, F. Du and G. Chen, Cu3V2O8 nanoparticles as intercalation-type anode material for lithium-ion batteries, *Chem.–Eur. J.*, 2016, **22**(32), 11405–11412.

201 L. Y. W. Linda, *Crystal Structure and Morphology of Band-Gap Engineered Titania and Titanates via Hydrothermal Synthesis*, Nanyang Technological University, 2010.

202 M. Shirpour, J. Cabana and M. Doeff, Lepidocrocite-type layered titanate structures: new lithium and sodium ion intercalation anode materials, *Chem. Mater.*, 2014, **26**(8), 2502–2512.

203 T. Hatchard and J. Dahn, In situ XRD and electrochemical study of the reaction of lithium with amorphous silicon, *J. Electrochem. Soc.*, 2004, **151**(6), A838.

204 M. Obrovac, L. Christensen, D. B. Le and J. R. Dahn, Alloy design for lithium-ion battery anodes, *J. Electrochem. Soc.*, 2007, **154**(9), A849.

205 J. Yin, M. Wada, S. Yoshida, K. Ishihara, S. Tanase and T. Sakai, New Ag-Sn alloy anode materials for lithium-ion batteries, *J. Electrochem. Soc.*, 2003, **150**(8), A1129.

206 B. Kang and G. Ceder, Battery materials for ultrafast charging and discharging, *Nature*, 2009, **458**(7235), 190–193.

207 N. Liu, H. Wu, M. T. McDowell, Y. Yao, C. Wang and Y. Cui, A yolk-shell design for stabilized and scalable Li-ion battery alloy anodes, *Nano Lett.*, 2012, **12**(6), 3315–3321.

208 L.-F. Cui, Y. Yang, C.-M. Hsu and Y. Cui, Carbon– silicon core– shell nanowires as high capacity electrode for lithium ion batteries, *Nano Lett.*, 2009, **9**(9), 3370–3374.

209 M. T. McDowell, I. Ryu, S. W. Lee, C. Wang, W. D. Nix and Y. Cui, Studying the kinetics of crystalline silicon nanoparticle lithiation with in situ transmission electron microscopy, *Adv. Mater.*, 2012, **24**(45), 6034–6041.

210 H. Song, H. X. Wang, Z. Lin, X. Jiang, L. Yu, J. Xu, Z. Yu, X. Zhang, Y. Liu and P. He, Highly Connected Silicon–Copper Alloy Mixture Nanotubes as High-Rate and Durable Anode Materials for Lithium-Ion Batteries, *Adv. Funct. Mater.*, 2016, **26**(4), 524–531.

211 W. Weppner and R. A. Huggins, Determination of the kinetic parameters of mixed-conducting electrodes and application to the system Li3Sb, *J. Electrochem. Soc.*, 1977, **124**(10), 1569.

212 J. Wang, I. Raistrick and R. A. Huggins, Behavior of some binary lithium alloys as negative electrodes in organic solvent-based electrolytes, *J. Electrochem. Soc.*, 1986, **133**(3), 457.

213 W. Xianming, T. Nishina and I. Uchida, Lithium alloy formation at bismuth thin layer electrode and its kinetics in propylene carbonate electrolyte, *J. Power Sources*, 2002, **104**(1), 90–96.

214 L. Zhang, X. Zhao, X. Jiang, C. Lv and G. Cao, Study on the insertion behaviors of lithium-ions into CoFe3Sb12 based electrodes, *J. Power Sources*, 2001, **94**(1), 92–96.

215 A. Trifonova, M. Wachtler, M. Winter and J. Besenhard, Sn-Sb and Sn-Bi alloys as anode materials for lithium-ion batteries, *Ionics*, 2002, **8**, 321–328.

216 M. V. Reddy, G. Subba Rao and B. Chowdari, Metal oxides and oxysalts as anode materials for Li ion batteries, *Chem. Rev.*, 2013, **113**(7), 5364–5457.

217 J. B. Goodenough and K.-S. Park, The Li-ion rechargeable battery: a perspective, *J. Am. Chem. Soc.*, 2013, **135**(4), 1167–1176.

218 Y. Oumellal, A. Rougier, G. Nazri, J. Tarascon and L. Aymard, Metal hydrides for lithium-ion batteries, *Nat. Mater.*, 2008, **7**(11), 916–921.

219 X. Li, X. He, C. Shi, B. Liu, Y. Zhang, S. Wu, Z. Zhu and J. Zhao, Synthesis of One-Dimensional Copper Sulfide Nanorods as High-Performance Anode in Lithium Ion Batteries, *ChemSusChem*, 2014, **7**(12), 3328–3333.

220 M. Zhou, N. Peng, Z. Liu, Y. Xi, H. He, Y. Xia, Z. Liu and S. Okada, Synthesis of sub-10 nm copper sulphide rods as high-performance anode for long-cycle life Li-ion batteries, *J. Power Sources*, 2016, **306**, 408–412.

221 H.-C. Tao, X.-L. Yang, L.-L. Zhang and S.-B. Ni, One-pot facile synthesis of CuS/graphene composite as anode materials for lithium ion batteries, *J. Phys. Chem. Solids*, 2014, **75**(11), 1205–1209.

222 D. Yuan, G. Huang, F. Zhang, D. Yin and L. Wang, Facile synthesis of CuS/rGO composite with enhanced electrochemical lithium-storage properties through microwave-assisted hydrothermal method, *Electrochim. Acta*, 2016, **203**, 238–245.

223 H. Li, Y. Wang, J. Huang, Y. Zhang and J. Zhao, Microwave-assisted synthesis of CuS/graphene composite for enhanced lithium storage properties, *Electrochim. Acta*, 2017, **225**, 443–451.

224 Y. Wang, H. Li, Y. Zhang, Y. Peng, P. Zhang and J. Zhao, Self-templating thermolysis synthesis of Cu 2–x S@ M (M= C, TiO 2, MoS 2) hollow spheres and their application in rechargeable lithium batteries, *Nano Res.*, 2018, **11**, 831–844.

225 Y. Wang, Y. Zhang, H. Li, Y. Peng, J. Li, J. Wang, B.-J. Hwang and J. Zhao, Preparation of one-dimensional bamboo-like Cu2-xS@ C nanorods with enhanced lithium storage properties, *Electrochim. Acta*, 2017, **247**, 271–280.

226 J. Yan, H. Huang, J. Zhang, Z. Liu and Y. Yang, A study of novel anode material CoS2 for lithium ion battery, *J. Power Sources*, 2005, **146**(1–2), 264–269.

227 Q. Wang, L. Jiao, Y. Han, H. Du, W. Peng, Q. Huan, D. Song, Y. Si, Y. Wang and H. Yuan, CoS2 hollow spheres: fabrication and their application in lithium-ion batteries, *J. Phys. Chem. C*, 2011, **115**(16), 8300–8304.

228 Z. Wang, L. Pan, H. Hu and S. Zhao, Co 9 S 8 nanotubes synthesized on the basis of nanoscale Kirkendall effect and their magnetic and electrochemical properties, *CrystEngComm*, 2010, **12**(6), 1899–1904.

229 X. Zhang, H. Wang and G. Wang, Cobalt sulfide nanoparticles anchored in three-dimensional carbon nanosheet networks for lithium and sodium ion batteries with enhanced electrochemical performance, *J. Colloid Interface Sci.*, 2017, **492**, 41–50.

230 G. Qu, H. Geng, D. Ge, M. Tang, J. Zheng and H. Gu, Porous carbon-wrapped mesoporous Co9S8 fibers as stable anode for Li-ion batteries, *Electrochim. Acta*, 2016, **211**, 305–312.

231 Y. Zhou, D. Yan, H. Xu, S. Liu, J. Yang and Y. Qian, Multiwalled carbon nanotube@ aC@ Co 9 S 8 nanocomposites: A high-capacity and long-life anode material for advanced lithium ion batteries, *Nanoscale*, 2015, **7**(8), 3520–3525.

232 S. Liu, J. Wang, J. Wang, F. Zhang and L. Wang, Highly uniform Co9S8 nanoparticles grown on graphene nanosheets as advanced anode materials for improved Li-storage performance, *Appl. Surf. Sci.*, 2016, **390**, 86–91.

233 P. Zeng, J. Li, M. Ye, K. Zhuo and Z. Fang, In situ formation of Co9S8/N-C hollow nanospheres by pyrolysis and sulfurization of ZIF-67 for high-performance lithium-ion batteries, *Chem.–Eur. J.*, 2017, **23**(40), 9517–9524.

234 Y. Zhou, D. Yan, H. Xu, J. Feng, X. Jiang, J. Yue, J. Yang and Y. Qian, Hollow nanospheres of mesoporous Co9S8 as a high-capacity and long-life anode for advanced lithium ion batteries, *Nano Energy*, 2015, **12**, 528–537.

235 H. Wang, J. Ma, S. Liu, L. Nie, Y. Chai, X. Yang and R. Yuan, CoS/CNTs hybrid structure for improved performance lithium ion battery, *J. Alloys Compd.*, 2016, **676**, 551–556.

236 Y. Tan, M. Liang, P. Lou, Z. Cui, X. Guo, W. Sun and X. Yu, In situ fabrication of CoS and NiS nanomaterials anchored on reduced graphene oxide for reversible lithium storage, *ACS Appl. Mater. Interfaces*, 2016, **8**(23), 14488–14493.

237 C. Xu, Y. Jing, J. He, K. Zhou, Y. Chen, Q. Li, J. Lin and W. Zhang, Self-assembled interwoven CoS2/CNTs/graphene architecture as anode for high-performance lithium ion batteries, *J. Alloys Compd.*, 2017, **708**, 1178–1183.

238 J. Zhang, L. Yu and X. W. D. Lou, Embedding CoS 2 nanoparticles in N-doped carbon nanotube hollow frameworks for enhanced lithium storage properties, *Nano Res.*, 2017, **10**, 4298–4304.

239 J. He, Y. Chen, P. Li, F. Fu, Z. Wang and W. Zhang, Self-assembled CoS2 nanoparticles wrapped by CoS2-quantum-dots-anchored graphene nanosheets as superior-capability anode for lithium-ion batteries, *Electrochim. Acta*, 2015, **182**, 424–429.

240 S. Tao, W. Huang, H. Xie, J. Zhang, Z. Wang, W. Chu, B. Qian and L. Song, Formation of graphene-encapsulated CoS 2 hybrid composites with hierarchical structures for high-performance lithium-ion batteries, *RSC Adv.*, 2017, **7**(63), 39427–39433.

241 J. Guo, F. Li, Y. Sun, X. Zhang and L. Tang, Graphene-encapsulated cobalt sulfides nanocages with excellent anode performances for lithium ion batteries, *Electrochim. Acta*, 2015, **167**, 32–38.

242 B. Qiu, X. Zhao and D. Xia, In situ synthesis of CoS2/RGO nanocomposites with enhanced electrode performance for lithium-ion batteries, *J. Alloys Compd.*, 2013, **579**, 372–376.

243 W. Chen, T. Li, Q. Hu, C. Li and H. Guo, Hierarchical CoS2@ C hollow microspheres constructed by nanosheets with superior lithium storage, *J. Power Sources*, 2015, **286**, 159–165.

244 Q. Wang, R. Zou, W. Xia, J. Ma, B. Qiu, A. Mahmood, R. Zhao, Y. Yang, D. Xia and Q. Xu, Facile synthesis of ultrasmall CoS2 nanoparticles within thin N-doped porous carbon shell for high performance lithium-ion batteries, *Small*, 2015, **11**(21), 2511–2517.

245 T. Stephenson, Z. Li, B. Olsen and D. Mitlin, Lithium ion battery applications of molybdenum disulfide (MoS 2) nanocomposites, *Energy Environ. Sci.*, 2014, **7**(1), 209–231.

246 Y. Wang, L. Yu and X. W. Lou, Synthesis of highly uniform molybdenum–glycerate spheres and their conversion into hierarchical MoS2 hollow nanospheres for lithium-ion batteries, *Angew. Chem.*, 2016, **128**(26), 7549–7552.

247 X. Y. Yu, H. Hu, Y. Wang, H. Chen and X. W. Lou, Ultrathin MoS2 nanosheets supported on N-doped carbon nanoboxes with enhanced lithium storage and electrocatalytic properties, *Angew. Chem.*, 2015, **127**(25), 7503–7506.

248 (*a*) J. Zhang, T. Wang, P. Liu, S. Liu, R. Dong, X. Zhuang, M. Chen and X. Feng, *Energy Environ. Sci.*, 2016, **9**, 2789; (*b*) M. Chhowalla, H. S. Shin, G. Eda, L.-J. Li, K. P. Loh and H. Zhang, *Nat. Chem*, 2013, **5**, 263.

249 Y. Zhu, X. Fan, L. Suo, C. Luo, T. Gao and C. Wang, Electrospun FeS2@ carbon fiber electrode as a high energy density cathode for rechargeable lithium batteries, *ACS Nano*, 2016, **10**(1), 1529–1538.

250 W. Huang, S. Li, X. Cao, C. Hou, Z. Zhang, J. Feng, L. Ci, P. Si and Q. Chi, Metal–organic framework derived iron sulfide–carbon core–shell nanorods as a conversion-type battery material, *ACS Sustain. Chem. Eng.*, 2017, **5**(6), 5039–5048.

251 H.-H. Fan, H.-H. Li, K.-C. Huang, C.-Y. Fan, X.-Y. Zhang, X.-L. Wu and J.-P. Zhang, Metastable marcasite-FeS2 as a new anode material for lithium ion batteries: CNFs-improved lithiation/delithiation reversibility and Li-storage properties, *ACS Appl. Mater. Interfaces*, 2017, **9**(12), 10708–10716.

252 H. Xue, Y. Denis, J. Qing, X. Yang, J. Xu, Z. Li, M. Sun, W. Kang, Y. Tang and C.-S. Lee, Pyrite FeS 2 microspheres wrapped by reduced graphene oxide as high-performance lithium-ion battery anodes, *J. Mater. Chem. A*, 2015, **3**(15), 7945–7949.

253 X. Xu, T. Cai, Z. Meng, H. Ying, Y. Xie, X. Zhu and W.-Q. Han, FeS2 nanocrystals prepared in hierarchical porous carbon for lithium-ion battery, *J. Power Sources*, 2016, **331**, 366–372.

254 J. Jiang, Y. Li, J. Liu and X. Huang, Building one-dimensional oxide nanostructure arrays on conductive metal substrates for lithium-ion battery anodes, *Nanoscale*, 2011, **3**(1), 45–58.

255 A. Samad, A. Shafique and Y.-H. Shin, Adsorption and diffusion of mono, di, and trivalent ions on two-dimensional TiS2, *Nanotechnology*, 2017, **28**(17), 175401.

256 W. Sun, L. Suo, F. Wang, N. Eidson, C. Yang, F. Han, Z. Ma, T. Gao, M. Zhu and C. Wang, "Water-in-Salt" electrolyte enabled LiMn2O4/TiS2 Lithium-ion batteries, *Electrochem. Commun.*, 2017, **82**, 71–74.

257 B. Radisavljevic, A. Radenovic, J. Brivio, I. V. Giacometti and A. Kis, *Nat. Nanotechnol.*, 2011, **6**(3), 147–150.

258 S. Liu, B. Shen, Y. Niu and M. Xu, Fabrication of WS2-nanoflowers@ rGO composite as an anode material for enhanced electrode performance in lithium-ion batteries, *J. Colloid Interface Sci.*, 2017, **488**, 20–25.

259 T. Wang, C. Sun, M. Yang, L. Zhang, Y. Shao, Y. Wu and X. Hao, Enhanced reversible lithium ion storage in stable 1T@ 2H WS2 nanosheet arrays anchored on carbon fiber, *Electrochim. Acta*, 2018, **259**, 1–8.

260 Q. Pang, Y. Gao, Y. Zhao, Y. Ju, H. Qiu, Y. Wei, B. Liu, B. Zou, F. Du and G. Chen, Improved lithium-ion and sodium-ion storage properties from few-layered WS2 nanosheets embedded in a mesoporous CMK-3 matrix, *Chem.–Eur. J.*, 2017, **23**(29), 7074–7080.

261 L. Zhang, W. Fan and T. Liu, Flexible hierarchical membranes of WS 2 nanosheets grown on graphene-wrapped electrospun carbon nanofibers as advanced anodes for highly reversible lithium storage, *Nanoscale*, 2016, **8**(36), 16387–16394.

262 Y. Wang, D. Kong, W. Shi, B. Liu, G. J. Sim, Q. Ge and H. Y. Yang, Ice templated free-standing hierarchically WS2/CNT-rGO aerogel for high-performance rechargeable lithium and sodium ion batteries, *Adv. Energy Mater.*, 2016, **6**(21), 1601057.

263 J. Zou, C. Liu, Z. Yang, C. Qi, X. Wang, Q. Qiao, X. Wu and T. Ren, Multilayer-Cake WS2/C Nanocomposite as a High-Performance Anode Material for Lithium-Ion Batteries:"Regular" and "Alternate", *ChemElectroChem*, 2017, **4**(9), 2232–2236.

264 W. Fang, H. Zhao, Y. Xie, J. Fang, J. Xu and Z. Chen, Facile hydrothermal synthesis of VS2/graphene nanocomposites with superior high-rate capability as lithium-ion battery cathodes, *ACS Appl. Mater. Interfaces*, 2015, **7**(23), 13044–13052.

265 Y. Zhou, J. Tian, H. Xu, J. Yang and Y. Qian, VS4 nanoparticles rooted by aC coated MWCNTs as an advanced anode material in lithium ion batteries, *Energy Storage Mater.*, 2017, **6**, 149–156.

266 J.-T. Jang, S. Jeong, J.-W. Seo, M.-C. Kim, E. Sim, Y. Oh, S. Nam, B. Park and J. Cheon, Ultrathin zirconium disulfide nanodiscs, *J. Am. Chem. Soc.*, 2011, **133**(20), 7636–7639.

267 H. Mukaibo, A. Yoshizawa, T. Momma and T. Osaka, Particle size and performance of SnS2 anodes for rechargeable lithium batteries, *J. Power Sources*, 2003, **119**, 60–63.

268 S. Liu, X. Yin, L. Chen, Q. Li and T. Wang, Synthesis of self-assembled 3D flowerlike SnS2 nanostructures with enhanced lithium ion storage property, *Solid State Sci.*, 2010, **12**(5), 712–718.

269 J. Zai, K. Wang, Y. Su, X. Qian and J. Chen, High stability and superior rate capability of three-dimensional hierarchical SnS2 microspheres as anode material in lithium ion batteries, *J. Power Sources*, 2011, **196**(7), 3650–3654.

270 J. Xia, G. Li, Y. Mao, Y. Li, P. Shen and L. Chen, Hydrothermal growth of SnS 2 hollow spheres and their electrochemical properties, *CrystEngComm*, 2012, **14**(13), 4279–4283.

271 J. Wang, J. Liu, H. Xu, S. Ji, J. Wang, Y. Zhou, P. Hodgson and Y. Li, Gram-scale and template-free synthesis of ultralong tin disulfide nanobelts and their lithium ion storage performances, *J. Mater. Chem. A*, 2013, **1**(4), 1117–1122.

272 T.-J. Kim, C. Kim, D. Son, M. Choi and B. Park, Novel SnS2-nanosheet anodes for lithium-ion batteries, *J. Power Sources*, 2007, **167**(2), 529–535.

273 C. Zhai, N. Du and H. Z. D. Yang, Large-scale synthesis of ultrathin hexagonal tin disulfide nanosheets with highly reversible lithium storage, *Chem. Commun.*, 2011, **47**(4), 1270–1272.

274 S. Liu, X. Yin, Q. Hao, M. Zhang, L. Li, L. Chen, Q. Li, Y. Wang and T. Wang, Chemical bath deposition of SnS2 nanowall arrays with improved electrochemical performance for lithium ion battery, *Mater. Lett.*, 2010, **64**(21), 2350–2353.

275 H. Zhong, G. Yang, H. Song, Q. Liao, H. Cui, P. Shen and C.-X. Wang, Vertically aligned graphene-like SnS2 ultrathin nanosheet arrays: excellent energy storage, catalysis, photoconduction, and field-emitting performances, *J. Phys. Chem. C*, 2012, **116**(16), 9319–9326.

276 X.-L. Gou, J. Chen and P.-W. Shen, Synthesis, characterization and application of SnSx (x= 1, 2) nanoparticles, *Mater. Chem. Phys.*, 2005, **93**(2–3), 557–566.

277 Y. Du, Z. Yin, X. Rui, Z. Zeng, X.-J. Wu, J. Liu, Y. Zhu, J. Zhu, X. Huang and Q. Yan, A facile, relative green, and inexpensive synthetic approach toward large-scale production of SnS 2 nanoplates for high-performance lithium-ion batteries, *Nanoscale*, 2013, **5**(4), 1456–1459.

278 H. S. Kim, Y. H. Chung, S. H. Kang and Y. E. Sung, Electrochemical behavior of carbon-coated SnS2 for use as the anode in lithium-ion batteries, *Electrochim. Acta*, 2009, **54**(13), 3606–3610.

279 M. He, L.-X. Yuan and Y.-H. Huang, Acetylene black incorporated three-dimensional porous SnS 2 nanoflowers with high performance for lithium storage, *RSC Adv.*, 2013, **3**(10), 3374–3383.

280 J.-G. Kang, G.-H. Lee, K.-S. Park, S.-O. Kim, S. Lee, D.-W. Kim and J.-G. Park, Three-dimensional hierarchical self-supported multi-walled carbon nanotubes/tin (iv) disulfide nanosheets heterostructure electrodes for high power Li ion batteries, *J. Mater. Chem.*, 2012, **22**(18), 9330–9337.

281 L. Ji, H. L. Xin, T. R. Kuykendall, S.-L. Wu, H. Zheng, M. Rao, E. J. Cairns, V. Battaglia and Y. Zhang, SnS 2 nanoparticle loaded graphene nanocomposites for superior energy storage, *Phys. Chem. Chem. Phys.*, 2012, **14**(19), 6981–6986.

282 H. Ren, J. Wang, Y. Cao, W. Luo and Y. Sun, Nickel sulfide nanoparticle anchored reduced graphene oxide with improved lithium storage properties, *Mater. Res. Bull.*, 2021, **133**, 111047.

283 H.-H. Kim, K.-H. Kim, J. Lee and S.-H. Hong, Electrochemical properties and reaction mechanism of NiTi2S4 ternary metal sulfide as an anode for lithium ion battery, *ACS Sustain. Chem. Eng.*, 2021, **9**(29), 9680–9688.

284 X. Jin, L. Sheng, L. Jiang, Z. Xiao, D. Wang, M. Jiang, X. Lin, X. Zhang, X. Duan and J. Shi, Manganese sulfate-derived α/γ-MnS embedded in N-doped layered carbon for high-

performance lithium-ion batteries, *Mater. Today Chem.*, 2022, **24**, 100992.

285 Z. Xiao, L. Gao, S. Su, D. Li, L. Cao, L. Ye, B. Zhang, L. Ming and X. Ou, Efficient fabrication of metal sulfides/graphite anode materials derived from spent lithium-ion batteries by gas sulfidation process, *Mater. Today Energy*, 2021, **21**, 100821.

286 N. M. Santhosh, N. Shaji, P. Stražar, G. Filipič, J. Zavašnik, C. W. Ho, M. Nanthagopal, C. W. Lee and U. Cvelbar, Advancing Li-ion storage performance with hybrid vertical carbon/Ni3S2-based electrodes, *J. Energy Chem.*, 2022, **67**, 8–18.

287 X.-G. Deng, L.-Q. Fan, X.-Y. Fu, T. Tang, S.-H. Lin, L. Chen, F.-D. Yu, Y.-F. Huang, M.-L. Huang and J.-H. Wu, Carbon-reinforced Ni3S2/Ti3C2Tx MXene composite as an anode for superior-performance lithium-ion capacitors, *J. Colloid Interface Sci.*, 2024, **661**, 237–248.

288 Z. Fu, Y. Wang, Y. Xu, H. Li, Q. Qiao, P. Yin, F. Wang, X. Guo and Z. Yang, The surface coating strategy enhances the lithium storage performance of Ni3S2@ PPy self-supporting as anode materials for lithium-ion batteries, *J. Alloys Compd.*, 2022, **926**, 166889.

289 I. Khan, R. Medwal, S. Fareed, A. Farid, J. V. Vas, M. Reddy and R. S. Rawat, Nanostructured polycrystalline Ni3S2 as electrode material for lithium ion batteries, *Mater. Res. Express*, 2020, **7**(1), 015517.

290 J.-L. Xu, L. Liu, Y.-H. Sun, W.-J. Yan, Z.-R. Wang and Q. Sun, Ni-doped Ni3S2 nanoflake intertexture grown on graphene oxide as sheet-like anode for high-performance lithium-ion batteries, *J. Alloys Compd.*, 2020, **835**, 155418.

291 L. Jiao, Y. Luo and L. Cheng, Ni3S2/NiSe2 hollow spheres with low bonding energy Ni-Se bonds for excellent lithium-ion charge-discharge stability, *Colloids Surf., A*, 2023, **664**, 131122.

292 Y. Fan, X. He, H. Li, Y. Huang, C. Sun, H. Liu, E. Huangzhang, F. Sun, X. Zhao and J. Nan, Lithiophilic Ni3S2 layer decorated nickel foam (Ni3S2@ Ni foam) with fast ion transfer kinetics for long-life lithium metal anodes, *Chem. Eng. J.*, 2022, **450**, 138384.

293 C. Wang, Q. Han, R. Xie, B. Wang, T. He, W. Xie, Q. Tang, Y. Li, J. Xu and B. Yu, Fabrication of petal-like Ni3S2 nanosheets on 3D carbon nanotube foams as high-performance anode materials for Li-ion batteries, *Electrochim. Acta*, 2020, **331**, 135383.

294 M. M. Sanad, S. W. Arafat, Z. K. Heiba, A. I. Alakhras and A. Toghan, Fabrication of Ni3S2-functionalized V2O3 nanospheres as promising anode materials for rechargeable batteries and supercapacitors, *Appl. Phys. A*, 2023, **129**(7), 516.

295 S. Jiang, M. Mao, M. Pang, Y. Du, W. He, M. Pang, R. Wang, Q. Pan and J. Zhao, Cost effective synthesis hetero-structured N-doped C-coated Ni9S8/Ni3S2/NiS1. 03 nanoparticles attached on 3D reduced graphene oxide anode to exceptional Li-ion performance, *Appl. Surf. Sci.*, 2023, **635**, 157697.

296 Q. Liang, J. Xu, T. Huang, S. Wang and H. Li, Preparation of VS2/rGO Nanosheet Composite Materials as High Capacity Anodes for Lithium-ion Batteries, *ChemistrySelect*, 2024, **9**(25), e202304355.

297 D. Wu, C. Wang, M. Wu, Y. Chao, P. He and J. Ma, Porous bowl-shaped VS2 nanosheets/graphene composite for high-rate lithium-ion storage, *J. Energy Chem.*, 2020, **43**, 24–32.

298 J. Li, Z. Shi, M. Law, Z. Chen, Q. Lin, Y. Zhang, M. Huo, Y. Wang, C.-T. Lin and P. Balaya, In-situ assembly of 3D VS2/Reduced graphene oxide with superior lithium ion storage performance: The role of heterojunction, *J. Power Sources*, 2024, **621**, 235296.

299 D. Xin, S. He, X. Zhang, R. Li, W. Qiang, S. Duan, Q. Lou, K. Deng, Z. Cheng and M. Xia, Interlayer-expanded and carbon-coated VS2 nanosheets self-assembled on 3D CNTs cross-linked network skeleton for ultrastable lithium-ion storage, *J. Energy Storage*, 2023, **72**, 108688.

300 Y. Tian, F. Lu, Y. Wang, T. Sun and Y. Liu, Branch-leaf structural VS2@ C/TiO2 anode for high-performance lithium-ion batteries, *J. Electroanal. Chem.*, 2024, **953**, 118005.

301 Z. Huang, X. Han, X. Cui, C. He, J. Zhang, X. Wang, Z. Lin and Y. Yang, Vertically aligned VS 2 on graphene as a 3D heteroarchitectured anode material with capacitance-dominated lithium storage, *J. Mater. Chem. A*, 2020, **8**(12), 5882–5889.

302 L. Wang, H. Dang, T. He, R. Liu, R. Wang and F. Ran, Vanadium sulfide decorated at carbon matrix as anode materials for "fast-charging" lithium-ion batteries, *J. Alloys Compd.*, 2024, **1002**, 175490.

303 J. Zheng, C. He, X. Li, K. Wang, T. Wang, R. Zhang, B. Tang and Y. Rui, CoS2–MnS@ Carbon nanoparticles derived from metal–organic framework as a promising anode for lithium-ion batteries, *J. Alloys Compd.*, 2021, **854**, 157315.

304 D. Hu, C. Zhu, Y. Yao, S. Liu, X. Meng, H. Yuan, Z. Chen, X. Jiang, Y. Li and S. Zhu, A facile ex situ strategy of α-MnS nanoparticles anchored on holey graphene as high-performance anode for lithium-ion batteries, *Appl. Surf. Sci.*, 2021, **542**, 148496.

305 F. Chen, D. Shi, M. Yang, H. Jiang, Y. Shao, S. Wang, B. Zhang, J. Shen, Y. Wu and X. Hao, Novel designed MnS-MoS2 heterostructure for fast and stable Li/Na storage: insights into the advanced mechanism attributed to phase engineering, *Adv. Funct. Mater.*, 2021, **31**(6), 2007132.

306 X.-H. Zhou, K.-M. Su, W.-M. Kang, B.-W. Cheng and Z.-H. Li, Nanosized α-MnS homogenously embedded in axial multichannel carbon nanofibers as freestanding electrodes for lithium-ion batteries, *J. Mater. Sci.*, 2020, **55**(17), 7403–7416.

307 X. Zhou, J. Gao, H. Xu, X. Xu, Z. Zhuang, Q. Wu, J. Lin and W. Li, Internally and externally modified Mn2SnS4@ ZnS@ NC nanocassettes for high-performance lithium-ion battery anodes, *J. Energy Storage*, 2025, **107**, 114980.

308 L. Zhang, F. Peng, Y. Li, M. Zhang, D. Li, Q. Pan, H. Wang, F. Zheng, Y. Huang and Q. Li, Construction of heterojunctions for Mn-Sn bimetallic sulfides@ N-doped carbon nanorods as high-performance anode for lithium-ion batteries, *J. Alloys Compd.*, 2023, **962**, 171209.

309 D.-A. Zhang, X. Zhao, L. Zhu and Q. Wang, Facile One-Pot Hydrothermal Synthesis of Hierarchical MoS2/α-MnS Nanocomposites with Good Cycling Performance as Anode Materials for Lithium-Ion Batteries, *Crystals*, 2022, **12**(12), 1763.

310 R. A. Adams, A. Varma and V. G. Pol, Carbon anodes for nonaqueous alkali metal-ion batteries and their thermal safety aspects, *Adv. Energy Mater.*, 2019, **9**(35), 1900550.

311 S. Alvin, H. S. Cahyadi, J. Hwang, W. Chang, S. K. Kwak and J. Kim, Revealing the intercalation mechanisms of lithium, sodium, and potassium in hard carbon, *Adv. Energy Mater.*, 2020, **10**(20), 2000283.

312 X. Chen, Y. Zheng, W. Liu, C. Zhang, S. Li and J. Li, High-performance sodium-ion batteries with a hard carbon anode: transition from the half-cell to full-cell perspective, *Nanoscale*, 2019, **11**(46), 22196–22205.

313 G. Yang, X. Li, Z. Guan, Y. Tong, B. Xu, X. Wang, Z. Wang and L. Chen, Insights into lithium and sodium storage in porous carbon, *Nano Lett.*, 2020, **20**(5), 3836–3843.

314 L. Xie, F. Su, L. Xie, X. Guo, Z. Wang, Q. Kong, G. Sun, A. Ahmad, X. Li and Z. Yi, Effect of pore structure and doping species on charge storage mechanisms in porous carbon-based supercapacitors, *Mater. Chem. Front.*, 2020, **4**(9), 2610–2634.

315 L. Xie, C. Tang, Z. Bi, M. Song, Y. Fan, C. Yan, X. Li, F. Su, Q. Zhang and C. Chen, Hard carbon anodes for next-generation Li-ion batteries: review and perspective, *Adv. Energy Mater.*, 2021, **11**(38), 2101650.

316 X. Wang, K. Han, D. Qin, Q. Li, C. Wang, C. Niu and L. Mai, Polycrystalline soft carbon semi-hollow microrods as anode for advanced K-ion full batteries, *Nanoscale*, 2017, **9**(46), 18216–18222.

317 X. Li, M. Chen, L. Wang, H. Xu, J. Zhong, M. Zhang, Y. Wang, Q. Zhang, L. Mei and T. Wang, Correction: Nitrogen-doped carbon nanotubes as an anode for a highly robust potassium-ion hybrid capacitor, *Nanoscale Horiz.*, 2020, **5**(12), 1643.

318 L. Zhang, W. Wang, S. Lu and Y. Xiang, Carbon anode materials: a detailed comparison between Na-ion and K-ion batteries, *Adv. Energy Mater.*, 2021, **11**(11), 2003640.

319 M. Zhao, H.-J. Peng, B.-Q. Li and J.-Q. Huang, Kinetic promoters for sulfur cathodes in lithium–sulfur batteries, *Acc. Chem. Res.*, 2024, **57**(4), 545–557.

320 H.-D. Lim, B. Lee, Y. Bae, H. Park, Y. Ko, H. Kim, J. Kim and K. Kang, Reaction chemistry in rechargeable Li–O 2 batteries, *Chem. Soc. Rev.*, 2017, **46**(10), 2873–2888.

321 L. Sun, Y. Liu, R. Shao, J. Wu, R. Jiang and Z. Jin, Recent progress and future perspective on practical silicon anode-based lithium ion batteries, *Energy Storage Mater.*, 2022, **46**, 482–502.

322 Y. Li, Y. Li, L. Zhang, H. Tao, Q. Li, J. Zhang and X. Yang, Lithiophilicity: The key to efficient lithium metal anodes for lithium batteries, *J. Energy Chem.*, 2023, **77**, 123–136.

323 X. Shen, X.-Q. Zhang, F. Ding, J.-Q. Huang, R. Xu, X. Chen, C. Yan, F.-Y. Su, C.-M. Chen, X. Liu, *et al.*, Advanced electrode materials in lithium batteries: Retrospect and prospect, *Energy Mater. Adv.*, 2021, **2021**, 1205324.

324 H.-g. Wang, Y. Wang, Q. Wu and G. Zhu, Recent developments in electrode materials for dual-ion batteries: Potential alternatives to conventional batteries, *Mater. Today*, 2022, **52**, 269–298.

325 D. B. Agusdinata, W. Liu, H. Eakin and H. Romero, Socio-environmental impacts of lithium mineral extraction: towards a research agenda, *Environ. Res. Lett.*, 2018, **13**(12), 123001.

326 F. Mendes and A. Martins, Selective sorption of nickel and cobalt from sulphate solutions using chelating resins, *Int. J. Miner. Process.*, 2004, **74**(1–4), 359–371.

327 L. A.-W. Ellingsen, C. R. Hung and A. H. Strømman, Identifying key assumptions and differences in life cycle assessment studies of lithium-ion traction batteries with focus on greenhouse gas emissions, *Transp. Res. Part D Transp. Environ.*, 2017, **55**, 82–90.

328 S. Chen, Z. Gao and T. Sun, Safety challenges and safety measures of Li-ion batteries, *Energy Sci. Eng.*, 2021, **9**(9), 1647–1672.

329 S. Wang and J. Yu, A comparative life cycle assessment on lithium-ion battery: Case study on electric vehicle battery in China considering battery evolution, *Waste Manage. Res.*, 2021, **39**(1), 156–164.

330 J. Ordoñez, E. J. Gago and A. Girard, Processes and technologies for the recycling and recovery of spent lithium-ion batteries, *Renewable Sustainable Energy Rev.*, 2016, **60**, 195–205.

331 P. Meister, H. Jia, J. Li, R. Kloepsch, M. Winter and T. Placke, Best practice: performance and cost evaluation of lithium ion battery active materials with special emphasis on energy efficiency, *Chem. Mater.*, 2016, **28**(20), 7203–7217.

332 J. Piatek, S. Afyon, T. M. Budnyak, S. Budnyk, M. H. Sipponen and A. Slabon, Sustainable Li-ion batteries: chemistry and recycling, *Adv. Energy Mater.*, 2021, **11**(43), 2003456.

333 C. Peng, J. Hamuyuni, B. P. Wilson and M. Lundström, Selective reductive leaching of cobalt and lithium from industrially crushed waste Li-ion batteries in sulfuric acid system, *Waste Manage.*, 2018, **76**, 582–590.

334 X. Li and K. Binnemans, Oxidative dissolution of metals in organic solvents, *Chem. Rev.*, 2021, **121**(8), 4506–4530.

335 G. Zante, A. Braun, A. Masmoudi, R. Barillon, D. Trébouet and M. Boltoeva, Solvent extraction fractionation of manganese, cobalt, nickel and lithium using ionic liquids and deep eutectic solvents, *Miner. Eng.*, 2020, **156**, 106512.

336 G. Lombardo, B. Ebin, M. R. S. J. Foreman, B.-M. Steenari and M. Petranikova, Incineration of EV Lithium-ion batteries as a pretreatment for recycling–Determination of the potential formation of hazardous by-products and effects on metal compounds, *J. Hazard. Mater.*, 2020, **393**, 122372.

337 S. Natarajan and V. Aravindan, An urgent call to spent LIB recycling: whys and wherefores for graphite recovery, *Adv. Energy Mater.*, 2020, **10**(37), 2002238.

338 Y. He, T. Zhang, F. Wang, G. Zhang, W. Zhang and J. Wang, Recovery of LiCoO2 and graphite from spent lithium-ion

batteries by Fenton reagent-assisted flotation, *J. Cleaner Prod.*, 2017, **143**, 319–325.

339 C. Liu, J. Lin, H. Cao, Y. Zhang and Z. Sun, Recycling of spent lithium-ion batteries in view of lithium recovery: A critical review, *J. Cleaner Prod.*, 2019, **228**, 801–813.

340 Z. J. Baum, R. E. Bird, X. Yu and J. Ma, Lithium-ion Battery Recycling-Overview of Techniques and Trends, *ACS Energy Lett.*, 2022, **7**(10), 3268–3269.

341 J. Neumann, M. Petranikova, M. Meeus, J. D. Gamarra, R. Younesi, M. Winter and S. Nowak, Recycling of lithium-ion batteries—current state of the art, circular economy, and next generation recycling, *Adv. Energy Mater.*, 2022, **12**(17), 2102917.

342 X. Feng, M. Ouyang, X. Liu, L. Lu, Y. Xia and X. He, Thermal runaway mechanism of lithium ion battery for electric vehicles: A review, *Energy Storage Mater.*, 2018, **10**, 246–267.

343 D. Ren, X. Feng, L. Lu, X. He and M. Ouyang, Overcharge behaviors and failure mechanism of lithium-ion batteries under different test conditions, *Appl. Energy*, 2019, **250**, 323–332.

344 M. Chen, S. Lin, W. Song, J. Lv and Z. Feng, Electrical and thermal interplay in lithium-ion battery internal short circuit and safety protection, *Int. J. Energy Res.*, 2020, **44**(8), 6745–6757.

345 C. Tian, F. Lin and M. M. Doeff, Electrochemical characteristics of layered transition metal oxide cathode materials for lithium ion batteries: surface, bulk behavior, and thermal properties, *Acc. Chem. Res.*, 2017, **51**(1), 89–96.

346 Z. Li, H. Zhao, P. Lv, Z. Zhang, Y. Zhang, Z. Du, Y. Teng, L. Zhao and Z. Zhu, Watermelon-like structured SiOx–TiO2@ C nanocomposite as a high-performance lithium-ion battery anode, *Adv. Funct. Mater.*, 2018, **28**(31), 1605711.

347 J. Liu, T. Zhao, S. Zhang and Q. Wang, A new metallic carbon allotrope with high stability and potential for lithium ion battery anode material, *Nano Energy*, 2017, **38**, 263–270.

348 M. Tang, P. Albertus and J. Newman, Two-dimensional modeling of lithium deposition during cell charging, *J. Electrochem. Soc.*, 2009, **156**(5), A390.

349 Q. Wang, P. Ping, X. Zhao, G. Chu, J. Sun and C. Chen, Thermal runaway caused fire and explosion of lithium ion battery, *J. Power Sources*, 2012, **208**, 210–224.

350 J. Duan, X. Tang, H. Dai, Y. Yang, W. Wu, X. Wei and Y. Huang, Building safe lithium-ion batteries for electric vehicles: a review, *Electrochem. Energy Rev.*, 2020, **3**, 1–42.

351 M. S. Whittingham, Lithium batteries and cathode materials, *Chem. Rev.*, 2004, **104**(10), 4271–4302.

352 M. Javed, A. Shah, J. Nisar, S. Shahzad, A. Haleem and I. Shah, Nanostructured design cathode materials for magnesium-ion batteries, *ACS Omega*, 2024, **9**(4), 4229–4245.

353 J. L. Afonso, L. A. L. Cardoso, D. Pedrosa, T. J. Sousa, L. Machado, M. Tanta and V. Monteiro, A review on power electronics technologies for electric mobility, *Energies*, 2020, **13**(23), 6343.

354 C. Zhao, Y. Lu, Y. Li, L. Jiang, X. Rong, Y. S. Hu, H. Li and L. Chen, Novel methods for sodium-ion battery materials, *Small Methods*, 2017, **1**(5), 1600063.

355 Y.-S. Hu and Y. Li, Unlocking sustainable Na-ion batteries into industry, *ACS Energy Lett.*, 2021, **6**(11), 4115–4117.

356 K. Abraham, How comparable are sodium-ion batteries to lithium-ion counterparts?, *ACS Energy Lett.*, 2020, **5**(11), 3544–3547.

357 M. Shalaby, M. O. Alziyadi, H. Gamal and S. Hamdy, Solid-state lithium-ion battery: The key components enhance the performance and efficiency of anode, cathode, and solid electrolytes, *J. Alloys Compd.*, 2023, **969**, 172318.

358 N. Oueldna and N. Sabi, Correlation between physical properties and the electrochemical behavior in inorganic solid-state electrolytes for lithium and sodium batteries: A comprehensive review, *J. Energy Storage*, 2024, **86**, 111254.

359 J. Yu, W. Yu, Z. Zhang and P. Tan, Reunderstanding the uneven deposition in aqueous zinc-based batteries, *Chem. Eng. J.*, 2024, **481**, 148556.

360 M. Abdelbaky, J. R. Peeters and W. Dewulf, On the influence of second use, future battery technologies, and battery lifetime on the maximum recycled content of future electric vehicle batteries in Europe, *Waste Manage.*, 2021, **125**, 1–9.

361 M. Fichtner, K. Edström, E. Ayerbe, M. Berecibar, A. Bhowmik, I. E. Castelli, S. Clark, R. Dominko, M. Erakca and A. A. Franco, Rechargeable batteries of the future—the state of the art from a BATTERY 2030+ perspective, *Adv. Energy Mater.*, 2022, **12**(17), 2102904.

362 K. Itani and A. De Bernardinis, Review on new-generation batteries technologies: trends and future directions, *Energies*, 2023, **16**(22), 7530.

363 Q. Liu, X. Zhao, Q. Yang, L. Hou, D. Mu, G. Tan, L. Li, R. Chen and F. Wu, The progress in the electrolytes for solid state sodium-ion battery, *Adv. Mater. Technol.*, 2023, **8**(7), 2200822.

364 K. Shi, B. Guan, Z. Zhuang, J. Chen, Y. Chen, Z. Ma, C. Zhu, X. Hu, S. Zhao and H. Dang, Recent Progress and Prospects on Sodium-Ion Battery and All-Solid-State Sodium Battery: A Promising Choice of Future Batteries for Energy Storage, *Energy Fuels*, 2024, **38**(11), 9280–9319.